

The Nanofactory Solution to Global Climate Change: Atmospheric Carbon Capture

© 2015 Robert A. Freitas Jr. All Rights Reserved.

Abstract. The new carbon capture technology proposed here, built by molecular manufacturing using first-generation nanofactories at a manufacturing cost of ~\$1000/kg, would enable the atmospheric capture of CO₂ at a total lifetime cost of about **\$21/tonne CO₂**, far less expensive than the \$70-\$200/tonne CO₂ and higher estimated for conventional atmospheric carbon capture technologies. For an installation cost of \$2.74 trillion/yr over 10 years followed by a maintenance cost of \$0.91 trillion per year, a network of direct atmospheric CO₂ capture plants could be emplaced that would be powerful enough to reduce global CO₂ levels by ~50 ppm per decade, easily overwhelming current anthropogenic emission rates. This is sufficient to return Earth's atmosphere to pre-industrial carbon dioxide levels near 300 ppm within 40 years from launch of program, and thereafter to maintain the atmosphere in this ideal condition indefinitely, eliminating one of the primary drivers of global climate change on our planet. Lower cost later-generation nanofactories may allow the deployment of a global system of similar capacity for an annual installation and maintenance cost of \$4.04 billion per year, capturing and permanently sequestering atmospheric CO₂ using marine "carbon capture islands" at a total lifetime cost of about **\$0.08/tonne CO₂**. The cost is driven so extraordinarily low because the mature nanofactory, manufacturing atomically precise product for ~\$1/kg, can also manufacture a cheap source of solar energy to power the CO₂ capture and sequestration process.

Cite as: Robert A. Freitas Jr., "The Nanofactory Solution to Global Climate Change: Atmospheric Carbon Capture," IMM Report No. 45, December 2015;
<http://www.imm.org/Reports/rep045.pdf>

Table of Contents

1. Introduction.....	4
2. Physical Properties of Carbon Dioxide.....	9
3. Conventional Carbon Capture Technologies.....	11
3.1 Carbon Capture from Flue Gases.....	12
3.2 Carbon Capture from Liquid Fuels.....	17
3.3 Carbon Capture from the Atmosphere.....	19
3.4 Carbon Transport.....	26
3.5 Carbon Storage.....	29
3.5.1 Geological Carbon Storage.....	30
3.5.2 Carbon Storage in Minerals.....	33
4. NEW APPROACH: Molecular Filters.....	35
4.1 Basic Molecular Filter Design.....	36
4.2 Binding Site Design for Carbon Dioxide.....	40
4.3 Filtering Carbon Dioxide Directly from the Atmosphere.....	44
5. Simple Nanofactory-Based Atmospheric CO₂ Capture System.....	46
5.1 An Exemplar CO₂ Capture Plant Scaling Design.....	46
5.1.1 Target Processing Rate.....	46
5.1.2 Sorting Rotor Power Requirement.....	46
5.1.3 Solar Panel Area.....	47
5.1.4 Solar Panel Cost.....	49
5.1.5 Number, Area, and Cost of Sorting Rotors.....	50
5.1.6 Air Throughput Rate.....	51
5.1.7 Layout of Nanofilter Sheets.....	52
5.1.8 Carbon Transport from Plant.....	52
5.1.9 Total Cost per Tonne.....	53
5.2 A Simple CO₂ Capture Plant Applied to Global Climate Change.....	55
5.2.1 Worldwide CO ₂ Capture Plant Network Scenarios.....	56
5.2.2 Network Size and Deployment.....	59
5.2.3 Network Issues: Wind Velocity and Vertical Convection.....	60

6. Advanced Nanofactory-Based Atmospheric CO₂ Capture System.....	61
6.1 Selection of Storage Pressure	62
6.2 Building and Loading Diamond Microtanks.....	65
6.3 Golfballs: Carbon Disposal at Sea.....	67
6.4 Golfcarts: Golfball Manufacturing at Sea	69
6.4.1 Onboard Solar Power.....	70
6.4.2 Number and Area of Sorting Rotors	72
6.4.3 Air Throughput Rate.....	73
6.4.4 Onboard Nanofactory	74
6.4.5 Paddlewheel Motive Power	75
6.4.6 Summary of Golfcart Mass, Volume and Productivity	76
6.5 The Siting of Carbon Capture Islands	77
6.6 Manufacturing Golfcarts Using Onshore Nanofactories.....	84
7. Conclusions.....	86

1. Introduction

Chemical substances released into the atmosphere as a result of industrial and other activities related to human civilization can remain aloft for a long time. Eventually the air becomes contaminated with gaseous and particulate waste materials that may not be optimal for human or ecological health.

Beyond these conventional air pollutants, more recently it has been determined that atmospheric concentrations of carbon dioxide are rising unusually rapidly by historical standards. This rise in atmospheric CO₂ levels appears to have a significant anthropogenic component (e.g., caused by human industrial activities, automobiles, worldwide agriculture, Amazon basin deforestation, and the like), with negative long-term effects on regional and global mean temperatures, rainfall, wind velocities, polar ice coverage, and so forth (i.e., climate change).¹ In this view, excessive amounts of CO₂ may be regarded as an additional “climate pollutant” in Earth’s atmosphere.

Since implementation of globally-effective regulations to reduce carbon dioxide and other climate pollutant emissions at their many sources faces significant economic and political challenges, there have been numerous suggestions for sequestration approaches in which, for example, carbon-rich pollutant gases that have already been released into the atmosphere would subsequently be extracted from the atmosphere and isolated in some form of long-term storage.² The best-known examples of carbon sequestration are active afforestation or reforestation programs³ that seek to sequester carbon as cellulosic biological matter in long-lived plants such as trees. While workable in theory, trees can all too easily be cleared by humans, felled by disease, burned by fire, or die of old age after a few decades, returning the sequestered carbon to the air. Another well-known biosequestration proposal is to seed the ocean surface with bulk quantities of iron-rich compounds, stimulating plankton growth that removes CO₂ from the air and carries the sequestered carbon to the ocean floor when the blooms later die off and sink,⁴ though the

¹ IPCC, 2014: Climate Change 2014: Synthesis Report. Contribution of Working Groups I, II and III to the Fifth Assessment Report of the Intergovernmental Panel on Climate Change [Core Writing Team, Pachauri RK, Meyer LA (eds.)]. IPCC, Geneva, Switzerland, 151 pp; <http://ipcc.ch/report/ar5/syr/>.

² Metz B, Davidson O, de Coninck HC, Loos M, Meyer LA, eds., Working Group III of the Intergovernmental Panel on Climate Change: IPCC Special Report on Carbon Dioxide Capture and Storage, Cambridge University Press, NY, 2005.

³ Canadell JG, Raupach MR. Managing forests for climate change. *Science* 320(13 June 2008):1456-1457; <http://www.sciencemag.org/cgi/content/full/320/5882/1456>.

⁴ Markels M Jr., Barber RT. Sequestration of CO₂ by ocean fertilization. NETL Conference on Carbon Sequestration, 14-17 May 2001; http://www.netl.doe.gov/publications/proceedings/01/carbon_seq/p25.pdf. Jin X, Gruber N, Frenzel H, Doney SC, McWilliams JC. The impact on atmospheric CO₂ of iron fertilization induced changes in the ocean’s biological pump. *Biogeosciences* 5(2008):385-406; <http://www.biogeosciences.net/5/385/2008/>.

effectiveness of this method has been questioned.⁵ Oceanic phosphorus seeding is a related possibility.⁶ Burial of biochar (anaerobic charcoal)⁷ and manufacture of CO₂-enriched concrete⁸ and “carbonate cement” (similar to marine cement)⁹ are under active investigation, and carbon capture and storage (CCS)¹⁰ from coal-fired power plant smokestacks is being tested. Others have proposed the direct capture of airborne CO₂ and permanently burying it deep underground¹¹ or at sea.¹² Free-standing scrubbing towers employing conventional chemistry have been proposed by Zeman and Lackner,¹³ and their team has worked to build a laboratory prototype at Global Research Technologies in Tucson, Arizona.¹⁴ A \$25M Virgin Earth Challenge prize¹⁵

⁵ Buesseler KO, Doney SC, Karl DM, Boyd PW, Caldeira K, Chai F, Coale KH, de Baar HJW, Falkowski PG, Johnson KS, Lampitt RS, Michaels AF, Naqvi SWA, Smetacek V, Takeda S, Watson AJ. Ocean iron fertilization – moving forward in a sea of uncertainty. *Science* 319(11 January 2008):162; http://marine.rutgers.edu/ebme/papers/Buesseler_et_al_Science_319_Jan_2008.pdf.

⁶ Lampitt RS, Achterberg EP, Anderson TR, Hughes JA, Iglesias-Rodriguez MD, Kelly-Gerreyn BA, Lucas M, Popove EE, Sanders R, Shepherd JG, Smythe-Wright D, Yool A. Ocean fertilization: a potential means of geoengineering. *Philos. T.R. Soc. A* 366(2008):3919-3945; <http://rsta.royalsocietypublishing.org/content/366/1882/3919.short>.

⁷ Lehmann J, Gaunt J, Rondon M. Bio-char sequestration in terrestrial ecosystems – a review. *Mitigation and Adaptation Strategies for Global Change* 11(2006):403-427; <http://citeseerx.ist.psu.edu/viewdoc/download?doi=10.1.1.436.7800&rep=rep1&type=pdf>.

⁸ Yixin S, Xudong Z, Monkman S. A new CO₂ sequestration process via concrete products production, 2006 IEEE EIC Climate Change Technology, 10-12 May 2006, pp. 1-6. Kashef-Haghighi S, Ghoshal S. CO₂ sequestration in concrete through accelerated carbonation curing in a flow-through reactor. *Ind. Eng. Chem. Res.* 48(21 October 2009); <http://pubs.acs.org/doi/pdf/10.1021/ie900703d>.

⁹ Biello D. Cement from CO₂: a concrete cure for global warming? *Scientific American*, 7 August 2008; <http://www.scientificamerican.com/article.cfm?id=cement-from-carbon-dioxide>.

¹⁰ Keith DW, Ha-Doung M, Stolaroff JK. Climate strategy with CO₂ capture from the air. *Climatic Change* 74(2006):17-45; http://scholar.harvard.edu/files/davidkeith/files/51.keith_2005.climatestratwithaircapture.e.pdf.

¹¹ “Bureau of Economic Geology Receives \$38 Million for First Large-Scale U.S. Test Storing Carbon Dioxide Underground,” Jackson School of Geosciences, The University of Texas at Austin, 24 October 2007; <http://www.jsg.utexas.edu/news/rels/102407.html>.

¹² Goldberg DS, Takahashi T, Slagle AL. Carbon dioxide sequestration in deep-sea basalt. *Proc. Natl. Acad. Sci. (USA)* 105(22 July 2008):9920-9925; <http://www.ncbi.nlm.nih.gov/pmc/articles/PMC2464617/>.

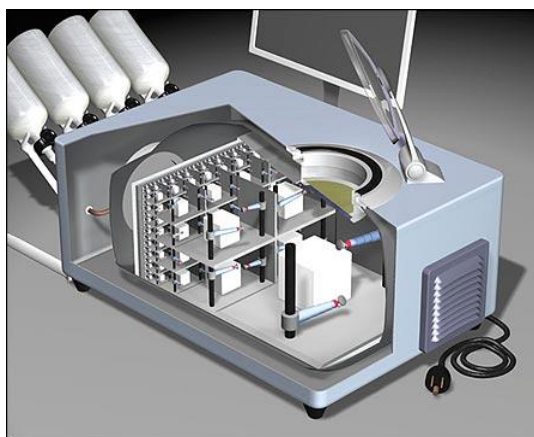
¹³ Zeman FS, Lackner KS. Capturing carbon dioxide directly from the atmosphere. *World Resour. Rev.* 16(2004):157-172; http://wordpress.ei.columbia.edu/lenfest/files/2012/11/ZEMAN_LACKNER_2004.pdf.

¹⁴ Andrea Thompson, “New Device Vacuums Away Carbon Dioxide,” *LiveScience*, 1 May 2007, http://www.livescience.com/technology/070501_carbon_capture.html; David Adam, “Could US scientist's ‘CO₂ catcher’ help to slow warming?” *The Guardian*, Saturday 31 May 2008, <http://www.guardian.co.uk/environment/2008/may/31/carbonemissions.climatechange>.

promises to reward the first inventor who demonstrates a practical way to remove a billion tons per year of CO₂ from the atmosphere. An X-Prize for carbon capture is also under development.¹⁶

In this paper we offer a novel method for global carbon sequestration that is made possible by the advent of the nanofactory – a proposed new technology for molecular manufacturing that can be developed at an R&D cost of under \$1B in a surprisingly short period of time. Even first-generation nanofactories will be able to manufacture key components of compact zero-carbon-footprint CO₂ capture plants that can extract, transport, and permanently sequester atmospheric CO₂ at a cost of under **\$21/tonne (Section 5)**. Systems built using later-generation nanofactories can offer substantially lower per-tonne CO₂ capture and sequester costs, on the order of **\$0.08/tonne (Section 6)**.

The nanofactory (image, right) is a proposed high quality, low cost, and very flexible manufacturing system in which products are built atom by atom.¹⁷ The nanofactory is sometimes colloquially called a “3D printer for atoms” – a molecular manufacturing system that employs controlled molecular assembly at the atomic scale. Nanofactories will enable the creation of fundamentally novel products having the intricate complexity and reliability currently found only in biological systems, but operating with greater speed, power, and predictability than biological systems – and, perhaps most importantly, entirely under human engineering control.



The principal inputs to a nanofactory may be simple hydrocarbon feedstock molecules such as natural gas or propane, along with water and small supplemental amounts of other simple molecules containing trace atoms of a few additional chemical elements needed to make useful products, such as oxygen, nitrogen, sulfur, or silicon. The nanofactory must also be provided with electricity or some other energy source, and a means for cooling the working unit.

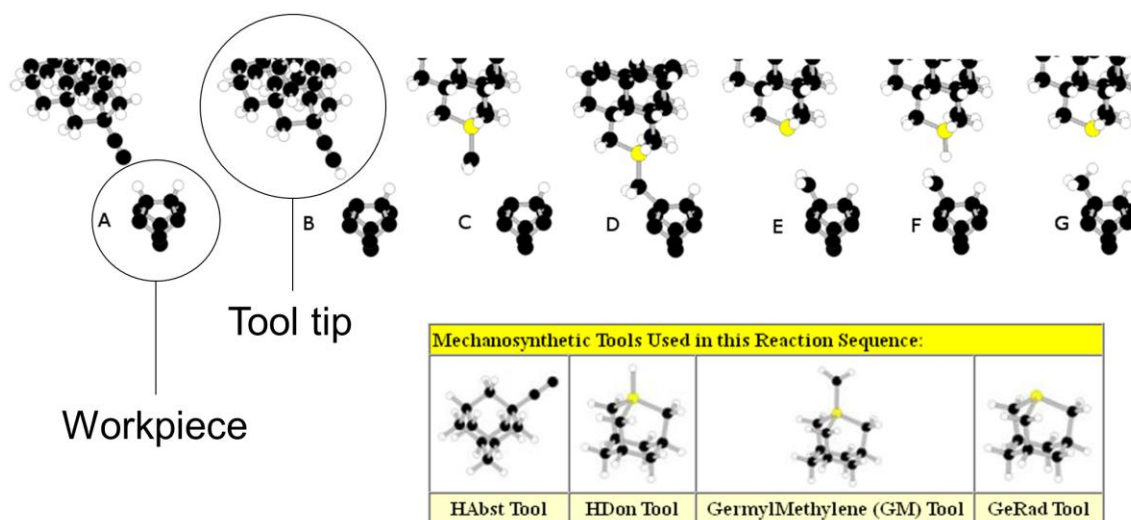
At the most basic level, the nanofactory will employ mechanosynthesis to fabricate atomically precise structures using molecular feedstock. Mechanosynthesis, involving molecular positional fabrication, is the formation of covalent chemical bonds using precisely applied mechanical

¹⁵ Virgin Earth Challenge, <http://www.virgin.com/subsites/virginearth/>.

¹⁶ <http://www.xprize.org/prizes/future-prizes/carbon>.

¹⁷ Drexler KE, Nanosystems, Wiley, 1992, Chapter 14. Freitas RA Jr, Merkle RC, Kinematic Self-Replicating Machines, Landes Bioscience, 2004; <http://www.molecularassembler.com/KSRM.htm>. See also: “Nanofactory Collaboration,” <http://www.MolecularAssembler.com/Nanofactory>.

forces to build, for example, diamondoid structures.¹⁸ Mechanochemistry employs chemical reactions driven by the mechanically precise placement of extremely reactive chemical species in an ultra-high vacuum environment (image, below). Mechanochemistry may be automated via computer control, enabling programmable molecular positional fabrication. Atomically precise fabrication involves holding feedstock atoms or molecules, and a growing nanoscale workpiece, in the proper relative positions and orientations so that when they touch they will chemically bond in the desired manner. In this process, a mechanochemical tool is brought up to the surface of a workpiece. One or more transfer atoms are added to, or removed from, the workpiece by the tool. Then the tool is withdrawn and recharged. This process is repeated until the workpiece (e.g., a growing nanopart) is completely fabricated to molecular precision with each atom in exactly the right place. Note that the transfer atoms are under positional control at all times to prevent unwanted side reactions from occurring. Side reactions are also prevented using proper reaction design so that the reaction energetics help us avoid undesired pathological intermediate structures.



The primary objective of this paper is to parameterize the mission design of a molecular manufacturing based air-scrubbing system called a CO₂ capture plant that is potentially capable of active continuous management of the concentrations of relevant greenhouse gases in the atmosphere. The purpose of a global network of these plants is to maintain the specified greenhouse gas constituents at programmed concentrations that are regarded as ideal for human health, proper ecological maintenance, and human esthetics. In this initial analysis, system specifications are dominated by the requirement for massive long-term sequestration of carbon

¹⁸ For mechanochemistry theory work generally, see: Freitas RA Jr, Merkle RC. A Minimal Toolset for Positional Diamond Mechanochemistry. *J Comput Theor Nanosci.* 2008 May;5:760-861; <http://www.molecularassembler.com/Papers/MinToolset.pdf>. For experimental mechanochemistry work, see: Sugimoto Y, Pou P, Custance O, Jelinek P, Abe M, Perez R, Morita S. Complex Patterning by Vertical Interchange Atom Manipulation Using Atomic Force Microscopy. *Science.* 2008 Oct 17;322:413-417; <http://www.sciencemag.org/content/322/5900/413.full>.

dioxide, but the same approach could readily be applied to control other climate-relevant greenhouse gases such as nitrous oxide¹⁹ and even to avoid the buildup of potentially catastrophic levels of methane²⁰ or hydrogen sulfide,²¹ adding only minor additional system costs.

After a brief description of the most relevant physical properties of carbon dioxide (**Section 2**), we review the conventional (and very expensive) methods for carbon capture, transport, and sequestration (**Section 3**). We next review our new approach to atmospheric carbon capture that uses “molecular filters” or “nanofilters” to be manufactured by nanofactories (**Section 4**). We then discuss how a simple CO₂ capture plant using molecular filters could serve as the basic module for a scalable approach to direct atmospheric carbon capture at the global level (**Section 5**). This would enable human-controlled modulation of the CO₂ content of the atmosphere and consequent human control over global climate change – at least to the extent that climate change is driven by the presence of excessive greenhouse gases. A more advanced and far less costly system for direct atmospheric carbon capture on a global scale – one that more fully exploits the tremendous power and efficiency of nanofactory-based molecular manufacturing – is described in **Section 6**. Our conclusions are in **Section 7**.

Throughout this paper, the unit “tonne” refers to a metric ton or 1000 kg, and the energy unit “zJ” refers to the zeptojoule or 10⁻²¹ joules. The cost of industrial electricity is assumed to be \$0.07/kWh ($p_{\text{elect}} = 1.94 \times 10^{-8}$ \$/J).²²

¹⁹ Elberling B, Christiansen HH, Hansen BU. High nitrous oxide production from thawing permafrost. *Nat Geosci.* 2010; 3:332-335; https://www.researchgate.net/profile/Birger_Hansen2/publication/44884749_High_nitrous_oxide_production_from_thawing_permafrost/links/550be9700cf2b2450b4dfed7.pdf. See also: “Overview of Greenhouse Gases: Nitrous Oxide Emissions,” U.S. Environmental Protection Agency, November 2015; <http://www3.epa.gov/climatechange/ghgemissions/gases/n2o.html>.

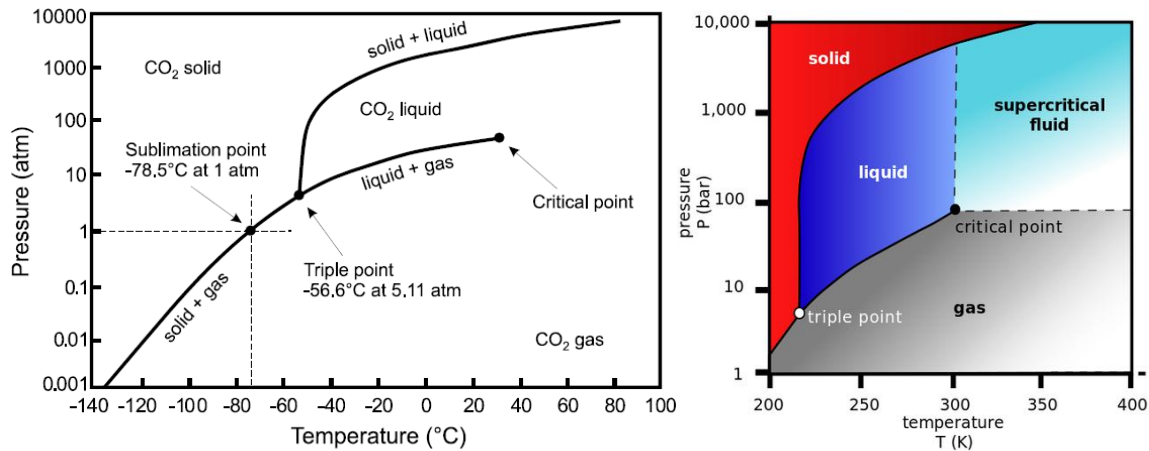
²⁰ Kennett JP, Cannariato KG, Hendy IL, Behl RJ. Methane hydrates in Quaternary climate change: the clathrate gun hypothesis. *American Geophysical Union*, 2003, <http://www.amazon.com/Methane-Hydrates-Quaternary-Climate-Change/dp/0875902960/>. See also: “Clathrate gun hypothesis,” https://en.wikipedia.org/wiki/Clathrate_gun_hypothesis.

²¹ Ward PD, *Under a Green Sky: Global Warming, the Mass Extinctions of the Past, and What They Can Tell Us About Our Future*, Harper Perennial, reprint edition, 2008; <http://www.amazon.com/Under-Green-Sky-Warming-Extinctions/dp/0061137928>. See also: “Anoxic event,” https://en.wikipedia.org/wiki/Anoxic_event,

²² U.S. Industrial Sector, \$0.0651/kWh in April 2013. “Electricity Monthly Update, End Use: April 2013, Retail Service by Customer Sector,” U.S. Energy Information Administration (EIA); http://www.eia.gov/electricity/monthly/update/end_use.cfm.

2. Physical Properties of Carbon Dioxide

The standard pressure-temperature (PT) phase diagram for carbon dioxide (CO₂) is shown below.²³



At the **triple point** in the PT phase diagram for CO₂ (pressure = 5.117 atm, 5.185×10^5 N/m², 5.185 bar, 75.2 psi; temperature = 216.58 K, -56.57 °C, -69.8 °F), all three phases exist in thermodynamic equilibrium with a density of 1179 kg/m³. Below the triple point pressure or temperature, CO₂ can only appear in the solid and gaseous states. Above the triple point pressure or temperature, CO₂ can exist in any of the three states depending on conditions.

At the **critical point** in the PT phase diagram for CO₂ (pressure = 72.8 atm, 73.8×10^5 N/m², 73.8 bar, 1070 psi; temperature = 304.18 K, 31.03 °C, 87.9 °F), the difference between the liquid and gaseous phase vanishes, creating a “fluid” known as “**supercritical CO₂**” with a density of 464.1 kg/m³ at critical pressure and temperature. Below the critical point pressure or temperature, CO₂ can exist in any of the three states depending on conditions. Above the critical point pressure and temperature, CO₂ can only appear in the solid and supercritical fluid states. Supercritical CO₂ expands to fill its container like a gas but has a density more like that of a liquid.²⁴

Sublimation is a transition between solid and gaseous states without passing through the liquid state. **Sublimation points** occur at specific pressures and temperatures defined by the curve labeled “solid + gas” in the PT phase diagram for CO₂. For example, at a pressure of 1 atm, solid CO₂ sublimates to gas at a temperature at, or above, -78.5 °C (194.7 K, -109.3 °F).

²³ [https://en.wikipedia.org/wiki/Carbon_dioxide_\(data_page\)](https://en.wikipedia.org/wiki/Carbon_dioxide_(data_page)).

²⁴ https://en.wikipedia.org/wiki/Supercritical_carbon_dioxide.

CO₂ is most commonly transported, bought and sold under pressure in liquid form, though the solid form (“dry ice”) is also sold. Carbon dioxide is generally liquefied by compression and refrigeration for storage or shipment. It is commonly stored and shipped as a liquid at pressures and temperatures ranging from 13.8 bar (13.6 atm) and -29 °C (200 psi and -20 °F) to 24.1 bar (23.8 atm) and -12 °C (350 psi and 11 °F).²⁵

²⁵ “Carbon Dioxide,” http://www.asiaiga.org/docs/AIGA_068_10_Carbon_Dioxide_reformatted_Jan_12.pdf.

3. Conventional Carbon Capture Technologies

To sequester unwanted carbon dioxide, the molecule must first be captured and concentrated from whatever source is generating it. Carbon capture technologies are generally aimed at one of three primary sources of carbon dioxide:

(1) flue gases at electrical power plants following their combustion of carbon-rich fuels, usually hydrocarbons (**Section 3.1**);

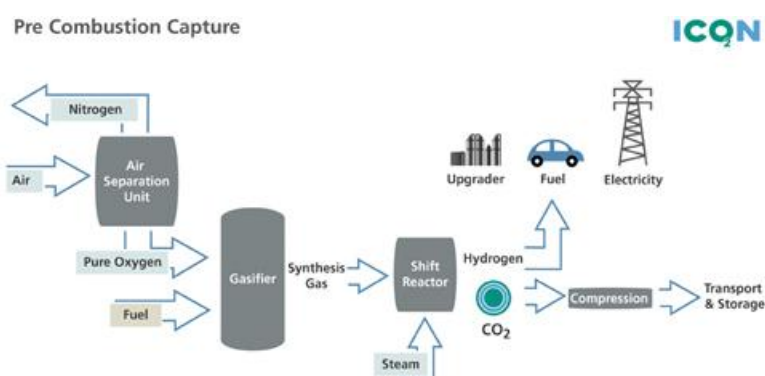
(2) liquid fuels being transported through pipes or stored in tanks in which large concentrations of CO₂ gas are dissolved (**Section 3.2**); and

(3) the free atmosphere, which has experienced rapidly rising CO₂ levels (**Section 3.3**).

3.1 Carbon Capture from Flue Gases

There are three CO₂-capture technologies for flue gas scrubbing in use today: pre-combustion, oxyfuel combustion, and post-combustion.²⁶

Pre-combustion capture²⁷ (image, below) is a process that separates and captures CO₂ from a fossil fuel before it is burned. In these cases, the fossil fuel is partially oxidized, for instance in a gasifier. Oxygen is added to turn the fossil fuel into a synthetic gas. The resulting syngas (CO and H₂O) is shifted into CO₂ and H₂. The H₂ can be burned cleanly as fuel while the resulting CO₂ is captured from a relatively pure exhaust stream before combustion takes place. The technology for pre-combustion is widely applied in fertilizer, chemical, gaseous fuel (H₂, CH₄), and power production.

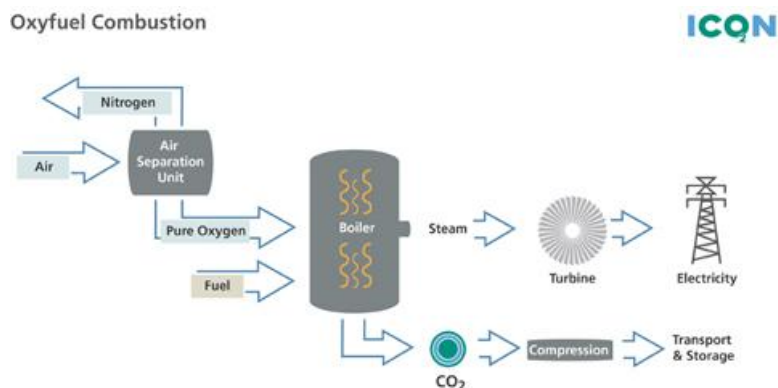


Oxyfuel combustion²⁸ (image, below) is a process that burns a fossil fuel in the presence of pure oxygen instead of air. This reduces fuel consumption and removes contaminants such as nitrogen. Cooled flue gas is recirculated and injected into the combustion chamber to limit the resulting flame temperatures to levels common during conventional combustion. An exhaust stream is created that contains primarily CO₂ and water (which is condensed through cooling), making it easier to capture the CO₂. The result is an almost pure carbon dioxide stream that can be transported to the sequestration site and stored. Carbon dioxide capture and storage is more commonly proposed on plants burning coal in oxygen extracted from the air, which means the CO₂ is highly concentrated and no scrubbing process is necessary. Concentrated CO₂ from the combustion of coal in oxygen is relatively pure and can be directly processed.

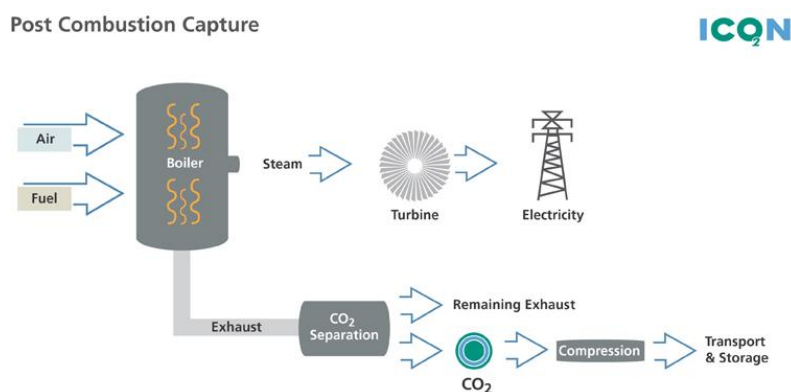
²⁶ "CO₂ Capture," <http://www.solutionsstarthere.ca/33.asp>. See also: http://en.wikipedia.org/wiki/Carbon_capture.

²⁷ "Gasification: Current Industry Perspective," U.S. Dept. of Energy, 2004; http://www.netl.doe.gov/publications/brochures/pdfs/Gasification_Brochure.pdf.

²⁸ "Winner: Clean Coal - Restoring Coal's Sheen," IEEE Spectrum 45(January 2008):57-60.



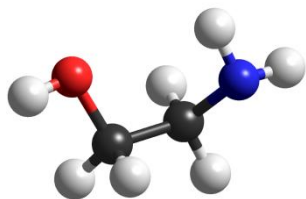
Post-combustion capture (image, below), the most common and widely used process, involves removing the CO₂ from flue gases after a fossil fuel has been burned. The CO₂ is separated from other gases by using a solvent, then removing the solvent through heating. This process is well developed and has existed for several decades. Current technology typically captures 85%-95% of the CO₂ in the exhaust stream and produces a 99.95%+ pure CO₂ product (dry basis). Capturing and compressing CO₂ may increase the fuel needs of a coal-fired carbon-capture power plant by 25%-40%; these and other system costs are estimated to increase the cost of the energy produced by 21%-91% for purpose built plants.²⁹ Applying the technology to existing plants would be more expensive especially if they are far from a sequestration site.



In the flue gas stack of power plants using post-combustion systems, the typical composition of the gas-fired flue gas is **7.4-7.7% CO₂** and 14.6% H₂O, 4.45% O₂, 0.02-0.03% CO, 0.006-0.007% NO_x, and 73-74% N₂; coal-fired flue gas is typically **12.5-12.8% CO₂**, 6.2% H₂O, 4.4% O₂, 0.005% CO, 0.042% NO_x, 0.042% SO₂, and 76-77% N₂. The temperature of the flue gas in the stack is maintained such that the water vapors in it do not condense, i.e., the temperature of the flue gas is a function of the dew point at a specific moisture percentage in the flue gas. So, flue gas with 15% moisture content would be exhausted above 55 °C (328 K) and flue gas with

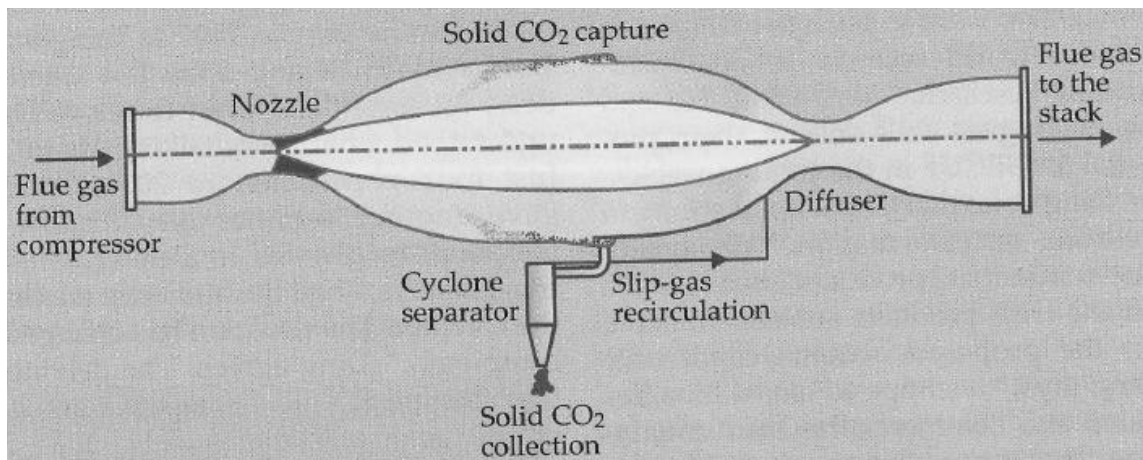
²⁹ Metz B, Davidson O, Coninck Hd, Loos M, Meyer L. IPCC Special Report on Carbon Dioxide Capture and Storage. Cambridge University Press, NY, 2005; http://www.ipcc.ch/pdf/special-reports/srccs/srccs_wholereport.pdf.

6% moisture would be exhausted above 45 °C (318 K).³⁰ Flue gas typically runs up the stack at about 1 atm pressure.



All carbon capture technologies consume energy. The current benchmark industrial technology, an absorber-desorber process that uses a monoethanol amine (MEA; molecule image, left) solvent, costs around **\$90/tonne CO₂** for gas capture.³¹ Applied to a power plant, this could add as much as 76% to the cost of producing electricity from coal.³² New technologies are being researched in the U.S. with ARPA-E funding.³³ For example, Alliant Techsystems is developing a device in which flue gas is compressed and then

accelerated through a special nozzle to supersonic velocities (see below). The process produces a rapid decrease in temperature and pressure, causing the CO₂ to desublimite and collect as dry ice. The proposed device is mechanically simple, contains no moving parts, and is readily scalable. The company projects low capital costs for system construction and operating costs are estimated to be significantly less than membrane- and absorption-based alternatives, possibly in the range of **\$48/tonne CO₂**.



As another example, phase-changing compounds called aminosilicones are being used by GE Global Research and partners to replace MEA as the CO₂ absorbent. GE's Robert Perry says the aminosilicones change from liquid to solid on contact with CO₂. Because the solid absorbent contains a higher percentage of CO₂ than the liquid MEA, the energy efficiency of the process is improved. The project's goals are to reduce parasitic power requirements to less than 23% and

³⁰ Puneet Mannan, personal communication, 25 June 2013.

³¹ Kramer D. Carbon capture may be a ways off, but ARPA-E is working on it. *Physics Today*, May 2013, pp. 23-25. See also: https://en.wikipedia.org/wiki/Amine_gas_treating.

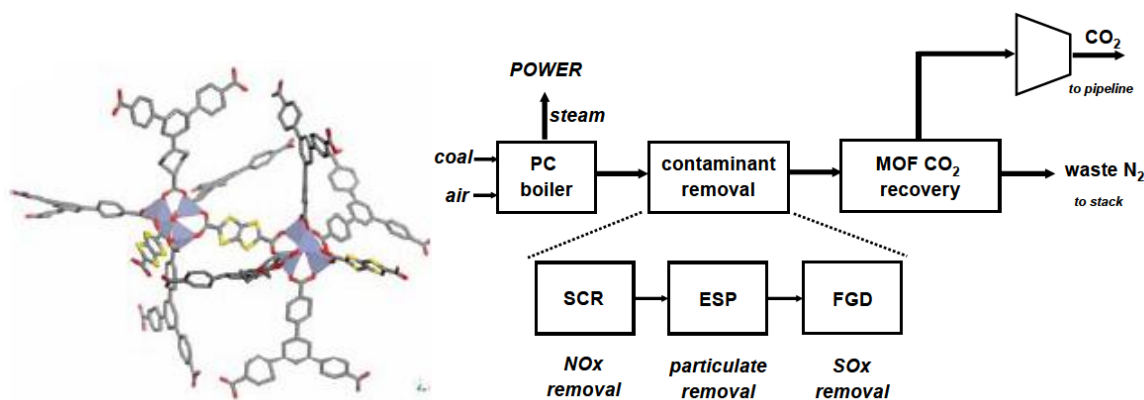
³² Chris Nelder, "Why carbon capture and storage will never pay off," ZDNet, 6 March 2013; <http://www.zdnet.com/article/why-carbon-capture-and-storage-will-never-pay-off/>.

³³ Kramer D. Carbon capture may be a ways off, but ARPA-E is working on it. *Physics Today*, May 2013, pp. 23-25.

lower the cost to **\$60/tonne CO₂** removed. It's more difficult to move a solid partway through the process loop compared with a liquid, but on the other hand, having a stable solid that can be heated to 160 °C or so to drive off the CO₂ at 5-6 atm means that less compression is required to liquefy the CO₂ for transport.

Another Columbia University project seeks to turn captured CO₂ into a solid that can be easily and safely transported, stored aboveground, or integrated into products such as paper filler, plastic filler, and construction materials. In nature, the reaction of CO₂ with various minerals over long periods of time – a process known as carbon mineralization – yields a solid carbonate. The Columbia team is using a process involving a combination of chemical catalysts to increase this rate. If successful, the Columbia project would produce a long-term solid CO₂ storage solution that would eliminate the worry of monitoring gas in underground storage. But that solution could have its limits: converting the gigatons of CO₂ produced annually into solid form would create “mountains of carbonate everywhere,” cautions GE’s Robert Perry.³⁴

A U.S. Department of Energy-sponsored study, completed in 2010 by Honeywell with four university participants, evaluated the state of the art in microporous metal-organic-frameworks (MOFs) for carbon capture from flue gas (images, below).³⁵ Their best-performing MOF material had 1D hexagonal pores about 11 Angstroms in diameter, outperformed all other MOF and zeolite materials with about 25 wt% CO₂ captured under flue gas conditions (~0.13 atm CO₂ pressure, 311 K), and if deployed industrially would extract 90% of the CO₂ in flue gas, yielding a product stream of 95%-97% pure CO₂. At their assumed busbar electricity cost of \$0.0633/kWh, their estimated cost of CO₂ capture was \$57/short ton, equivalent to **\$69/tonne CO₂** assuming our standard \$0.07/kWh electricity cost and converting to metric tonnes. The estimated total capital cost to implement this system at a power plant was \$354 million, to be preceded by “extensive process modeling” and R&D leading to an initial demo unit costing \$5-\$10 million/year for 5 years, plus 2 years of pilot plant operation at \$5 million/year.



³⁴ Kramer D. Carbon capture may be a ways off, but ARPA-E is working on it. *Physics Today*, May 2013, pp. 23-25.

³⁵ Willis R. Carbon Dioxide Removal from Flue Gas Using Microporous Metal Organic Frameworks. Final Technical Report, DOE Award No. DE-FC26-07NT43092, October 2010; <http://www.netl.doe.gov/technologies/coalpower/ewr/co2/pubs/43092F1.pdf>.

Another approach is a variant on the conventional amine approach in which a solution containing amines selectively binds carbon dioxide, then releases it upon heating, requiring a large amount of energy that would come from steam that could otherwise be used to generate power. MIT researchers have devised a new process that gets the amine solution to release carbon dioxide without heating it by running the solution through a device that resembles a battery having positive and negative electrodes made of copper. The solution of CO₂-rich amines is pumped to one electrode where electricity is applied, producing copper ions. There, the copper ions bind more strongly to the amines than the carbon dioxide does, displacing the carbon dioxide and causing it to bubble off. The copper-amine solution is then pumped to the opposite electrode, where the copper is removed, allowing the amines to capture more carbon dioxide. Small scale tests suggest that the process consumes only 45 KJ/mole (~\$20/tonne) compared with 77 KJ/mole (~\$34/tonne) for the conventional amine system.³⁶

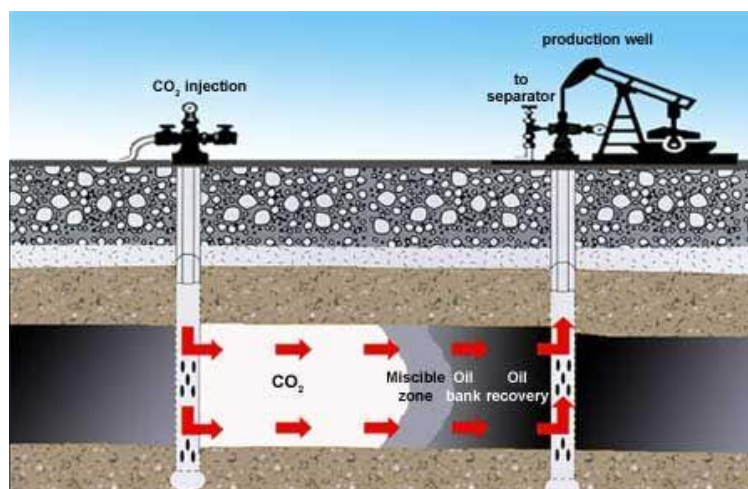
Even further afield, a molten carbonate fuel cell made by the Danbury CT-based company FuelCell Energy could provide a cheap way to selectively remove carbon dioxide from the exhaust gases of fossil-fuel power plants, both concentrating the CO₂ so it can be stored underground and generating electricity that provides revenue to offset its cost.³⁷ Normally, molten carbonate fuel cells take carbon dioxide in at one electrode which is then used to form ions that conduct current to the opposite electrode, where the carbon dioxide is emitted. Finally, it is pumped back to the first electrode to be reused, forming a complete loop. To capture carbon dioxide, this loop would be interrupted. Instead of recycling carbon dioxide, the fuel cell would get the CO₂ it needs from the exhaust in a power plant, selectively take it up and use it to form ions, then emit it in a much more concentrated stream at the opposite electrode. The gases emitted there would be about 70% CO₂ and the rest mostly water vapor, which is easy to condense out, leaving an almost pure stream of carbon dioxide that can be pressurized and pumped underground for storage. FuelCell Energy optimistically calculates that the process could capture CO₂ at \$20-\$30/ton, but so far the technology has only been demonstrated at a small scale in a lab. Some DOE funding will allow building larger systems, but several questions remain about how well it will work and how much it will cost. In particular, power plant exhaust gases are contaminated with sulfur and other pollutants that could interfere with the operation of a fuel cell, so the capture cost will depend on how much the gases need to be cleaned up before they're introduced into a fuel cell.

³⁶ Kevin Bullis, "Cheaper Ways to Capture Carbon Dioxide," MIT Technology Review, 12 June 2013; <http://www.technologyreview.com/news/515881/cheaper-ways-to-capture-carbon-dioxide/>.

³⁷ Kevin Bullis, "Fuel Cells Could Offer Cheap Carbon Dioxide Storage," MIT Technology Review, 24 May 2013; <http://www.technologyreview.com/news/515026/fuel-cells-could-offer-cheap-carbon-dioxide-storage/>.

3.2 Carbon Capture from Liquid Fuels

Enhanced Oil Recovery (abbreviated EOR) is a generic term for techniques for increasing the amount of crude oil that can be extracted from an oil field.³⁸ Using EOR, 30% to 60% or more of the reservoir's original oil can be extracted, compared with 20% to 40% using primary and secondary recovery. Gas injection or miscible flooding is presently the most-commonly used approach in enhanced oil recovery. Miscible flooding is a general term for injection processes that introduce miscible gases into the reservoir (image below, left side). The fluid most commonly used for miscible displacement is carbon dioxide because it reduces the oil viscosity and is less expensive than liquefied petroleum gas. In mature oil fields, extensive pipe networks are used to carry the carbon dioxide to the injection points.



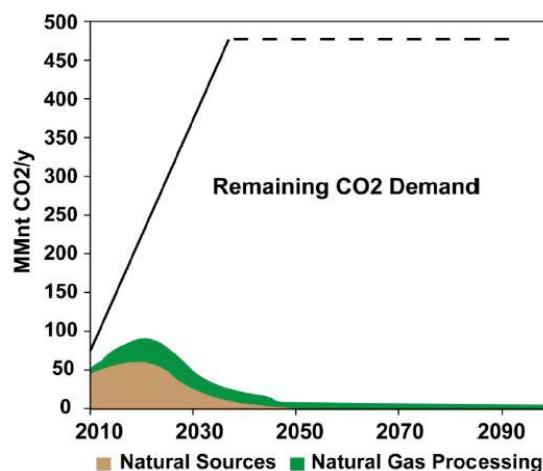
Carbon dioxide flooding is particularly effective in reservoirs deeper than 600 meters, with an injection pressure of at least 100 atm to ensure that the CO₂ will be in a supercritical state. In high pressure applications with lighter oils, CO₂ is miscible with the oil, with resultant swelling of the oil, and reduction in viscosity, and possibly also with a reduction in the surface tension with the reservoir rock. In these applications, between one-half and two-thirds of the injected CO₂ returns with the produced oil and is usually re-injected into the reservoir to minimize operating costs. The remainder is trapped in the oil reservoir by various means.

During successful CO₂ EOR operations, carbon dioxide is produced along with oil and brine through production wells (image above, right side). As fluids are brought from reservoir depths to the surface, dense-phase CO₂ (supercritical or liquid) flashes to gas and CO₂ comes out of

³⁸ http://en.wikipedia.org/wiki/Enhanced_Oil_Recovery.

solution with oil and water.³⁹ Although venting this CO₂ to the atmosphere would be permissible, the purified gas is a valuable commodity (e.g., bringing \$15-\$40/tonne CO₂ if sold commercially)⁴⁰ so operators invest in separation facilities that extract this CO₂ from the oil, recompress it, and return it to the injection stream (image, above; “to separator”). Efficiency of this return depends on CO₂ handling losses from separation, during equipment maintenance, from connections, and during equipment malfunctions. One proprietary assessment from Kinder Morgan’s West Texas in 2009 showed losses during handling of <0.5% of total CO₂ in the system,⁴¹ while another report from Oxy’s Elk Hills CO₂ EOR projects reports about 0.3% CO₂ losses due to “venting and fugitive emissions”.⁴² At 293 K and 1 atm pressure, the solubility of CO₂ in oil is about 0.0307 mol/kg, or 0.135% by weight.⁴³ Total CO₂ costs (both purchase price and recycle costs) amount to 25% to 50% of the cost per barrel of oil produced.⁴⁴

Additional sources of liquid CO₂ might also find a ready market – one chart (image, right) of projected CO₂ supply and demand suggests that reclamation of very large volumes of anthropogenic CO₂ might be necessary to realize the estimated 100 billion bbls of economic stranded oil.⁴⁵



³⁹ Hovorka SD. EOR as Sequestration—Geoscience Perspective. White Paper for Symposium on Role of EOR in Accelerating Deployment of CCS, 2010; <http://mitei.mit.edu/system/files/hovorka.pdf>.

⁴⁰ Hill B, Hovorka S, Melzer S. Geologic carbon storage through enhanced oil recovery. Energy Procedia (2013) preprint; http://www.catf.us/resources/publications/files/201301-Geologic_carbon_storage_through_enhanced_oil_recovery.pdf.

⁴¹ Chuck Fox, oral presentation, 7th Annual EOR Carbon Management Workshop, December 2009; cited in <http://mitei.mit.edu/system/files/hovorka.pdf>.

⁴² Hill *et al.*, 2013, *supra*, Ref. [14].

⁴³ Stefan Iglauer, “Dissolution Trapping of Carbon Dioxide in Reservoir Formation Brine – A Carbon Storage Mechanism,” Table 2, p. 243; <http://www.intechopen.com/download/pdf/23520>.

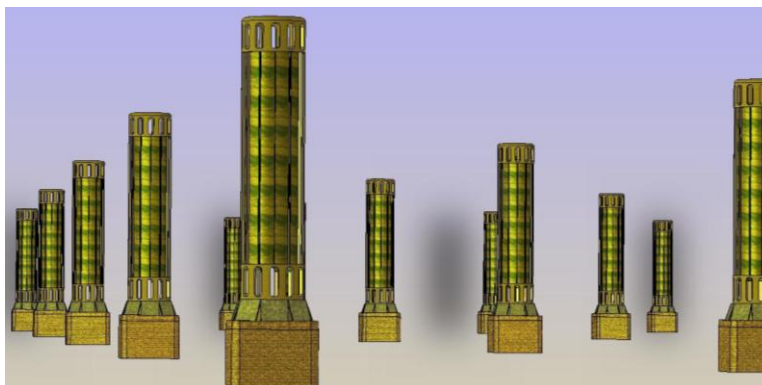
⁴⁴ “Carbon Dioxide Enhanced Oil Recovery,” NETL, March 2010; http://www.netl.doe.gov/technologies/oil-gas/publications/EP/CO2_EOR_Primer.pdf.

⁴⁵ Kuuskraa V. Advanced Resources International, Inc. Using the economic value of CO₂-EOR to accelerate the deployment of CO₂ capture, utilization and storage. (CCUS, EPRI Cost Workshop, Palo Alto, CA, April 25-26, 2012. Cited in Hill *et al.*, 2013, *supra*, Ref. [23].

3.3 Carbon Capture from the Atmosphere

A few engineering proposals have been made for the more difficult task of capturing CO₂ directly from the air.⁴⁶ Capture costs are generally assumed to be much higher than from point sources, in part because the CO₂ concentration in air is 100-300 times lower than in flue gases which increases the mass flow that must be processed (per ton of carbon dioxide extracted).

Most notably, in 2007 Klaus Lackner of Columbia University and Global Research Technologies LLC (Lackner's R&D company) reported the first successful demonstration of an "air extraction" prototype that captures CO₂ directly from the atmosphere.⁴⁷ Lackner's 2009 technical paper⁴⁸ described his method for direct carbon capture from ambient air, based on a solid sorbent in the form of an anionic exchange resin that absorbs carbon dioxide when dry and releases it when exposed to moisture. Moisture cycling releases 0.05 atm CO₂ that was previously extracted from ambient air with a CO₂ partial pressure of 0.0004 atm (400 ppm), after which standard pumps compress the 0.05 atm gas up to a 66 atm pipeline pressure at 300 K, whereupon the gas liquefies. Unfortunately, large filter units would have to be physically removed from the air collector system (image, below), transported to a vacuum chamber on a conveyor belt, moisture-cycled, then returned to the air collector.



Lackner concluded that for a successful air capture design the cost of contacting the air is not likely to drive the cost of the overall system. Instead, the cost of air capture is likely to be driven by the cost of sorbent recycling. Total system cost was estimated to be **1.1 GJ/tonne CO₂**, at a

⁴⁶ http://en.wikipedia.org/wiki/Carbon_dioxide_air_capture.

⁴⁷ "First Successful Demonstration of Carbon Dioxide Air Capture Technology Achieved by Columbia University Scientist and Private Company," The Earth Institute, Columbia University, 24 April 2007; <http://www.earth.columbia.edu/news/2007/story04-24-07.php>.

⁴⁸ Lackner KS. Capture of carbon dioxide from ambient air. Eur. Phys. J. Special Topics 176(2009):93-106; http://death.ocf.berkeley.edu/~step/Journal_Club/paper4_02092010.pdf. See also http://www.netl.doe.gov/publications/proceedings/01/carbon_seq/7b1.pdf.

mature-system cost of **\$36/tonne CO₂** assuming electric power is supplied at \$0.07/kWh, although “we expect that the first prototypes could break even at **\$200/tonne CO₂**”.



Lackner’s previous company, Kilimanjaro Energy (<http://www.kilimanjaroenergy.com/>), appears to be dormant or out of business. But he continues to push the concept. According to a 2014 report,⁴⁹ Lackner has been developing his own system for nearly a decade and says he has a successful prototype that he will soon be testing extensively outside the laboratory. In the laboratory model (image, left), a fan pushes air through coils of dry resin filters with openings the size of drinking straws. As the air passes through, the CO₂ interacts with carbonate and hydroxide in the resin

walls, forming bicarbonate. When the filters become fully saturated, they are recharged by stacking the coils like poker chips in a glass tube. Water is poured over them, causing a chemical reaction that releases the CO₂ gas into the tube. From there, the CO₂ could be stored as a gas or compressed into a liquid for storage. Much of the energy cost associated with air capture would come from converting the gas to a liquid.

So far, Lackner’s team (which is still seeking commercial backing) has found the prototype works best in very dry desert conditions. The current design for their prototype air capture facility (image, right) would be about the size of a small house, with the ability to capture 1 ton/day of carbon. The coiled filters would be placed in panels that are 3 feet wide by 7.5 feet tall. These panels, about 30 in all, would rotate on the top of the building structure. This would allow air to passively flow through the filters. As the filters reach their saturation point, a robotic device would remove the panel and bring it to a storage box below where the filters would be recharged and a fresh panel would be put up in its place. In order to achieve negative emissions, there would need to be about 100 million of his 1-ton/day structures worldwide. The resulting carbon dioxide could be buried underground or used for industrial purposes like exploratory oil drilling or in commercial greenhouses. Unfortunately, Lackner now estimates that the cost of this method of carbon capture could be as high as **\$1000/tonne**,⁵⁰ and that the price would have to fall below \$100/tonne for the technology to be economically feasible.

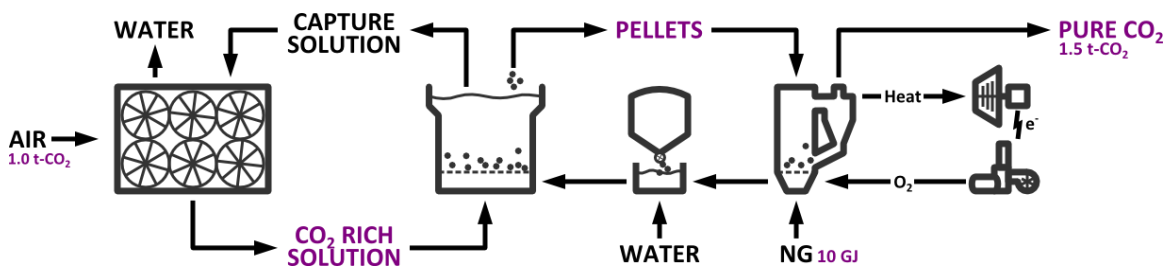


⁴⁹ Niina Heikkinen, “CO₂ capture from air could ripen into a global warming solution, researcher predicts,” E&E News, 7 August 2014; <http://www.eenews.net/stories/1060004175>.

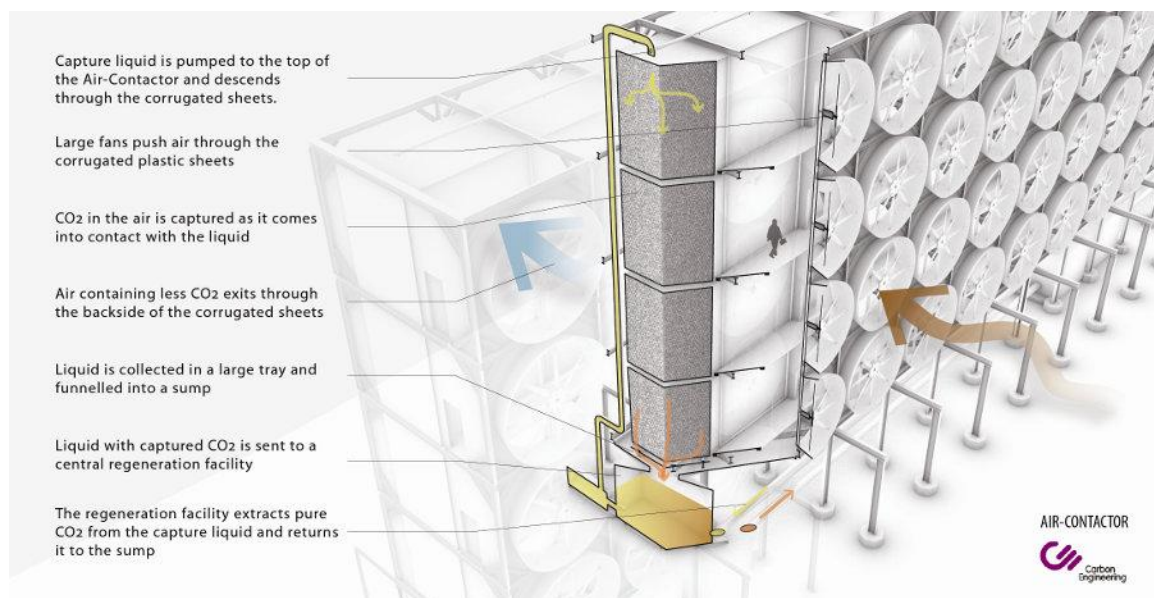
⁵⁰ *Ibid.*

There currently appear to be three active startup companies pursuing direct atmospheric carbon capture as of 2015,⁵¹ described below.

Carbon Engineering, founded in 2009, is a private company located in Calgary, Canada, that is pursuing a related method for scrubbing CO₂ directly out of the air.⁵² Their Direct Air Capture (DAC) system integrates two processes, an air contactor and a regeneration cycle, to continuously capture atmospheric carbon dioxide.



In the first process, their air contactor (image, below) brings atmospheric air containing CO₂ into contact with a chemical solution of caustic potassium hydroxide that naturally absorbs CO₂, producing a liquid solution that is rich in CO₂.

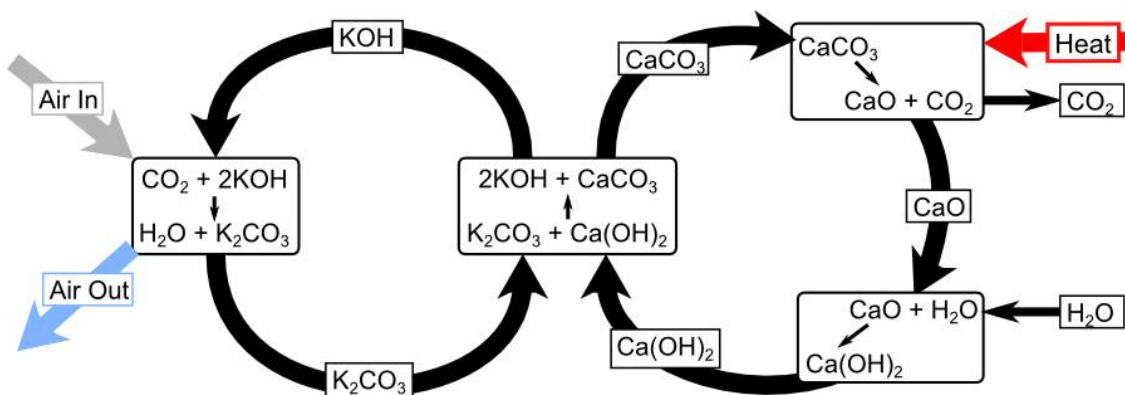


⁵¹ “Startups have figured out how to remove carbon from the air. Will anyone pay them to do it?” The Guardian, 14 July 2015; <http://www.theguardian.com/sustainable-business/2015/jul/14/carbon-direct-air-capture-startups-tech-climate>.

⁵² <http://carbonengineering.com/>.

In the second process, the solution containing the captured CO_2 is sent to a regeneration cycle (image, below) that simultaneously extracts the CO_2 while regenerating the original chemical solution, for re-use in the contactor. From the company website:⁵³

“After CO_2 is captured in the air contactor, it forms a chemical known as potassium carbonate [K_2CO_3], which is carried to the regeneration cycle dissolved in solution. This solution is fed into a device called a pellet reactor which simultaneously reacts it with calcium hydroxide [$\text{Ca}(\text{OH})_2$] to regenerate the potassium hydroxide [KOH] for reuse in the air contactor and precipitates the CO_2 out of solution as solid calcium carbonate [CaCO_3]. Once the solid calcium carbonate [CaCO_3] has been separated from the solution, it is sent to a device called a fluid-bed calciner. The calciner operates at about 900°C which causes the calcium carbonate [CaCO_3] to decompose into calcium oxide (CaO), during which pure CO_2 is released as a gas. The calciner burns fuel, such as natural gas, in an oxygen environment to supply the heat needed to perform this reaction. The calciner also generates heat that is used to supply electricity for the rest of the air capture plant. The CO_2 produced by burning the fuel mixes with the captured atmospheric CO_2 and all the CO_2 is sent to a final “compression and clean-up” stage to produce pure, pipeline-quality CO_2 . After the solids have released their CO_2 , they are then sent to a mixing tank where they react with water to re-form fresh calcium hydroxide [$\text{Ca}(\text{OH})_2$]. This calcium hydroxide is recycled to the pellet reactor for reuse.”



These two processes work together to enable continuous capture of CO_2 from atmospheric air, with energy (and small amounts of make-up chemicals) as an input, and pure CO_2 as an output. The stream of pure CO_2 can be sold and used in industrial applications and/or permanently sequestered (geologically stored) deep underground. The basic process was demonstrated experimentally several years ago. According to their website, the company recently concluded a second round of investment funding to fabricate and test a fully-integrated end-to-end pilot plant of their technology. Their plan was to work through a pilot phase during 2013-2015, which is the last step before building a full-up commercial air capture plant in ~2017. When their technology reaches maturity, the company estimates it can deliver industrial CO_2 for about **\$70-\$100/tonne**. Carbon Engineering also plans to split water into hydrogen and oxygen, and then combine the hydrogen with CO_2 to make a diesel fuel that could power local buses or be exported to California, which subsidizes low-carbon fuels.⁵⁴

⁵³ <http://carbonengineering.com/our-technology/>.

⁵⁴ <http://www.theguardian.com/sustainable-business/2015/jul/14/carbon-direct-air-capture-startups-tech-climate>.

Climeworks, a Zurich-based private company, sells a stand-alone mobile capture device that can extract 8 kg/day of >99% pure CO₂ from ambient air (image, below). It is designed for demonstration and test purposes and is suitable for autonomous 24/7 operation,⁵⁵ and uses a cyclic adsorption/desorption process. During adsorption, atmospheric CO₂ is chemically bound to the sorbent's surface. Once the sorbent is saturated, the CO₂ is driven off the sorbent by heating it to 95 °C, thereby delivering high-purity gaseous CO₂, and the now-CO₂-free sorbent can be re-used for many adsorption/desorption cycles. About 90% of the energy demand can be supplied by low-temperature heat; the remaining energy is required in the form of electricity for pumping and control purposes.⁵⁶



At the 3rd Conference on Carbon Dioxide as Feedstock for Chemistry and Polymers in December 2014 in Germany,⁵⁷ it was announced that after successful operation of a 1 ton/yr CO₂ capture demonstrator for over 20 months, in August 2014 Climeworks commissioned a full-scale, industrial CO₂ capture module (CO₂ Collector) with a nominal CO₂ capture capacity of 50 tons/yr. The CO₂ Collector was presented to the public at the Swiss Energy and Climate Summit, Bern in September 2014 together with Audi, Climeworks' partner in the mobility sector. In 2015,

⁵⁵ "Climeworks CO₂ Capture Demonstrator"; <http://www.climeworks.com/demonstrator.html>.

⁵⁶ http://www.climeworks.com/capture_process.html.

⁵⁷ "CO₂ Supply through Direct Air Capture – Update on Climeworks Activities," p.12; <http://co2-chemistry.eu/media/files/journal/14-11-24CO2Journal.pdf>.

Climeworks was to build up production infrastructure for the manufacturing of 20 CO₂ collectors, which would be contained in a first commercial CO₂ capture plant. Industrial CO₂ capture plants consist of arrays of CO₂ Collectors with a modular design for various applications. No data are readily available regarding their estimated cost/tonne of CO₂ capture.

A third startup company in this sector is Global Thermostat, a New York-based company founded in 2006 that uses dry amine-based sorbents in “carbon capture cubes” (image, right)⁵⁸ to pull CO₂ out of the air, then strip it off using low-temperature steam to produce 98% pure gas at 1 atm pressure.⁵⁹ According to their website, GT’s plants are “are completely modular – from a single 50,000 tonne/yr module to a 40-module, 2 million tonne/yr plant, and larger – a GT plant grows by adding more modules. GT Plants also have a small footprint –



capturing from 20-500 tonnes of CO₂/yr/m² or more, depending on the embodiment used.” Results from an early version of their system (image, left), built using an \$18M investment by the Bronfman family, led to perhaps over-optimistic early public cost estimates for atmospheric CO₂ capture of **\$15-\$50/ton**,⁶⁰ “depending on how long the amine surfaces last,” but the company has not revealed more recent estimates.



A fourth company, Tucson AZ-based Global Research Technologies was founded in 2004 and planned to use a commercially-sold resin that absorbs CO₂ when dry, and releases it when exposed to humid air, providing a very simple, low-energy way to mine CO₂ from the air unless the resin proves vulnerable to contamination in scaled-up systems. Frank Zeman, director of the Center for Metropolitan Sustainability at the New York Institute of Technology, estimates Global Research Technology’s approach will cost something like **\$100-\$200/tonne** of CO₂ “in an optimistic world”, and in 2008 the company itself was claiming a **\$125/tonne** figure.⁶¹ Lackner is associated with this company,⁶² but by 2015 it appeared mostly inactive.

⁵⁸ Rob Wile, “How Carbon Capture Technology Can Almost Turn CO₂ Into Cash,” Business Insider, 2 April 2013; <http://www.chichilnisky.com/wp-content/uploads/2013/10/Global-Thermostat-Carbon-Capture-tech-2013-4.pdf>.

⁵⁹ <http://globalthermostat.com/who-we-are/about-global-thermostat/>.

⁶⁰ Eli Kintisch, “Can Sucking CO₂ Out of the Atmosphere Really Work?,” MIT Technology Review, 7 October 2014; <http://www.technologyreview.com/featuredstory/531346/can-sucking-co2-out-of-the-atmosphere-really-work/>.

⁶¹ Nicola Jones, “Sucking carbon out of the air,” Nature, 17 December 2008; <http://www.nature.com/news/2008/081217/full/news.2008.1319.html>.

⁶² <https://sustaintechs.wordpress.com/2008/05/03/global-research-technologies/>.

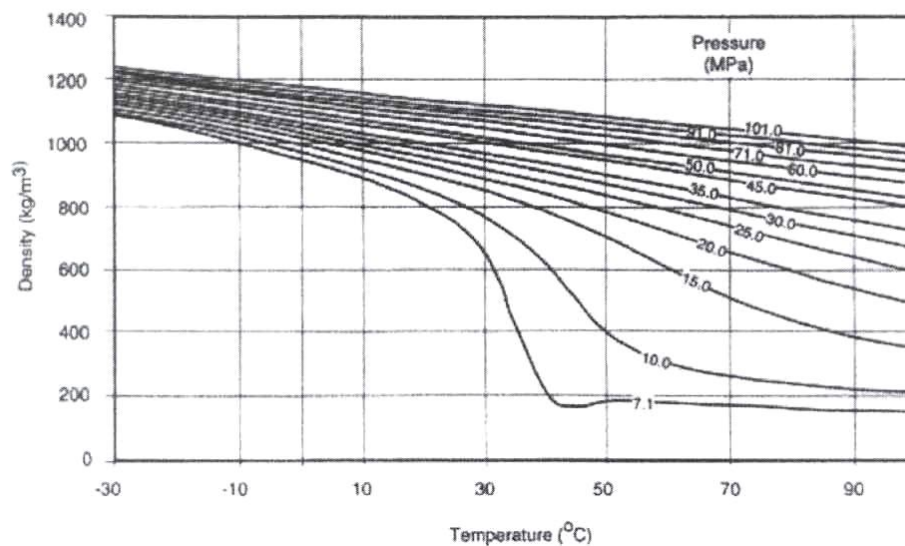
A 2011 technology assessment panel under the auspices of the American Physical Society pessimistically concluded that the cost of atmospheric CO₂ capture using all currently-known chemical-based approaches would likely approach **\$600/tonne** in any actual fielded large-scale system.⁶³

⁶³ “Direct Air Capture of CO₂ with Chemicals,” American Physical Society, 1 June 2011; <http://www.aps.org/policy/reports/assessments/upload/dac2011.pdf>.

3.4 Carbon Transport

After CO₂ is captured from its source and adequately pressurized, it usually must be transported somewhere else – either to be used in some industrial process or to be stored (**Section 3.5**). Carbon dioxide is typically compressed under great pressure to become a liquid (**Section 2**). It can then be transported by pipeline or truck. For example, industrial players have significant experience transporting CO₂ by truck and pipeline to field sites for enhanced oil recovery or EOR (**Section 3.2**).

The figure below shows the density of CO₂ as the pressures and temperatures vary.⁶⁴ Above the critical pressure of 7.38 MPa (72.8 atm) and at temperatures lower than 20 °C, CO₂ would have a density between 800 to 1200 kg/m³ (cf. the density of water, ~1000 kg/m³). A higher density is favorable when transporting liquid CO₂, as it is easier to move a dense liquid than a gas. Therefore it is typical to compress CO₂ to above 7.38 MPa for efficient transport.

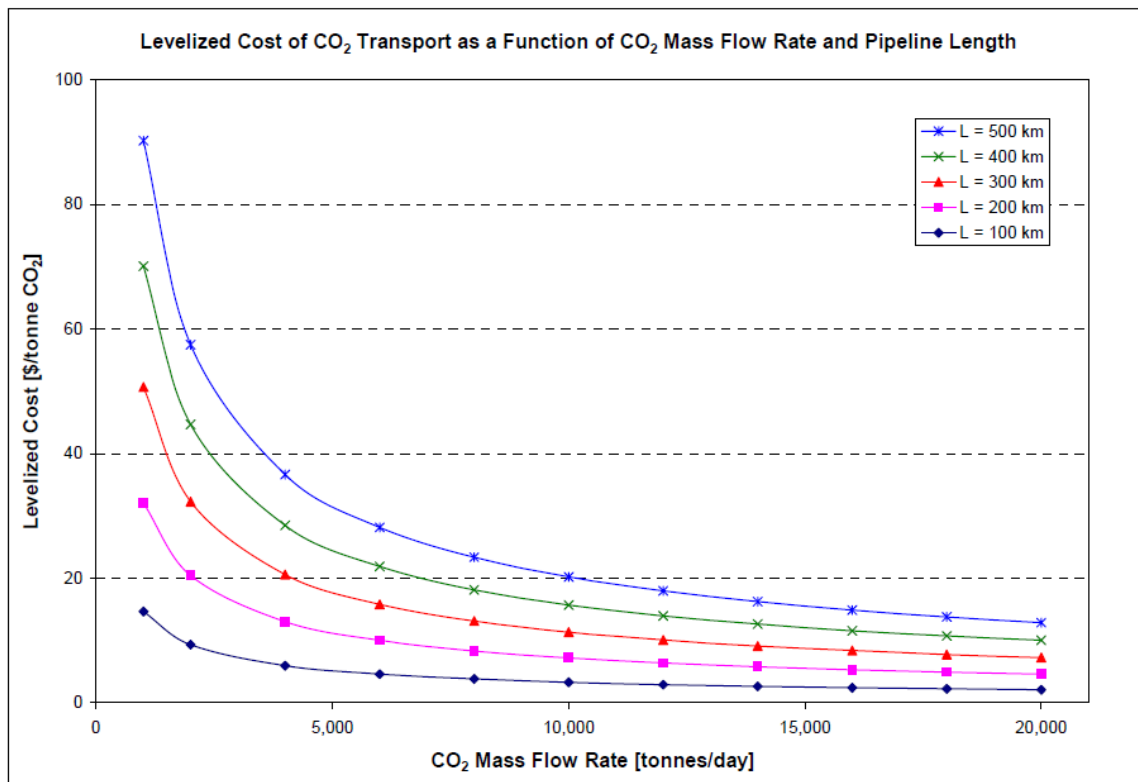


There is frictional loss as the CO₂ flows through a pipeline. Typically the frictional loss can range from 4 to 50 kPa per km, depending on the pipe diameter, mass, CO₂ flow rate and the pipe roughness factor. As a rule, the larger the pipeline diameter, the lower the frictional loss. Maintaining the CO₂ in the dense phase for the whole pipeline would require either (1) holding the inlet pressure to the pipeline at a high enough pressure to overcome all the losses while still above 7.38 MPa or (2) installing booster stations every 100 to 150 km to make up the pressure losses. Industry preference is to operate the pipeline at greater than 10.3 MPa at the inlet (i.e., the compressor discharge pressure) so that the CO₂ remains in the supercritical phase throughout the

⁶⁴ Wong S. CO₂ Compression and Transportation to Storage Reservoir, ARC-APEC-Beijing, Module 4, 2006; http://science.uwaterloo.ca/~mauriced/earth691-duss/CO2_Materials_From_ARC_APEC_Beijing_2006/CarSeq_Module4.pdf.

pipeline. When CO₂ remains in the dense phase, operators can revert to pumping rather than compression to achieve the higher pressure needed.

According to Wong, **pipelining** is currently the most economical method of transporting large quantities of CO₂, and therefore the preferred option. There are currently some 2,400 km of large CO₂ pipelines in operation, most of which are in the USA. In addition, there are some 700 km of lateral pipelines, which distribute CO₂ from the main lines. Altogether there are some 3,100 km of CO₂ pipelines worldwide, with a capacity of 44.7 million tonnes per year of CO₂. These pipelines transport CO₂ in the supercritical or dense phase. In 2006 the estimated cost to construct a pipeline was \$20,989/inch-km (“inch” refers to pipe diameter), with an additional cost of \$3,100/km for maintenance and lines built near population centers or over difficult terrain that tend to be most costly. The estimated annual transportation cost is **\$1.5-\$2/tonne of CO₂ per 100 km** for a mass flow rate of 2.16 million tonnes of CO₂ per year (~5900 tonnes/day). Wong’s range is consistent with the mathematical model for pipeline transport costs shown in the figure below, as published by McCollum and Ogden in 2006.⁶⁵



⁶⁵ McCollum DL, Ogden JM. Techno-Economic Models for Carbon Dioxide Compression, Transport, and Storage. Institute of Transportation Studies, U.C. Davis, October 2006, Figure 8; http://pubs.its.ucdavis.edu/download_pdf.php?id=1047.

The **railway system** has a large carrying capacity that enables it to handle large volumes of bulk commodities over long distances. CO₂ can be transported in specially developed tank cars that are approved to transport liquid CO₂ at a pressure of 2.6 MPa (25.7 atm). However, there is no large scale CO₂ transport by railway at this point. Rail transport will only become a competitive transport option if the logistics can fit the volumes in the existing railway system. However, loading and unloading infrastructure and temporary CO₂ storage would also have to be included and would be costly. One estimate by Odenberger⁶⁶ was that rail transport costs could be as low as **\$2.2/tonne of CO₂ per 100 km**, but this cost did not include any loading and unloading infrastructure or temporary CO₂ storage, meaning that the actual cost would be higher. Often rail lines do not extend to CO₂ source and storage sites, and fitting these sites with the existing rail system is logistically complicated and problematic. If a new railway line had to be laid, the cost would be still higher.

Liquefied CO₂ can be transported in motor carriers such as **tank trucks** with trailers and stored in cryogenic vessels. Tank trucks are flexible, adaptable and reliable means for transporting CO₂, but are much more expensive than pipelining – roughly \$3.5 per km for a 15-20 tonne truck with the truck returning empty, or about **\$17/tonne of CO₂ per 100 km** or farther. There is also boil-off loss during truck transport, which can be as high as 10% of the CO₂ depending on the length of time the liquid CO₂ is kept in the truck, typically at 1.7 MPa (16.8 atm) and -30 °C.

Ships can be used for long distance transport of CO₂ across oceans. Smaller dedicated CO₂ ships are in operation today. Such ships are up to 1,500 m³ in size, and the transport pressure is about 1.4-2 MPa (13.9-19.8 atm). These ships are not suitable for large-scale ship-based transport of CO₂ because at these pressures the ship must be constructed as a pressure vessel, which makes costs very high. Lower pressure is required for enlarged storage and ship tanks. Currently there is no large ship suited to carrying CO₂ at low pressure, but liquid petroleum gas (LPG) tankers could be used for CO₂ transport.

***In situ* Carbon Capture.** The cost of transporting captured CO₂ to a distant site is reduced essentially to zero if the gas can be captured at the same location where it is to be used, stored, or re-purposed. Unfortunately, power plants are rarely located conveniently atop geological formations (**Section 3.5.1**) or mineral formations (**Section 3.5.2**) that are suitable for conventional bulk-gas long-term storage. However, if a mass of carbon dioxide exactly equivalent to the mass of CO₂ released in the flue gas by a distant power plant can be extracted from the atmosphere by an extraction plant located atop an appropriate storage site, then the net carbon footprint is the same as if the CO₂ had been directly captured from the flue gas emitted by the distant power plant and then transported to the storage site via pipeline or truck. This allows CO₂ capture plants to be sited in locations having ideal solar energy and storage conditions, anywhere in the world, without regard to the location of the original source(s) of the CO₂ emissions. In such cases, we are allowing the atmosphere to provide most of the CO₂ transport function for free.

⁶⁶ Odenberger M, Svensson R. Transportation systems for CO₂ – Application to carbon sequestration. Chalmers University of Technology, Goteborg, Sweden, 2003, 48 pp; <http://www.entek.chalmers.se/~klon/msc>.

3.5 Carbon Storage

Carbon capture and storage (CCS) (or carbon capture and sequestration) is the process of capturing waste carbon dioxide (CO₂) from large point sources, such as fossil fuel power plants, transporting it to a storage site, and permanently depositing it where it cannot quickly re-enter the atmosphere, normally an underground geological formation.⁶⁷ The aim is to prevent the release of large quantities of CO₂ into the atmosphere from fossil fuel use in power generation and other industries. CCS is a potential means of mitigating the contribution of fossil fuel emissions to global warming and ocean acidification.

Long-term storage of captured CO₂ is typically envisaged either in deep geological formations (**Section 3.5.1**) or chemically combined in the form of mineral carbonates (**Section 3.5.2**). Deep ocean storage⁶⁸ of free (uncontainerized) CO₂ is no longer considered feasible because it greatly increases the problem of ocean acidification. Continental geological formations are currently considered the most promising sequestration sites. The National Energy Technology Laboratory (NETL) has reported that North America has enough storage capacity of this type to accommodate more than 900 years' worth of carbon dioxide at current production rates.⁶⁹

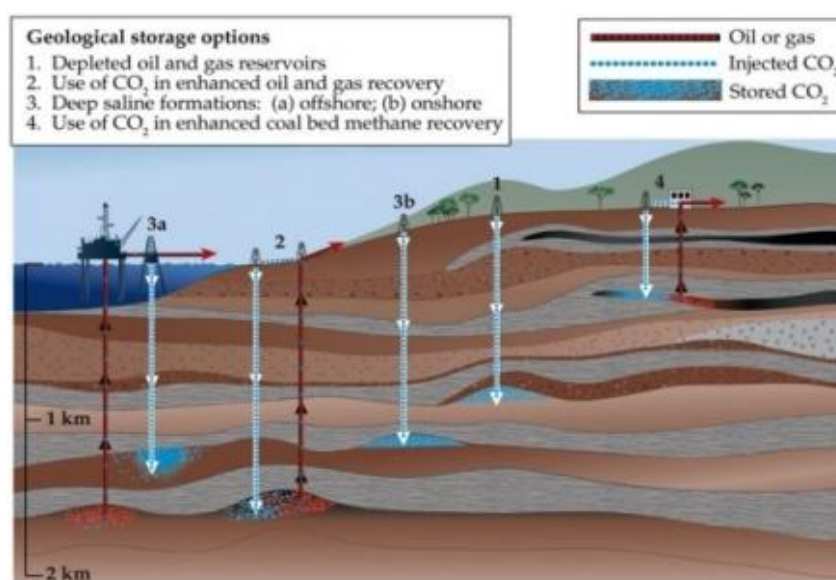
⁶⁷ http://en.wikipedia.org/wiki/Carbon_capture.

⁶⁸ Herzog H, Caldeira K, Adams E. Carbon sequestration via direct injection. RWOS 41, 2001; http://dge.stanford.edu/DGE/CIWDGE/labs/caldeiralab/Caldeira_research/pdf/Herzog_Caldeira_Adams_2001.pdf.

⁶⁹ NETL 2007 Carbon Sequestration Atlas; http://www.netl.doe.gov/technologies/carbon_seq/refshelf/atlas/index.html.

3.5.1 Geological Carbon Storage

Geological storage, also known as geo-sequestration, involves injecting carbon dioxide, generally in supercritical form, directly into underground geological formations. Oil fields, gas fields, saline formations, unmineable coal seams, and saline-filled basalt formations have been suggested as storage sites.⁷⁰ Various physical (e.g., highly impermeable cap rock) and geochemical trapping mechanisms would prevent the CO₂ from escaping to the surface. Approximately 30 to 50 million metric tonnes of CO₂ are injected annually into declining oil fields to increase oil recovery in the United States (**Section 3.2**). This option is attractive because the geology of hydrocarbon reservoirs is generally well understood and storage costs may be partly offset by the sale of additional oil that is recovered.



A major safety concern is the possible leakage of stored CO₂. For well-selected, well-designed and well-managed geological storage sites, IPCC estimates that risks are comparable to those associated with current hydrocarbon activity.⁷¹ CO₂ could be trapped for millions of years, and although some leakage occurs upwards through the soil, well-selected storage sites are likely to retain over 99% of the injected CO₂ over 1000 years.⁷² Leakage through the injection pipe is

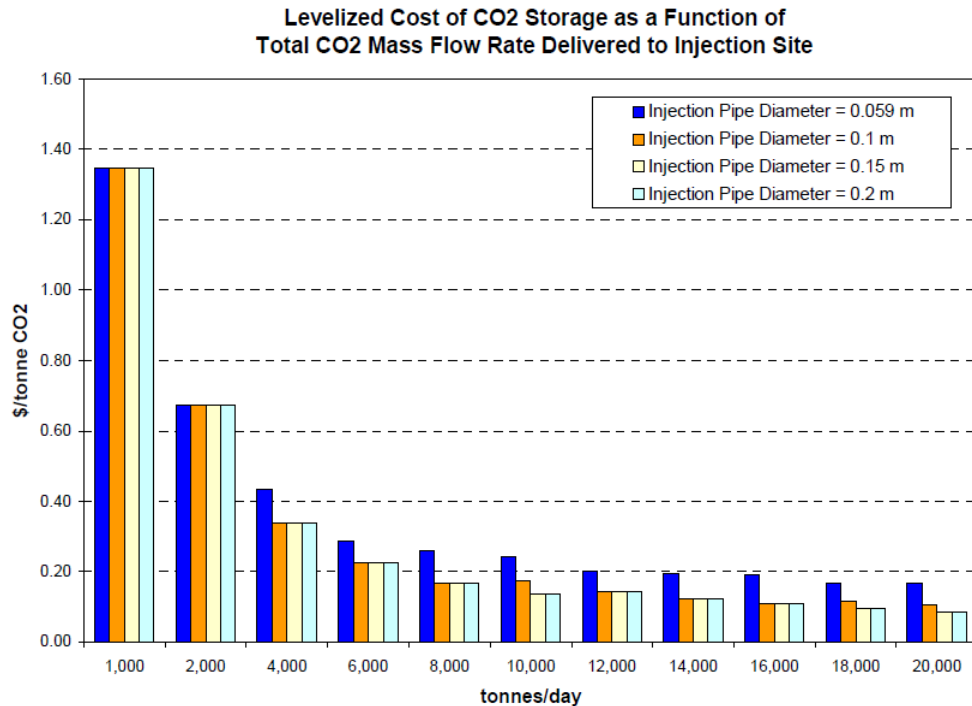
⁷⁰ 2010 Carbon Sequestration Atlas of the United States and Canada, Third Edition, NETL, U.S. Department of Energy, 2010; <http://large.stanford.edu/courses/2010/ph240/chenw2/docs/2010atlasIII.pdf>.

⁷¹ IPCC Special Report: Carbon Dioxide Capture and Storage Technical Summary, Intergovernmental Panel on Climate Change; http://www.ipcc.ch/pdf/special-reports/srccs/srccs_technicalsummary.pdf.

⁷² Global Status of BECCS Projects 2010 - Storage Security; <http://www.globalccsinstitute.com/publications/global-status-beccs-projects-2010/online/27051#storage-security>.

probably a greater risk. Although the injection pipe is usually protected with non-return valves to prevent release during a power outage, there is still a risk that the pipe itself could tear and leak due to the high pressure. For example, a modest release of CO₂ from a pipeline under a bridge during the Berkel en Rodenrijs incident in December 2008 resulted in the deaths of some ducks sheltering there,⁷³ and a few other instances of CO₂ leakage-related deaths are known.⁷⁴

EOR (Enhanced Oil Recovery; **Section 3.2**) gas sequestration is mostly attractive because it is extremely cheap – usually under **\$1/tonne CO₂**, as estimated by McCollum and Ogden⁷⁵ as a function of total CO₂ mass flow rate delivered to the injection site (chart, below).



⁷³ <http://www.berkelenrodenrijs.net/main.php?lees=3329>.

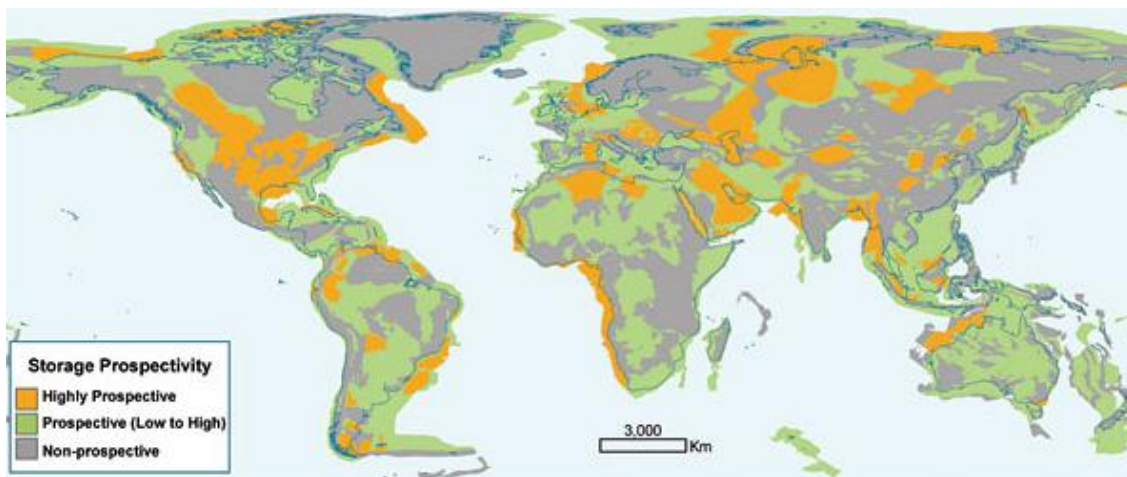
⁷⁴ In 1986 a large leakage of naturally sequestered CO₂ rose from Lake Nyos in Cameroon and asphyxiated 1,700 people. While the carbon had been sequestered naturally, some commentators point to the event as evidence for the potentially catastrophic effects of sequestering carbon artificially. The Lake Nyos disaster resulted from a volcanic event, which very suddenly released as much as a cubic kilometer of CO₂ gas from a pool of naturally occurring CO₂ under the lake in a deep narrow valley. The location of this pool of CO₂ is not a desirable site to inject or store CO₂, and this pool was not known about nor monitored until after the occurrence of the natural disaster. See http://www.forbes.com/2008/10/06/carbon-sequestration-biz-energy-cx_wp_1007capture.html.

⁷⁵ McCollum DL, Ogden JM. Techno-Economic Models for Carbon Dioxide Compression, Transport, and Storage. Institute of Transportation Studies, U.C. Davis, October 2006, Figure 9; http://pubs.its.ucdavis.edu/download_pdf.php?id=1047.

Other sources⁷⁶ put the cost of geological storage in saline formations or depleted oil or gas fields in the range of **\$0.50-\$8/tonne CO₂** injected, plus an additional \$0.10-\$0.30/tonne for monitoring costs.

Geologic sequestration typically involves storage in old oil fields, natural gas reservoirs, deep saline aquifers and unmineable coal beds, hundreds to thousands of meters underground. Viable locations must have a cap rock, or an impermeable layer above the reservoir shaped like an upside-down bowl, that traps the gas and keeps it from escaping.

The map below shows the locations of potential carbon dioxide storage regions around the world.⁷⁷ There appear to be many useful siting opportunities. Estimates of worldwide storage capacity range from 2000-10,000 billion tonnes of carbon dioxide, equal to 50-250 years of global anthropogenic CO₂ production at current rates, according to the Intergovernmental Panel on Climate Change (IPCC) in its report on carbon capture and storage.

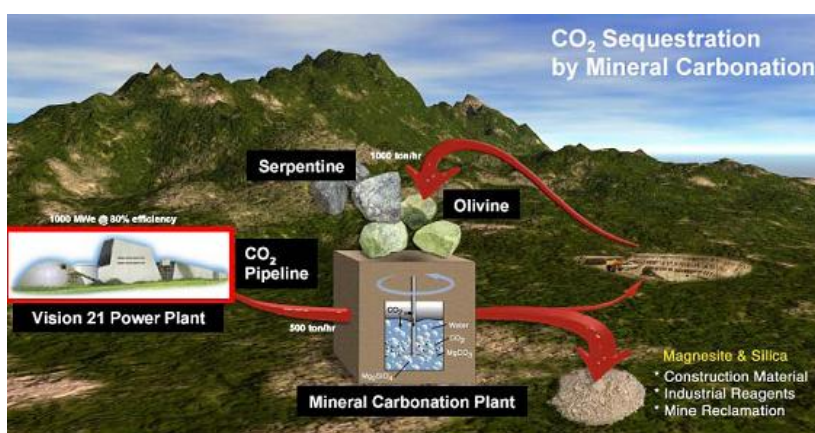


⁷⁶ http://en.wikipedia.org/wiki/Carbon_capture.

⁷⁷ Annie Jia, "Researchers examine carbon capture and storage to combat global warming," Stanford Report, 13 June 2007; <http://news.stanford.edu/news/2007/june13/carbon-061307.html>.

3.5.2 Carbon Storage in Minerals

Mineral storage of chemically fixated carbon dioxide is another theoretical, but apparently very costly, alternative.⁷⁸ Geologists have mapped 6,000 miles of large rock formations in the United States containing minerals that react naturally with carbon dioxide to form solid minerals, a process called mineral carbonation that could make for an ideal storage mechanism. In this process, CO₂ is exothermically reacted with available metal oxides which in turn produces stable carbonates. The process occurs naturally over many years and produces much surface limestone. The carbonation rate can be made faster by reacting at higher temperatures and/or pressures, or by pre-treatment of the minerals, but that requires significant additional energy. The IPCC estimates that a power plant using mineral storage of carbon will need 60%-180% more energy than a power plant without capture.⁷⁹



In situ mineral sequestration is a process in which highly pressurized (super-critical) carbon dioxide is pumped into basaltic rock formations in the earth. These basaltic rock formations are rich in mineral silicates that react with CO₂ to form mineral carbonates or bicarbonates. This is an

exothermic and, thus, thermodynamically favorable reaction that runs deep below ground, sequestering CO₂ in a mineral form.⁸⁰ *Ex situ* mineral sequestration is the reaction of carbon dioxide (CO₂) with minerals to form stable carbonates above ground. It involves laboratory techniques that catalyze the dissolution of minerals to release cations, which may then react with dissolved CO₂ to form geologically stable carbonates. The two main types of rock with which the CO₂ interacts are forsterite rock, which is low in magnesium concentration, and serpentine rock, which is high in magnesium concentration – and each of which reacts with the CO₂ differently.

⁷⁸ CO₂ Mineral Sequestration Studies in US, National Energy Technology Laboratory, 1998; http://www.netl.doe.gov/publications/proceedings/01/carbon_seq/6c1.pdf. See also: "Rocks Found That Could Store Greenhouse Gas," LiveScience, 9 March 2009; <http://www.livescience.com/3364-rocks-store-greenhouse-gas.html>.

⁷⁹ IPCC Special Report on Carbon Dioxide Capture and Storage (IPCC, 2005), prepared by working group III of the Intergovernmental Panel on Climate Change, Cambridge University Press; http://www.ipcc.ch/pdf/special-reports/srccs/srccs_wholereport.pdf.

⁸⁰ Lackner KS. Climate change. A guide to CO₂ sequestration. Science. 2003 Jun 13;300(5626):1677-8; <http://www.sciencemag.org/content/300/5626/1677.long>.

Lackner gives a theoretical estimate of less than \$10/tonne CO₂ for an ideal realization of this process, covering mining and preparation costs but omitting the cost of capturing and transporting the CO₂. One experimental reality: the CarbFix project's pilot project⁸¹ has cost \$11 million to sequester 2000 tons of CO₂ in 9 months, a **\$5500/tonne CO₂** cost that lies far above Lackner's theoretical estimate – though admittedly pilot programs usually cost much more than industrial implementation because the knowledge gained from a pilot program can allow costs to be markedly reduced. Early estimates⁸² put mineral sequestration at about **\$70/tonne CO₂** sequestered. If future research can reduce pre-treatment costs and overcome separation problems, the costs could theoretically be reduced to \$30/tonne of carbon dioxide sequestered. But right now the total estimated cost of this process is about **\$120/tonne CO₂**.⁸³

⁸¹ The Earth Institute at Columbia University, International Conference on CO₂ sequestration processes, First Science, 2009; http://www.firstscience.com/home/news/atmospheric-science/international-conference-on-co2-sequestration-processes-page1-1_67717.html.

⁸² Herzog H, Eliasson B, Kaarstad O. Capturing greenhouse gases. *Sci. Am.* 282(2002):72-80.

⁸³ "Mineral Basalt Sequestration," Mission 2013 Carbon Sequestration, MIT; <http://igutek.scripts.mit.edu/terrascopes/?page=Basalt>.

4. NEW APPROACH: Molecular Filters

The potential value of using motorized micromachines to assist in CO₂ capture has already been illustrated experimentally.⁸⁴ Here, we propose to achieve direct atmospheric carbon capture using a new technique based on atomically precise nanomachines called “molecular filters” that maximize the efficiency of molecular capture and transport across barrier membranes. Molecular filters can be fabricated in commercially useful quantities using molecular manufacturing methods such as nanofactories (**Section 1**).

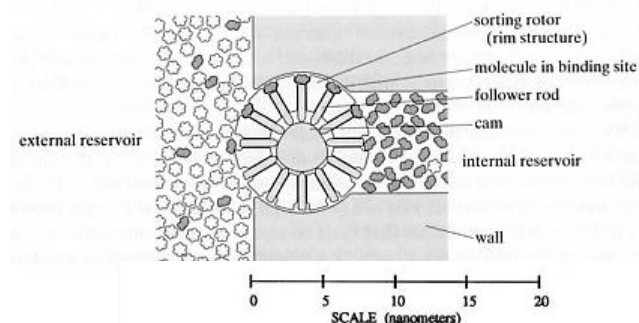
The most efficient of all modes of molecular transport involves receptor sites capable of recognizing and selectively binding specific molecular species. Many receptors reliably bind only a single molecular type. Other receptors, such as sugar molecule transporters in biochemistry, can recognize and transport several related sugar molecule types. In nanomechanical systems, artificial binding sites with a wide variety of size, shape, and electronic charge characteristics can be created and employed in the construction of a range of highly efficient molecular sortation and transport devices.

Basic molecular filter design using sorting rotors with binding sites is discussed in **Section 4.1**, followed by an analysis of a surprisingly simple CO₂ binding site that may be very efficient in separating CO₂ from all other atmospheric constituents under direct capture conditions (**Section 4.2**). We then provide a high-level description of one possible molecular filter systems for the direct filtration of CO₂ from ambient air (**Section 4.3**), followed by a description of a simple modular CO₂ capture plant that could be installed almost anywhere in the world (**Section 5**).

⁸⁴ Uygun M, Singh VV, Kaufmann K, Uygun DA, de Oliveira SDS, Wang J. Micromotor-Based Biomimetic Carbon Dioxide Sequestration: Towards Mobile Microscrubbers. *Angew. Chem. Int. Ed.* (4 Sep 2015); <http://onlinelibrary.wiley.com/doi/10.1002/anie.201505155/abstract>. See also: Mary Beth Griggs, “Tiny Motorized Robots Can Clean Carbon Dioxide Out of Seawater,” *Popular Science*, 23 September 2015; <http://www.popsci.com/tiny-motorized-robots-clean-carbon-dioxide-out-seawater>.

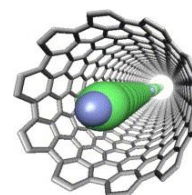
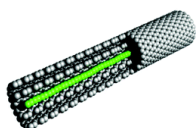
4.1 Basic Molecular Filter Design

The molecular filter consists of a barrier or wall penetrated by one or more nanomechanical devices that act as molecule-specific pumps, analogous to the transporter pumps found on the surfaces of living biological cells. One simple such pump is a nanomechanical device called a “molecular sorting rotor” that is capable of selectively binding molecules from solution and then



transporting these bound molecules against concentration gradients (image, left), moving only the molecules of a specific type (such as CO_2) from one side of the wall to the other. Each pump mechanically transports individual molecules, one by one, through the barrier. The molecular filter is simply a sheet with large numbers of surface-embedded pumps.

The classical sorting rotor illustrated above⁸⁵ is a disk about 10 nm in diameter and about 3 nm thick having 12 binding site “pockets” along the rim that are exposed alternately to the source fluid at left and the receiving chamber at right by the clockwise axial rotation of the disk. (Other designs may have more, or fewer, pockets.) Each pocket selectively binds a specific molecule when exposed to the source fluid at left. The rotor turns clockwise, moving the pocket containing the bound molecule through the wall from left to right. Once the binding site has rotated far enough to expose it to the receiving chamber at right, the bound molecules are forcibly ejected by rods (e.g., polyynes) thrust outward by the cam surface. Note that short polyynes (C_{10}H_2) have been synthesized experimentally inside carbon nanotubes (image, right),⁸⁶ longer polyynes have been assembled inside double-walled carbon nanotubes (image, left),⁸⁷ and isolated 44-carbon-atom polyyne chains (stabilized with end caps) also appear to be stable.⁸⁸ Of course, other means, whether mechanical or electronic, could also be used to reversibly alter the binding site affinity for the transported molecule during the transport process.

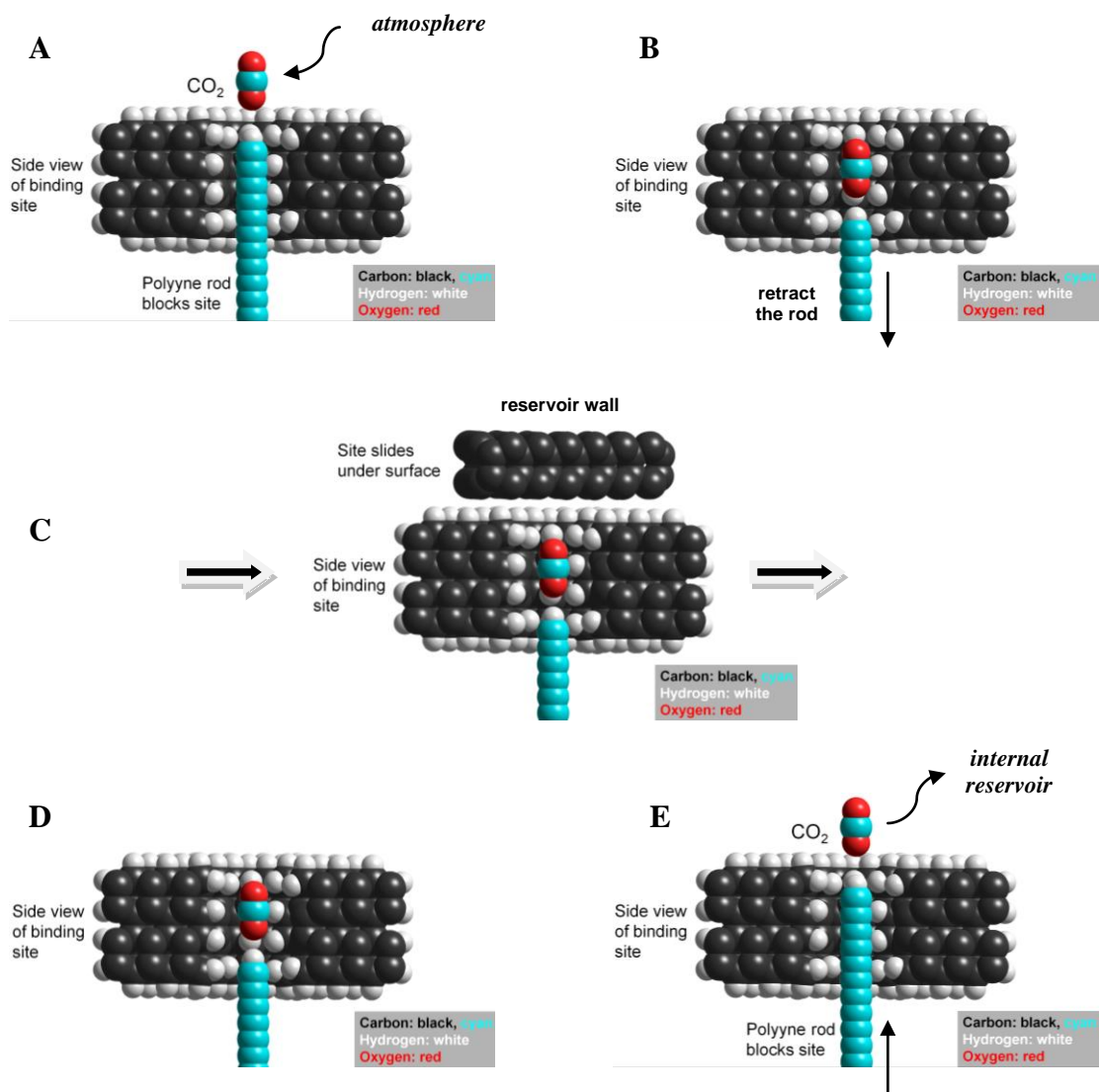


⁸⁵ Drexler KE, *Nanosystems*, Wiley, 1992, Section 13.2.1(a).

⁸⁶ Nishide D, Dohi H, Wakabayashi T, Nishibori E, Aoyagi S, Ishida M, Kikuchi S, Kitaura R, Sugai T, Sakata M, Shinohara H. Single-wall carbon nanotubes encaging linear chain C_{10}H_2 polyyne molecules inside. *Chem Phys Lett*. 2006 Sep 20;428(4-6):356-360; <http://www.sciencedirect.com/science/article/pii/S0009261406010256>.

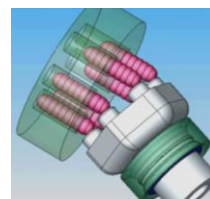
⁸⁷ Zhao C, Kitaura R, Hara H, Irle S, Shinohara H. Growth of linear carbon chains inside thin double-wall carbon nanotubes. *J Phys Chem*. 2011 Jun 7;115(27):13166-13170; <http://pubs.acs.org/doi/abs/10.1021/jp201647m>.

⁸⁸ Chalifoux WA, Tykwinski RR. Synthesis of polyynes to model the sp-carbon allotrope carbyne. *Nat Chem*. 2010;2:967-971; www.nature.com/nchem/journal/v2/n11/full/nchem.828.html.



A specific sequence, focusing on a single binding pocket, is illustrated above. Such molecular pumps generally operate in a four-phase sequence: (1) recognition (and binding) by the transporter of the target molecule from a variety of molecules presented to the pump in the source fluid; (2) translocation of the target molecule through a wall, into the interior of the transporter mechanism; (3) release of the molecule by the transporter mechanism; and (4) return of the transporter to its original condition, outside the wall, so that it is ready to accept another target molecule. Molecular transporters that rely on protein conformational changes are ubiquitous in biological systems.

Mechanical molecular sorting rotors (including the newer “revolver” motif; image, right) can be designed from about 100,000 atoms, comprising ~20,000 atoms for the rotor mechanism with binding sites plus another ~80,000 atoms for the rotor housing and pro rata share of the mechanical drive system. Each complete rotor mechanism might measure roughly 7 nm (wide) x 14 nm (tall) x 14 nm (deep) in size with a mass of about 2×10^{-21} kg



if composed mostly of diamondoid structure. The classic sorting rotor can turn at up to ~86,000 rev/sec which exposes 1 million binding sites per second to the source fluid, giving a conservative rim speed of 2.7 mm/sec, sorting and transporting small molecules at a rate of up to 10^6 molecules/sec assuming laminar flow as in the case of an aqueous source fluid.

The minimum energy required to pump⁸⁹ uncharged molecules is the change in free energy ΔG_c (joules) in transporting the species from one environment having concentration c_1 to a second environment having concentration c_2 , given by:⁹⁰

$$\Delta G_c = k_B T \ln(c_2/c_1) \quad (1)$$

where $k_B = 0.01381$ zJ/K (Boltzmann constant) and T = temperature in kelvins. For example, transport of one uncharged molecule from a low concentration to a high concentration environment across a $c_2/c_1 = 1000$ gradient (typical in biology) costs $\Delta G_c \sim 30$ zJ/molecule at 300 K. Pumping against a more aggressive $c_2/c_1 = 10^6$ concentration gradient costs $\Delta G_c \sim 60$ zJ/molecule.

Besides the compression energy ΔG_c , there is also less disorder (lower entropy) in the world when two gases are separated than when they share a common volume, and the entropy of the world can only be decreased by the expenditure of energy. Thermodynamics predicts the minimum amount of energy ΔG_s needed to achieve such a separation, a value that depends on the absolute temperature and the initial and final concentrations and pressures. If X_{CO_2} is the mole fraction of carbon dioxide, and if all of the captured CO_2 is pure and all of the CO_2 in the original mixture is removed, then the minimum energy per unit mass of CO_2 removed is given by:⁹¹

$$\Delta G_s = -k_B T [X_{CO_2} \ln(X_{CO_2}) + (1-X_{CO_2}) \ln(1-X_{CO_2})] / X_{CO_2} \quad (2)$$

For air capture of CO_2 at $T = 300$ K, $X_{CO_2} = 0.0004$ (400 ppm) and $\Delta G_s = 36.6$ zJ/molecule CO_2 .

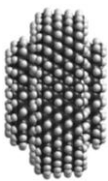
The total energy of CO_2 compression and separation is therefore:

$$\Delta G_{CO_2} = \Delta G_c + \Delta G_s. \quad (3)$$

⁸⁹ If molecules are allowed to flow in the reverse direction from higher concentration to lower concentration, then the sorting rotor becomes a pressure-driven motor, selectively transporting just the target molecular species from right to left while generating power rather than consuming it.

⁹⁰ Lackner KS. Capture of carbon dioxide from ambient air. Eur. Phys. J. Special Topics 176(2009):93-106, Eqn. (1), p. 95; http://death.ocf.berkeley.edu/~step/Journal_Club/paper4_02092010.pdf.

⁹¹ "Direct Air Capture of CO_2 with Chemicals," American Physical Society, 1 June 2011; <http://www.aps.org/policy/reports/assessments/upload/dac2011.pdf>.



If we plausibly assume the use of incommensurate-surfaced molecular bearings (image, left) exhibiting superlubricity⁹² inside the rotor mechanism, then the primary source of energy loss is speed-dependent viscous drag of the rotor surface as it moves through the fluid environment on either side of the barrier wall. For a fluid environment having the approximate viscosity of water ($\sim 10^{-3}$ kg/m-sec at 20 °C) on both sides of the wall, the sorting rotor described and operated as above has an estimated continuous drag power loss of 10^{-16} W while transporting 10^6 molecules/sec,⁹³ or ~ 0.1 zJ/molecule transported. At low speeds, drag power scales linearly with viscosity, so rotors turning in air at STP (viscosity $\sim 0.02 \times 10^{-3}$ kg/m-sec) for the purpose of CO₂ extraction from the atmosphere would dissipate ~ 0.002 zJ/molecule transported. This is 10^{-2} to 10^{-4} of the required ΔG_{CO_2} transport energy, hence this source of energy loss may be regarded as negligible in the carbon capture application.

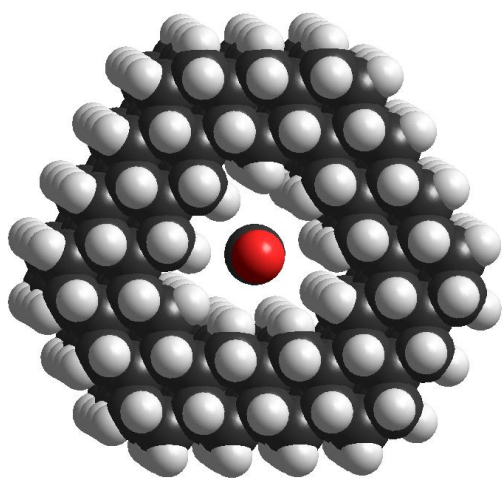
CO₂ gas molecules, having passed through the sorting rotor and being collected in the internal reservoir at ~ 100 atm pressure, are now ready for export to the sequestration system.

⁹² Dienwiebel M, Verhoeven GS, Pradeep N, Frenken JWM, Heimberg JA, Zandbergen HW. Superlubricity of graphite. *Phys. Rev. Lett.* 2004; 92:126101. Erdemir A, Martin J-M, eds., *Superlubricity*, Elsevier, 2007; <http://www.sciencedirect.com/science/book/9780444527721>. Liu Z, Yang J, Grey F, Liu JZ, Liu Y, Wang Y, Yang Y, Cheng Y, Zheng Q. Observation of superlubricity in microscale graphite. *Phys. Rev. Lett.* 2012; 108:205503.

⁹³ Drexler KE, *Nanosystems*, Wiley, 1992, Section 13.2.1(e).

4.2 Binding Site Design for Carbon Dioxide

The strength of the binding of the target molecule to the artificial receptor site can be designed to be sufficient to achieve high occupancy of all pockets (e.g., 99%) at the given relatively low speeds of rotor rotation. The mechanical energy consumed to force the target molecule out of its binding site into the receiving chamber is delivered from the cam to the rods, but this energy is largely returned with minimal losses to the cam on the source side by the compression of the rods during the binding of the target molecule to the receptor, a process that regenerates mechanical energy. The artificial receptors are best designed for high affinity binding in the presence of a dominant background of quite different molecules. Analogies with antibodies suggest that a rotor with binding pockets of this type could deliver a product stream with impurity fractions on the order of 10^{-4} to 10^{-9} (i.e., 99.99% purity or better) depending on affinities, specificities, and the concentrations of the effectively competing ligands.⁹⁴ A detailed computational modeling and simulation effort will be required to create ideal selective binding site designs for CO₂ and also for possible alternative specific target atmospheric molecules of interest including NO_x, SO_x, CO, N₂, O₂, H₂O, H₂S, H₂, Ar, and other competing molecular species.



However, even an extremely simple binding site may be surprisingly effective. The figure at left⁹⁵ is an example of a very simple 420-atom binding site (C = black, H = white, O = red) that does not employ strong covalent bonds between the site and the target molecule. To make this binding site, we took a thin sheet of hydrogen-terminated diamond with the C(111) lattice on the top and bottom horizontal faces, cut out a hexagonal perimeter with the C(100) lattice on all six vertical sides, punched a small hole in the center, and hydrogenated the inner walls of the pore, making a 420-atom (C₂₄₀H₁₈₀) all-hydrocarbon binding site. Such a structure could readily be nanofabricated as a solid block using a specific sequence of positionally-controlled tip-based

mechanosynthetic reactions.⁹⁶ The image shows a single CO₂ molecule nestled snugly inside the hydrogen-terminated pore, which employs only van der Waals attractions to provide the necessary binding interaction.

⁹⁴ Drexler KE, Nanosystems, Wiley, 1992, Section 13.2.2(b).

⁹⁵ Design by Ralph C. Merkle; personal communication, 2015.

⁹⁶ For mechanosynthesis theory work generally, see: Freitas RA Jr, Merkle RC. A Minimal Toolset for Positional Diamond Mechanosynthesis. *J Comput Theor Nanosci.* 2008 May;5:760-861; <http://www.molecularassembler.com/Papers/MinToolset.pdf>. For experimental mechanosynthesis work, see: Sugimoto Y, Pou P, Custance O, Jelinek P, Abe M, Perez R, Morita S. Complex Patterning by Vertical Interchange Atom Manipulation Using Atomic Force Microscopy. *Science.* 2008 Oct 17;322:413-417; <http://www.sciencemag.org/content/322/5900/413.full>.

To assess the performance of our simple binding site for atmospheric carbon capture, we first list 38 major and trace atmospheric constituents typically found in non-urban air along with their fractional molar concentration,⁹⁷ then employ molecular mechanics methods using the AMBER99 force field⁹⁸ (known to be highly parameterized for nonbonded interactions, using the computational tools of quantum chemistry) to estimate the binding energy (E_b) of the pore for each molecular species (**Table 1**). This is calculated as the difference between the total energy of the binding site with the molecule bound inside it and the sum of the total energies of the empty binding site and the isolated molecule. The fractional binding site occupancy of a molecular species, or $\exp(-E_b/k_B T)$ where $k_B = 8.625 \times 10^{-5}$ eV/molecule-K and ambient temperature $T = 300$ K, is then multiplied by the fractional atmospheric molar concentration (f_{air}) of that molecule, then renormalized to obtain the percentage of each molecular species likely to pass through the binding site filtration mechanism in the first pass. Our simple binding site pore has very high affinity for CO_2 and even higher affinity for eight other molecules, but those other eight molecules are present in normal air at such low concentrations that the resulting gaseous filtrate is ~99% pure CO_2 , with just ~1% of O_2 and N_2 and mere traces of everything else.

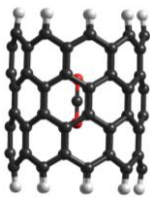
Filtrate purity will vary slightly with ambient environmental temperature (e.g., 99.26% CO_2 at 290 K, 98.49% CO_2 at 310 K). Note also that a single-stage filter of this type applied to flue gas from a coal-fired power plant would produce filtrate gas containing 52% CO_2 and 48% SO_2 ; applying a second stage of the same filters to the first-stage filtrate would extract essentially all of the SO_2 , since the second-stage filtrate would be 99.6% SO_2 and 0.4% CO_2 .

⁹⁷ Killinger DK, Churnside JH, Rothman LS. Chapter 44. Atmospheric Optics. Bass M, Van Stryland EW, Williams DR, Wolfe WL, eds., Handbook of Optics, Volume I: Fundamentals, Techniques, and Design, Second Edition, McGraw-Hill, Inc., New York, 1995, pp. 44.1-44.50. Weast RC, Handbook of Chemistry and Physics, 49th Edition, CRC, Cleveland OH, 1968.

⁹⁸ Cornell WD, Cieplak P, Bayly CI, Gould IR, Merz KM Jr, Ferguson DM, Spellmeyer DC, Fox T, Caldwell JW, Kollman PA. A second generation force field for the simulation of proteins, nucleic acids, and organic molecules. J Am Chem Soc. 1995;117: 5179-5197; http://homepage.univie.ac.at/mario.barbatti/papers/method/amber_1995.pdf. Wang J, Cieplak P, Kollman PA. How well does a restrained electrostatic potential (RESP) model perform in calculating conformational energies of organic and biological molecules? J Comput Chem. 2000;21(12):1049-1074; http://banana.cns.msu.edu/ffamber/pdfs/wang_amber99_2000jcc.pdf.

Table 1. Gas molecule concentration in ambient U.S. dry atmosphere, their binding energy in a simple pore of a molecular filter, and their concentration in the resulting filtrate.

Atmospheric Molecular Component	Fractional Atmospheric Concentration (f_{air})	Amber99 Binding Energy of Molecular Component in Simple Binding Site (E_b)	% Concentration of Air Component in Gas Filtrate
Nitrogen (N ₂)	7.80840 x 10 ⁻¹	-0.2521 eV	0.1386%
Oxygen (O ₂)	2.09460 x 10 ⁻¹	-0.3336 eV	0.8665%
Water vapor (H ₂ O)	~1.00 x 10 ⁻²	-0.2936 eV	0.0088%
Argon (Ar)	9.340 x 10 ⁻³	-0.0586 eV	< 1 ppm
Carbon Dioxide (CO ₂)	3.870 x 10 ⁻⁴	-0.6190 eV	98.9341%
Neon (Ne)	1.818 x 10 ⁻⁵	-0.1021 eV	< 1 ppm
Helium (He)	5.24 x 10 ⁻⁶	-0.0535 eV	< 1 ppm
Methane (CH ₄)	1.79 x 10 ⁻⁶	-0.3210 eV	< 1 ppm
Krypton (Kr)	1.14 x 10 ⁻⁶	-0.0904 eV	< 1 ppm
Hydrogen (H ₂)	5.50 x 10 ⁻⁷	-0.0461 eV	< 1 ppm
Nitrous Oxide (N ₂ O)	3.20 x 10 ⁻⁷	-0.4611 eV	0.0002%
Carbon Monoxide (CO)	1.50 x 10 ⁻⁷	-0.2999 eV	< 1 ppm
Xenon (Xe)	8.70 x 10 ⁻⁸	-0.1028 eV	< 1 ppm
Ozone (O ₃)	2.66 x 10 ⁻⁸	-0.6287 eV	0.0099%
Formaldehyde (H ₂ CO)	2.4 x 10 ⁻⁹	-0.5542 eV	0.0001%
Ethane (C ₂ H ₆)	2.0 x 10 ⁻⁹	-0.6816 eV	0.0058%
Hydrogen Chloride (HCl)	1.0 x 10 ⁻⁹	-0.3833 eV	< 1 ppm
Methyl Chloride (CH ₃ Cl)	7.0 x 10 ⁻¹⁰	-0.6842 eV	0.0022%
Carbonyl Sulfide (OCS)	6.0 x 10 ⁻¹⁰	-0.7324 eV	0.0123%
Acetylene (C ₂ H ₂)	3.0 x 10 ⁻¹⁰	-0.5079 eV	< 1 ppm
Sulfur Dioxide (SO ₂)	3.0 x 10 ⁻¹⁰	-0.7650 eV	0.0216%
Nitric Oxide (NO)	3.0 x 10 ⁻¹⁰	-0.3052 eV	< 1 ppm
Hydrogen Peroxide (H ₂ O ₂)	2.0 x 10 ⁻¹⁰	-0.4974 eV	< 1 ppm
Hydrogen Cyanide (HCN)	1.7 x 10 ⁻¹⁰	-0.5523 eV	< 1 ppm
Nitric Acid (HNO ₃)	5.0 x 10 ⁻¹¹	-0.4311 eV	< 1 ppm
Ammonia (NH ₃)	5.0 x 10 ⁻¹¹	-0.1887 eV	< 1 ppm
Nitrogen Dioxide (NO ₂)	2.3 x 10 ⁻¹¹	-0.5395 eV	< 1 ppm
Hypochlorous Acid (HOCl)	7.7 x 10 ⁻¹²	-0.5970 eV	< 1 ppm
Hydrogen Iodide (HI)	3.0 x 10 ⁻¹²	-0.4993 eV	< 1 ppm
Hydrogen Bromide (HBr)	1.7 x 10 ⁻¹²	-0.4707 eV	< 1 ppm
Hydroxyl radical (OH [•])	4.4 x 10 ⁻¹⁴	-0.3443 eV	< 1 ppm
Hydrogen Fluoride (HF)	1.0 x 10 ⁻¹⁴	-0.2439 eV	< 1 ppm
Chlorine Monoxide (ClO)	1.0 x 10 ⁻¹⁴	-0.6515 eV	< 1 ppm
Formic Acid (HCOOH)	1.0 x 10 ⁻¹⁴	-0.7281 eV	< 1 ppm
Carbonyl Fluoride (COF ₂)	1.0 x 10 ⁻¹⁴	-0.3756 eV	< 1 ppm
Sulfur Hexafluoride (SF ₆)	1.0 x 10 ⁻¹⁴	0.3578 eV	< 1 ppm
Hydrogen Sulfide (H ₂ S)	1.0 x 10 ⁻¹⁴	-0.3699 eV	< 1 ppm
Phosphine (PH ₃)	1.0 x 10 ⁻²⁰	-0.4062 eV	< 1 ppm



The 420-atom binding site design presented above is offered as just one example of a wide range of possibilities. An even simpler binding site based on the (9,0) carbon nanotube (image, left),⁹⁹ similarly evaluated using AMBER, appears to prefer CO₂ (-0.73 eV) over SO₂ (-0.62 eV), with additional binding energies of -0.49 eV (O₂), -0.45 eV (CO), -0.35 eV (H₂O), -0.33 eV (N₂), and -0.06 eV (H₂). There is already widespread interest in using nanotubes for efficient CO₂ capture.¹⁰⁰ An actual binding site that would be used in a molecular filter would necessarily be the result of an extensive design process – validated by higher-quality quantum chemistry simulations – that carefully balanced a large number of competing technical and operational requirements.

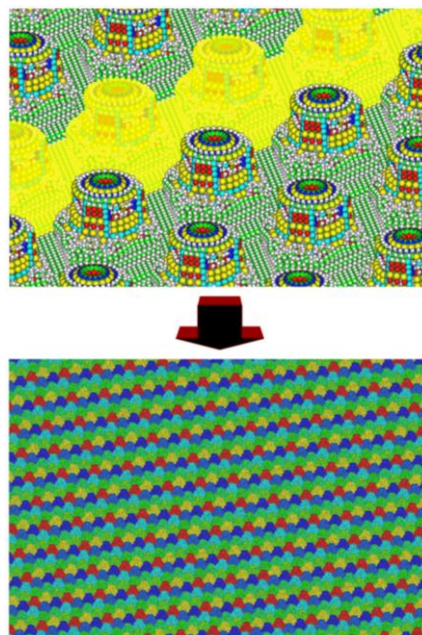
⁹⁹ Design by Ralph C. Merkle; personal communication, 2015.

¹⁰⁰ Rahimi M, Babu DJ, Singh JK, Yang Y-B, Schneider JJ, Müller-Plathe F. Double-walled carbon nanotube array for CO₂ and SO₂ adsorption. *J Chem Phys.* 2015;143:124701; <http://www.ncbi.nlm.nih.gov/pubmed/26429026>.

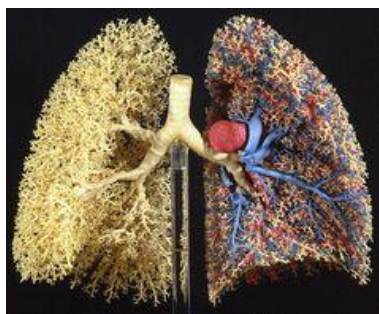
4.3 Filtering Carbon Dioxide Directly from the Atmosphere

Using molecular filters instead of more conventional approaches (**Section 3.3**), carbon dioxide can be extracted directly from the atmosphere at any convenient location on Earth, with the gas thus extracted applied as an economic offset to the effluents of a possibly very distant electrical power plant, either via carbon credits or by other related means.

A large array of sorting rotors (image, right) will be operated as pumps requiring external electrical power input to transport the target molecule in the source fluid, e.g., CO₂ in ambient air, from a relatively low-pressure environment to a high-pressure collection system at the final product target pressure of 100 atm. The current concentration of CO₂ in the atmosphere is about 400 ppm (i.e., 0.04%, 0.0004 atm partial pressure). A single extraction facility cannot appreciably decrease the ambient concentration, so we assume that our source has a fixed concentration of $P_{\text{init}} = 0.0004$ atm throughout the entire filtration process. Some additional design effort will be required to determine the best method for delivering external power to the rotors.



In this scheme, the molecular filter is comprised of sorting rotors tightly packed side by side to form a sheet of adjacent mechanical devices (image, right). The sheet must be of sufficient thickness to withstand pressure differentials on the order of ~ 100 atm without tearing. If the sheet of rotors is rolled into a seamless tube through which extracted CO₂ gas molecules may flow for collection downstream, this requirement is readily achieved by reducing the diameter of the largest branches in the collection system from 1 mm to 10 μm . In that case, the minimum wall thickness of a cylinder wall of radius $R_{\text{cyl}} = 10$ μm made of diamondoid material with a conservative failure strength of $\sigma_w = 10^{10}$ N/m² (~ 0.2 times the failure strength of diamond) that can withstand a pressure differential of $\Delta P = 100$ atm without bursting is $t_{\text{wall}} \geq R_{\text{cyl}} \Delta P / \sigma_w \sim 10$ nm, roughly comparable to the 14 nm thickness of the exemplar sorting rotor housing described in **Section 4.1**. These tubes will be short enough in length to avoid significant energy losses due to Poiseuille fluid flow drag.



The exemplar sorting rotor design includes a channel ~ 5 nm deep that can be employed to carry off the selected gas molecules once they have been selectively removed from the source fluid in which the molecular filter resides. The most efficient filter system architecture has yet to be determined, but might consist of a multiscale branching collection system roughly analogous to the structure of the human lung (image, left) – an architecture that nature has already optimized for efficient gas exchange and transport – but using continuous unidirectional flow rather than the pulsatile flow commonly

employed in biological lungs. The lowest-level branches might possibly be some tens of nanometers in diameter. Filtered gases would pass to progressively larger branches, finally

reaching the uppermost branches measuring on the order of millimeters in diameter, whereupon the gas is emptied into a large macroscale collection plenum for further processing. In sum, the collection system has short initial collector tubes that connect to progressively larger tubes, and the system is operated at 100 atm throughout.

With the gas collecting channel behind each sorting rotor maintained at $P_{\text{final}} = 100$ atm, the sorting rotors will function as pumps over the full pressure range of gas extraction and will require an energy input (e.g., electrical) to drive them forward. Given a constant 0.04% CO_2 concentration ($P_{\text{init}} = 0.0004$ atm) in the input stream and an average environmental temperature of 300 K, then $c_2/c_1 = P_{\text{final}}/P_{\text{init}} = 250,000$ and the rotors will be continuously drawing $\Delta G_{\text{CO}_2} = k_B T \ln(c_2/c_1) + \Delta G_s = 88$ zJ/molecule of CO_2 transported. Since the product is already compressed to the desired 100-atm final pressure, there is no requirement for any further compression.

In summary, using a high-pressure molecular filter a single facility located almost anywhere in the world can extract unlimited quantities of CO_2 directly out of the atmosphere for an energy cost of about 88 zJ/molecule (~ 1200 kJ/kg CO_2), delivered at a 100 atm exhaust pressure and 99%+ purity.

5. Simple Nanofactory-Based Atmospheric CO₂ Capture System

As a simple scaling exercise, consider the design of a small atmospheric CO₂ capture plant with a target of extracting $m_{\text{plant}} = 1 \text{ tonne/day of CO}_2 \text{ from ambient air}$ with zero carbon footprint, powered by *in situ* photovoltaics and located in a high-solar-intensity low-latitude installation site. This exercise provides a crude estimate of the Balance of Plant (BOP) costs for a CO₂ capture plant built around a core mechanism employing inexpensive atomically precise molecular filters, but it is only a scaling study and not a complete plant design.

We present a scaling design for an exemplar CO₂ capture plant in **Section 5.1**, then apply this design to the broader challenge of global climate change in **Section 5.2**.

5.1 An Exemplar CO₂ Capture Plant Scaling Design

From the outside, our CO₂ capture plant would look like a long, low-ceiling 10,000 SF rectangular (4:1) metal shed with rooftop solar panels.



The basic design analysis is as follows.

5.1.1 Target Processing Rate

To extract 1 tonne/day of CO₂ from ambient air, the required processing rate is:

$$(1 \text{ tonne CO}_2/\text{day}) (1000 \text{ kg CO}_2/\text{tonne}) / (86400 \text{ sec}/\text{day}) = 1.16 \times 10^{-2} \text{ kg CO}_2/\text{sec}$$

or

$$(1.16 \times 10^{-2} \text{ kg CO}_2/\text{sec}) (6.023 \times 10^{23} \text{ molecules CO}_2/\text{mole}) / (0.044 \text{ kg CO}_2/\text{mole}) = 1.58 \times 10^{23} \text{ molecules CO}_2/\text{sec}.$$

5.1.2 Sorting Rotor Power Requirement

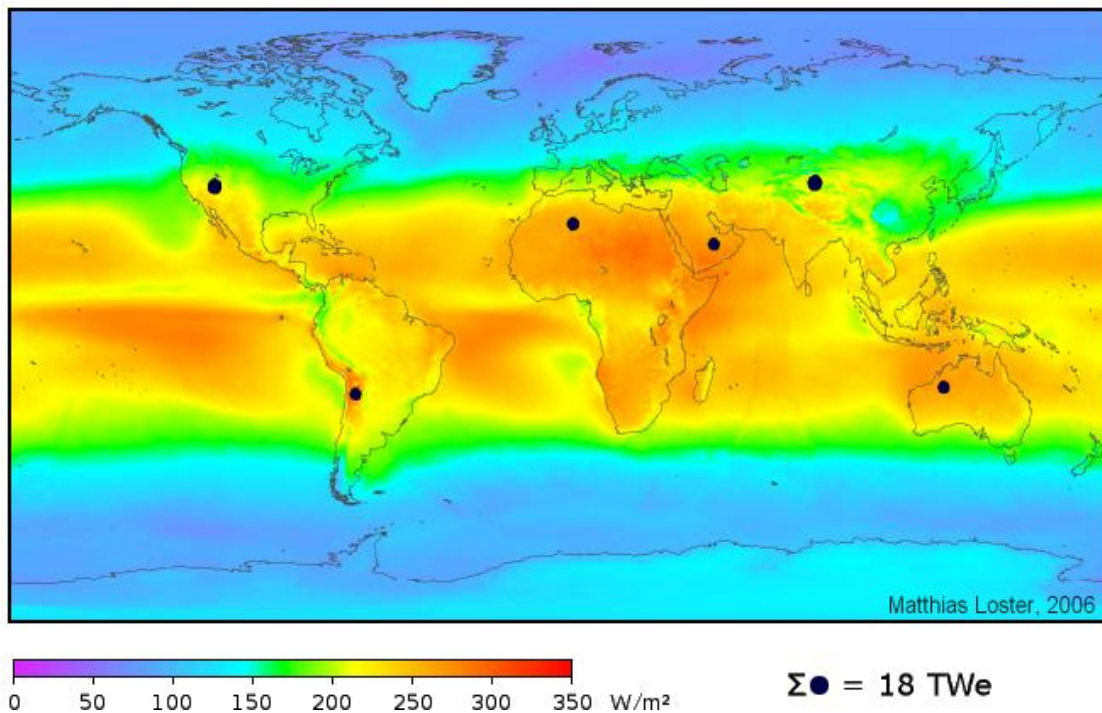
The required power input to drive all the sorting rotors for capture of CO₂ from 400 ppm air, purify it, and output pure CO₂ gas at 100 atm, at an energy cost of $\Delta G_{\text{CO}_2} \sim 88 \text{ zJ/molecule}$ of CO₂ transported (**Section 4.3**), is:

$$(1.58 \times 10^{23} \text{ molecules CO}_2/\text{sec}) (88 \times 10^{-21} \text{ J/molecule CO}_2) \sim 13,900 \text{ watts}.$$

5.1.3 Solar Panel Area

The map below (**Figure 1**) shows worldwide solar irradiance averaged over 3 years from 1991-1993 for 24 hours/day, taking into account the cloud coverage available from weather satellites.¹⁰¹ Solar areas defined by the dark disks could provide 18 terawatts (electrical), more than the world's total primary energy demand in 2009, assuming only 8% conversion efficiency.

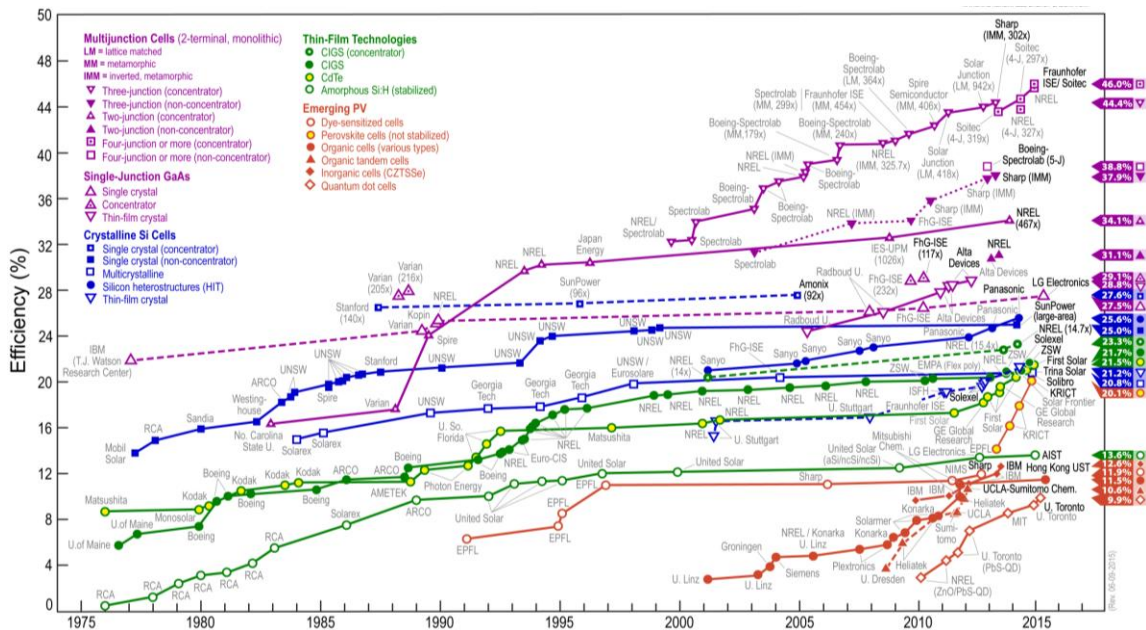
Figure 1. Average total solar irradiance at Earth's surface.



However, data tabulated by the National Renewable Energy Laboratory (NREL) (**Figure 2**) indicate that crystalline silicon solar cells have improved in photoelectric conversion efficiency from ~14% in the mid-1970s to the 21%-25% range by 2015. This efficiency will probably improve a bit more by the future decade in which our CO₂ capture plants would be built.

¹⁰¹ http://en.wikipedia.org/wiki/File:Solar_land_area.png.

Figure 2. Best research-cell efficiencies for photovoltaic energy generation (NREL).¹⁰²



Conservatively assuming a 20% efficiency is available from crystalline silicon photovoltaics, then the rotor power requirement for the CO₂ capture plant may be supplied with a zero carbon footprint by a rooftop solar power array having 6 hours/day of daytime sunlight operation and effective daytime ambient lighting of ~300 W/m² at high-solar-intensity low-latitude installation sites,¹⁰³ of areal size:

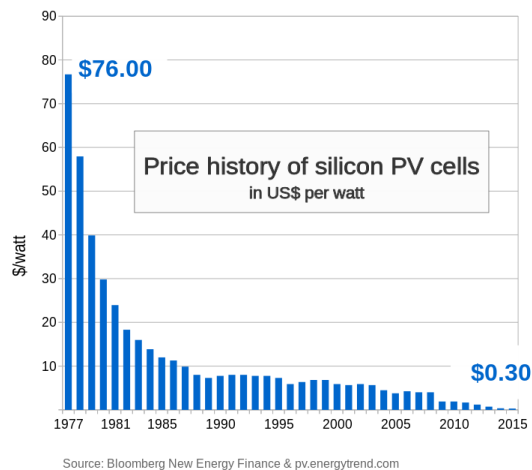
$$a_{\text{plant}} = (13,900 \text{ W}) / [(20\%) (6 \text{ hr} / 24 \text{ hr}) (300 \text{ W/m}^2)] = 927 \text{ m}^2 \text{ of solar panels} \\ \sim 10,000 \text{ SF.}$$

¹⁰² <https://upload.wikimedia.org/wikipedia/commons/e/e4/PVeff%28rev150609%29.jpg>.

¹⁰³ Supplementing with purchased electricity at installation sites with lower solar intensity doesn't significantly increase the estimated net cost per tonne of CO₂ extraction, but would create a net nonzero carbon footprint if the purchased electricity is not derived from renewable sources.

5.1.4 Solar Panel Cost

Wholesale photovoltaic prices have fallen from \$76.67 per watt in 1977 to an estimated \$0.30 per watt in 2015, for crystalline silicon solar cells (chart, right).¹⁰⁴ The average retail price of solar installations as monitored by the Solarbuzz group fell from \$5.50/watt in 2001 to \$2.29/watt by 2012, with 34% of monitored vendors selling below \$2/watt.¹⁰⁵ For large-scale installations, prices below \$1/watt were achieved by 2012 – e.g., a module price of \$0.78/watt was published for a large scale 5-year deal in April 2012.¹⁰⁶



If we assume favorable pricing at around \$1/watt for installed photovoltaics by the future decade in which our CO₂ capture plants would be built, then these solar panels, commercially installed on a turnkey basis, will cost:

$$(13,900 \text{ watts of solar panels}) (\$1/\text{watt}) = \$13,900.$$

¹⁰⁴ <http://pv.energytrend.com/pricequotes.html>. Chart: https://en.wikipedia.org/wiki/Cost_of_electricity_by_source#/media/File:Price_history_of_silicon_PV_cells_since_1977.svg.

¹⁰⁵ “Module pricing: Retail Price Summary – March 2012 Update; <http://www.solarbuzz.com/facts-and-figures/retail-price-environment/module-prices>.

¹⁰⁶ “Chinese PV producer Phono Solar to supply German system integrator Sybac Solar with 500 MW of PV modules,” 30 April 2012; <http://web.archive.org/web/20130414074440/http://www.solarserver.com/solar-magazine/solar-news/current/2012/kw18/chinese-pv-producer-phono-solar-to-supply-german-system-integrator-sybac-solar-with-500-mw-of-pv-modules.html>.

5.1.5 Number, Area, and Cost of Sorting Rotors

Taking the atmospheric CO₂ diffusion-limited maximum cycle time of 1800 Hz per binding site¹⁰⁷ and assuming 5 binding sites are exposed to atmosphere at any one time, we can run the rotors at ~10,000 Hz and all binding sites will stay fully occupied. This means the required number of ~100,000-atom sorting rotors is:

$$(1.58 \times 10^{23} \text{ molecules CO}_2 / \text{sec}) / (10,000 \text{ molecules CO}_2 / \text{rotor-sec}) = 1.58 \times 10^{19} \text{ rotors,}$$

having a mass:

$$(1.58 \times 10^{19} \text{ rotors}) (2 \times 10^{-21} \text{ kg/rotor}) = 0.0316 \text{ kg,}$$

having a surface area of:

$$(1.58 \times 10^{19} \text{ rotors}) (7 \text{ nm} \times 14 \text{ nm per rotor}) = 1548 \text{ m}^2,$$

and costing to manufacture¹⁰⁸ via a first-generation nanofactory:

$$(0.0316 \text{ kg}) (\$1000/\text{kg}) = \$32.$$

¹⁰⁷ Using Eqn. 4.3 in Freitas RA Jr., Nanomedicine, Vol. I, Landes Bioscience, 1999, p. 94 (<http://www.nanomedicine.com/NMI/3.2.2.htm#p2>), and taking the relevant variables as follows: $N_{\text{encounters}} = 100$, $A = 0.1 \text{ nm}^2$ for $\text{CO}_2 = 1 \times 10^{-19} \text{ m}^2$, $c_{\text{ligand}} = 9.58 \times 10^{-6} \text{ nm}^{-3}$ (e.g., 400 ppm CO₂ in ambient air implies: (0.0004 atm partial pressure) $(2.37 \times 10^{25} \text{ molecules/atm-m}^3 \text{ at STP}) = 9.48 \times 10^{21} \text{ CO}_2 \text{ molecules/m}^3 = 9.58 \times 10^{-6} \text{ nm}^{-3}$), $MW_{\text{kg}} = 0.044 \text{ kg/mole}$, $N_A = 6.023 \times 10^{23} \text{ molecules/mole}$, $k = 1.381 \times 10^{-23} \text{ J/molecule-K}$, and $T = 300 \text{ K}$, yields an equilibration time (or guaranteed occupancy time) of $t_{\text{EQ}} = 5.55 \times 10^{-4} \text{ sec}$, or $t_{\text{EQ}}^{-1} = 1800 \text{ Hz}$ rotor cycle time, assuming CO₂ concentration remains constant at 400 ppm.

¹⁰⁸ The estimated manufacturing cost for atomically precise diamondoid products using the first nanofactory is ~\$1000/kg of finished product, falling to ~\$10/kg for second-generation nanofactories that are constructed from components fabricated by the first nanofactory. Manufacturing cost for a mature later-generation nanofactory should approximate ~\$1/kg – see Drexler KE, Nanosystems: Molecular Machinery, Manufacturing, and Computation, John Wiley & Sons, New York, 1992; Section 14.5.6(h). Freitas RA Jr. Economic impact of the personal nanofactory. Nanotechnology Perceptions: A Review of Ultraprecision Engineering and Nanotechnology 2(May 2006):111-126, <http://www.rfreitas.com/Nano/NoninflationaryPN.pdf>. Freitas RA Jr., Merkle RC. Kinematic Self-Replicating Machines, Landes Bioscience, Georgetown, TX, 2004, pp. 202-204; <http://www.molecularassembler.com/KSRM/6.2.2.htm>).

5.1.6 Air Throughput Rate

Assume the building interior volume is 1400 m^3 ($927 \text{ m}^2 \times 1.5 \text{ m}$ high) and therefore contains (2.37×10^{25} molecules CO_2/m^3 at STP) (400 ppm CO_2) ($7.31 \times 10^{-26} \text{ kg/molecule CO}_2$) (1400 m^3) = 0.970 kg of CO_2 . To extract 1000 kg/day requires about $(1000 \text{ kg/day}) / (0.970 \text{ kg}) \sim 1000$ whole-building air exchanges per day, a total airflow of (1400 m^3) ($1000 \text{ exchanges/day}$) = $1.4 \times 10^6 \text{ m}^3/\text{day}$, equivalent to $16 \text{ m}^3/\text{sec}$, or:

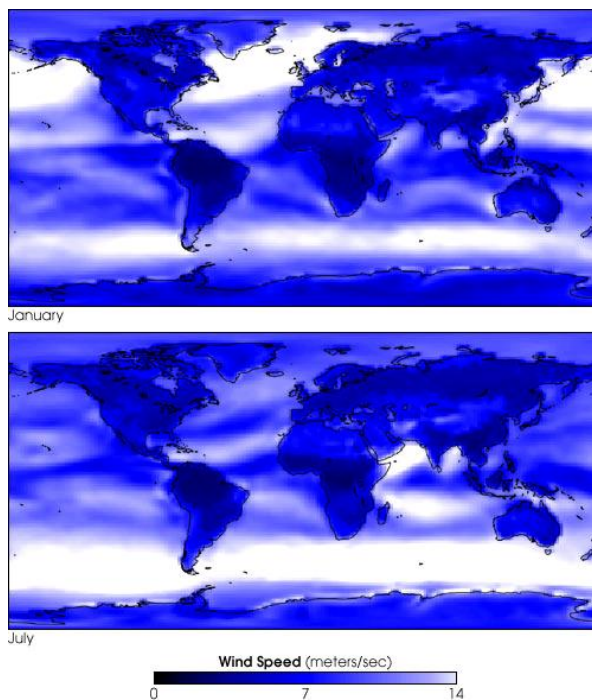
$$(1.4 \times 10^6 \text{ m}^3/\text{day}) (35.3147 \text{ cubic feet}/\text{m}^3) / (1440 \text{ min}/\text{day}) = 35,000 \text{ CFM}.$$

However, we shouldn't need any circulating fans.¹⁰⁹ If the 927 m^2 building is rectangular, measuring $62 \text{ m} \times 15 \text{ m} \times 1.5 \text{ m}$, and if we allow prevailing winds to blow through the building perpendicular to the long side, with chicken wire screens installed on both sides, then the frontal area facing into the wind is $62 \text{ m} \times 1.5 \text{ m} = 93 \text{ m}^2$ and the minimum wind speed required to clear the whole building 1000 times a day is only:

$$(16 \text{ m}^3/\text{sec}) / (93 \text{ m}^2) = 0.17 \text{ m}/\text{sec}.$$

However, this calculation assumes that all CO_2 present in the passing air is extracted, e.g., that the CO_2 concentration in the exiting air is $\sim 0 \text{ ppm}$, which is unrealistic given our assumptions about sorting rotor equilibration time. A more realistic assumption might be that only about half of the CO_2 is removed, giving a CO_2 exit concentration of $\sim 200 \text{ ppm}$ and a required minimum wind speed of $\sim 0.34 \text{ m}/\text{sec}$.

The mean horizontal surface wind speeds are typically 10-20 times higher than this at most places in the world having high solar irradiance (image, right).¹¹⁰



¹⁰⁹ A typical 30" whole-house fan blows 6000 CFM, draws 480 W, and costs \$318 at Home Depot (<http://www.homedepot.com/p/Master-Flow-6000-CFM-30-in-Belt-Drive-Deluxe-Whole-House-Fan-with-Shutter-30BWHFS/202067896>). We could use 6 of them to actively push 35,000 CFM, costing \$1908 and drawing 2880 W of power. The extra power to drive them could be purchased at the usual cost of industrial electricity, or $\$0.07/\text{kWh}$ ($1.94 \times 10^{-8} \text{ \$/J}$), which would add $(1.94 \times 10^{-8} \text{ \$/J}) (2880 \text{ W}) (30 \text{ yr}) (3.14 \times 10^7 \text{ sec/yr}) = \$52,600$ to the lifetime cost of the plant and would increase the total cost of atmospheric CO_2 capture by $(\$52,600)/(10,950 \text{ tonnes CO}_2) = \$4.80/\text{tonne CO}_2$.

¹¹⁰ http://commons.wikimedia.org/wiki/File:Wind_speed_climatology.jpg.

5.1.7 Layout of Nanofilter Sheets

The 1548 m² of thin sheets containing the molecular filters are arranged side by side in the building, oriented along the direction of airflow, in sheets of size (15 m x 1.5 m =) 22.5 m² each. The nanofilter sheets are (1548 m²) / (22.5 m²) = 69 in number, and each sheet is spaced at most (62 m building length) / (69 sheets) = 90 cm apart from its neighboring sheet. Each sheet is held in a rigid frame and includes connector plumbing to allow the purified 100 atm CO₂ gas to be drawn off for export from the plant.

A subsystem capable of automatically cleaning and keeping dust-free the nanofilter sheets, possibly including electrostatic filters, sheet wipers, sprayers, or other means, along with specific structures and methods for minimizing binding site fouling, will likely be essential but their precise design is beyond the scope of this paper.

5.1.8 Carbon Transport from Plant

Using *in situ* carbon capture, the cost of transporting captured CO₂ is reduced essentially to zero because the gas can be captured at the same location where it is to be sequestered. Carbon capture plants will be co-located with a pipe transport system able to carry the pressurized CO₂ effluent fluid directly to a nearby geological burial storage site (**Section 3.5.1**).

Assuming our CO₂ capture plants are located ~1000 meters apart and thus each require ~1 km of piping to transport the captured CO₂ into the sequestration system, the additional cost for pipelining may approximate (~1 km) (\$1.5-\$2/tonne CO₂ per 100 km) ~ \$0.02/tonne CO₂, a negligible addition to system cost.

5.1.9 Total Cost per Tonne

The baseline exemplar system will be a facility with a $t_{\text{lifetime}} = 30$ -year useful life.

We start by constructing a 10,000 SF flat-top industrial metal shed building for \$10/SF costing \$100,000, on remote or desert land costing \$2000/acre¹¹¹ giving a purchase cost of $(\$2000/\text{acre})(10,000 \text{ SF})/(43560 \text{ SF}/\text{acre}) = \459 . We spend another \$13,900 to have the solar electrical system installed to provide power. This system has a minimum lifetime of 15 years,¹¹² so we allow that it will be replaced once at the 15-year point for another \$13,900, although prices should have fallen significantly by then. We manufacture the sorting rotors for \$32,¹¹³ embedding them in a small mass of additional atomically precise manufactured structures and bulk support frames for the nanofilter sheets at a manufacturing cost of $(\$5/\text{m}^2) (1548 \text{ m}^2 \text{ nanofilter sheets}) = \7740 . We add pressure piping and valving for the 100 atm CO₂, electronic control and monitoring systems, installation labor and other capital costs for which we allocate another \$33,969, giving a total capital cost of \$170,000 to build the CO₂ capture plant. Source power is provided free by the sun, and we assume that operations at these simple and highly automated facilities can be maintained for an additional labor cost of $(\$1000/\text{yr}) (30 \text{ years}) = \$30,000$, giving a total lifetime cost per plant of $c_{\text{plant}} = \$200,000$.

If the facility has a useful lifetime of 30 years, then during that lifetime it extracts a total of:

$$(30 \text{ years}) (365 \text{ days/year}) (1 \text{ tonne CO}_2/\text{day}) = 10,950 \text{ tonnes of CO}_2.$$

Hence the net cost of atmospheric CO₂ extraction is:

$$(\$200,000) / (10,950 \text{ tonnes CO}_2) = \$18.26/\text{tonne CO}_2.$$

To this must be added the pipelining cost of \$0.02/tonne CO₂ (**Section 5.1.8**), plus the cost of geological carbon storage which has been estimated at \$0.50-\$8/tonne CO₂ injected (**Section 3.5.1**). Assuming a mid-range cost of \$2.72/tonne CO₂ for geological sequestration, the final

¹¹¹ In 2014, U.S. farmland averaged \$2950/acre, with the Mountain region having the lowest average farmland value at \$1070/acre and U.S. pasture land averaging \$1300/acre. See: "Agricultural Land Values Highlights," August 2014; <http://www.agweb.com/land/farmland-value-guide/>. Land costs may be significantly lower in underdeveloped and developing countries.

¹¹² Tests show that solar panel power output degrades less than 1%/yr, giving a plausible lifetime of 20-30 years; "How long do solar electric PV panels last?" <http://info.cat.org.uk/questions/pv/life-expectancy-solar-pv-panels>. Warranty limits are typically 20-25 years at 80% rated power on silicon solar cells, 10-20 years on the power inverters; "Lifespan and Reliability of Solar Photovoltaics - Literature Review," 22 September 2012; http://www.appropedia.org/Lifespan_and_Reliability_of_Solar_Photovoltaics_-_Literature_Review.

¹¹³ The lifetime of sorting rotors is presently unknown; but since the manufacturing cost for all the nanofilter sheets in one facility is \$32, annually replacing the entire set for 30 years would add \$948 to manufacturing expenses, increasing the total cost of atmospheric CO₂ capture by only \$0.087/tonne CO₂.

total net cost of atmospheric carbon capture, using the simple CO₂ capture plant described in this Section, is:

$$\$18.26/\text{tonne CO}_2 + \$0.02/\text{tonne CO}_2 + \$2.72/\text{tonne CO}_2 = \mathbf{\$21/\text{tonne CO}_2}.$$

Note that the emission factors for the combustion of motor gasoline and crude oil are 8.91 kg CO₂/gallon and 10.29 kg CO₂/gallon, respectively,¹¹⁴ so the energy cost to capture from the atmosphere all of the carbon dioxide emitted from using these fuels is (\$0.021/kg CO₂)(8.91 kg CO₂/gallon =) \$0.187 per gallon of gasoline and (\$0.021/kg CO₂)(10.29 kg CO₂/gallon)(42 gallons/barrel =) \$9.08 per barrel of crude oil. The emission factor for coal combustion in the electric power sector is 95.52 kg CO₂/MMBtu, so the capture cost is (\$0.021/kg CO₂)(95.52 kg CO₂/MMBtu)(0.003412 MMBtu/kWh =) \$0.0068 per kWh of electric power produced.



Therefore, atmospheric capture via molecular filters could make the combustion of fossil fuels **carbon-neutral** at a cost of **19¢/gallon of gasoline** consumed or **\$9/barrel of crude oil** shipped, or a cost of **0.7¢/kWh** for coal-fired electric power plants, perhaps provided by a small, nearly painless carbon emission fee.

“Green gasoline”, anyone?

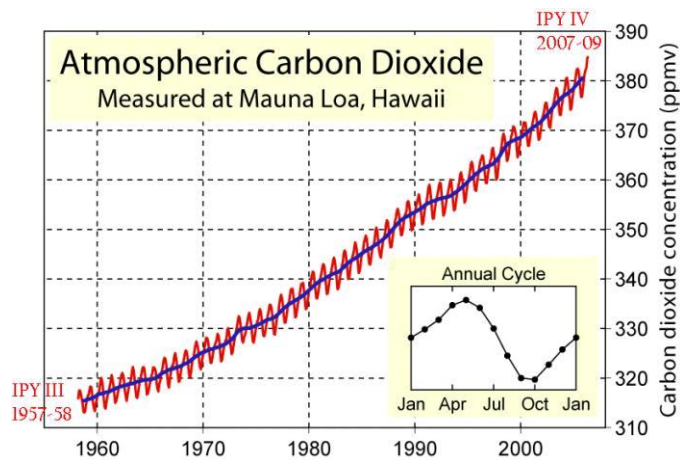
¹¹⁴ “Voluntary Reporting of Greenhouse Gases Program Fuel Carbon Dioxide Emission Coefficients,” U.S. Energy Information Administration, 31 January 2011; <http://www.eia.gov/oiaf/1605/coefficients.html>.

5.2 A Simple CO₂ Capture Plant Applied to Global Climate Change

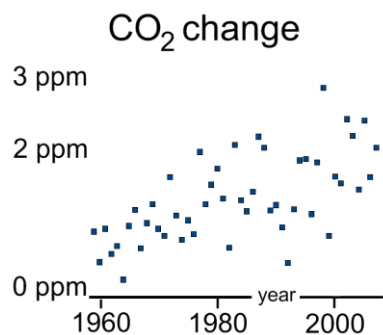
With a conceptual design for a CO₂ capture plant now in hand (**Section 5.1**), we can investigate the possibility of continuous active management of greenhouse gas concentration in the atmosphere. The purpose of a global network of these plants is to maintain the specified greenhouse gas constituents at programmed concentrations that are regarded as ideal for controlling climate change on Earth.

5.2.1 Worldwide CO₂ Capture Plant Network Scenarios

What is the optimal ambient concentration of all the molecular constituents of the air that we seek to control? This is a complex issue whose details lie beyond the scope of this paper. In the case of “climate pollutant” molecules, a proper detailed analysis should include, for example, a weighting of each atmospheric component by its heat-trapping efficiency as a greenhouse gas to determine its ideal atmospheric concentration.



However, for purposes of the present analysis, it will be naively assumed that permanently rolling back CO₂ concentrations to near-preindustrial levels of 300 ppm worldwide (leaving 2340×10^{12} kg, or 2340 gigatonnes (Gt), of CO₂ in the atmosphere) should suffice to eliminate any possible anthropogenic influence on global climate change from that source. Such a rollback requires removing 680×10^{12} kg of CO₂ from the air.



Of course, CO₂ emissions from human sources are slowly rising over time (e.g., the Keeling curve; above, left)¹¹⁵ and the rate of that increase is also rising over time (below, left).¹¹⁶ In 2009, roughly 11.8×10^{12} kg (~2.3 ppm) of anthropogenic CO₂ was added to the global load, far larger than the $0.130\text{-}0.230 \times 10^{12}$ kg/yr normally added from volcanic sources.¹¹⁷ Linearly extrapolating the historical rate rise of 1 ppm/yr in 1970 to 2 ppm in 2000, the rate of increase reaches 3 ppm/yr by 2030 and 4 ppm/yr by 2060.

¹¹⁵ Keeling CD. Rewards and penalties of monitoring the Earth. *Annual Review of Energy and the Environment* 23(1998):25-82. See also: “Keeling Curve,” http://icestories.exploratorium.edu/dispatches/wp-content/uploads/2008/05/keeling_graph.jpg.

¹¹⁶ Pieter Tans, “Annual CO₂ mole fraction increase (ppm) for 1959-2007,” National Oceanic and Atmospheric Administration, Earth System Research Laboratory, Global Monitoring Division, 3 May 2008; ftp://ftp.cmdl.noaa.gov/ccg/co2/trends/co2_gr_mlo.txt. See additional details at <http://www.esrl.noaa.gov/gmd/ccgg/trends/>. Image from: http://en.wikipedia.org/wiki/File:CO2_increase_rate.png.

¹¹⁷ Sigurdsson H, Houghton BF, *Encyclopedia of Volcanoes*, Academic Press, San Diego, 2000.

The chart below (**Figure 3**) shows three possible scenarios for future global CO₂ management.

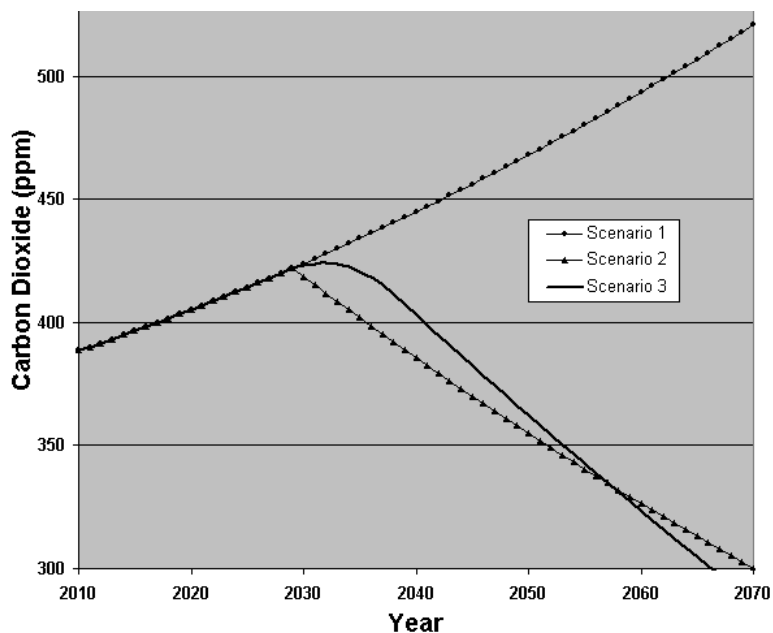
In **Scenario 1**, there is no sequestration and carbon emissions continue to grow at current rates, allowing CO₂ levels rise to 521 ppm by 2070.

In **Scenario 2**, a global network of CO₂ capture plants capable of removing 42×10^{12} kg/yr (42 Gt/yr) of CO₂ is built and begins extraction operations at full capacity in 2030, resulting in a peak at 422 ppm in 2029 and a reduction to the target 300 ppm level by 2070.

In **Scenario 3**, the CO₂ capture plant network is more realistically linearly ramped from 10% of maximum CO₂ extraction capacity in 2030 to full capacity at 50×10^{12} kg/yr (50 Gt/yr) by 2039, producing a peak at 424 ppm in 2032 and a reduction to 300 ppm by 2067.

In each case, the CO₂ content of the atmosphere in a given year is calculated as the content in the previous year plus the net mass added in the current year less the mass extracted by CO₂ capture plants in the current year, converted to ppm concentrations.

Figure 3. Three scenarios for global CO₂ management: (1) no sequestration, (2) 42 Gt/yr CO₂ capture plant network runs continuously during 2030-70, and (3) 50 Gt/yr CO₂ capture plant network ramps up linearly during 2030-39, then runs continuously thereafter.¹¹⁸



¹¹⁸ Freitas RA Jr. Diamond Trees (Tropostats): A Molecular Manufacturing Based System for Compositional Atmospheric Homeostasis. IMM Report 43, 10 February 2010; <http://www.imm.org/Reports/rep043.pdf>.

Our goal in the present work is to achieve Scenario 3: a global network of CO₂ capture plants powerful enough to extract up to $M_{\text{extract}} = 50 \times 10^{12}$ kg/yr (50 Gt/yr) of CO₂, sufficient to return Earth's atmosphere expeditiously to pre-industrial carbon levels and thereafter to maintain the atmosphere in this condition indefinitely – even assuming that the current anthropogenic carbon footprint continues growing on its present course without any abatement throughout the 21st century, which seems unlikely for various reasons. This calculation also assumes that there are no sudden massive releases of carbon into the atmosphere such as might occur in the aftermath of a supervolcano eruption or a thermonuclear war. A 50 Gt/yr removal rate should also suffice to accommodate possible slow outgassing from the oceans, where another $\sim 150,000 \times 10^{12}$ kg of dissolved CO₂ is stored as carbonic acid and in other forms such as carbonate and bicarbonate ions. The release of CO₂ from deeper geological stores such as the $\sim 10^{19}$ kg of carbon sequestered as carbonates in rocks takes place over even longer timescales and can safely be ignored in this analysis.

5.2.2 Network Size and Deployment

A global CO₂ capture plant network capable of selectively filtering out $M_{\text{extract}} \sim 50 \times 10^{12}$ kg/yr of CO₂ gas would require a continuous systemwide power generation of $P_{\text{network}} \approx M_{\text{extract}} \Delta G_{\text{CO}_2} / \tau_{\text{yr}} = (50 \times 10^{12} \text{ kg CO}_2 / \text{yr}) (1200 \text{ kJ/kg CO}_2) / (3.14 \times 10^7 \text{ sec/yr}) = 1.91 \times 10^{12} \text{ W}$ (~ 2 terawatts), about equal to the worldwide electricity consumption of $\sim 2 \times 10^{12} \text{ W}$ in 2008 but only a modest fraction of the total worldwide energy consumption of $\sim 15.04 \times 10^{12} \text{ W}$ for 2008.¹¹⁹ It is worth noting for comparison that worldwide biomass traps ~ 100 terawatts via photosynthesis¹²⁰ and the entire disk of the Earth receives 1370 W/m^2 of continuous solar illumination or $\sim 175,000$ terawatts ($1.75 \times 10^{17} \text{ W}$).

Since the global CO₂ capture plant system runs entirely on solar power that is intercepted before it hits the ground, any waste heat that is released will not exceed the heat that would otherwise have been re-radiated by the now-shadowed ground underneath the machines. Thus even a closely-packed field of CO₂ capture plants should produce no localized heat-island effects.

In this scenario, the number of plants required is $N_{\text{plants}} = M_{\text{extract}} / m_{\text{plant}} = (50 \times 10^{12} \text{ kg/yr}) (1 \text{ yr} / 365 \text{ days}) / (1 \text{ tonne/plant-day}) = 137 \text{ million CO}_2 \text{ capture plants}$, covering a total surface area of $A_{\text{plants}} = N_{\text{plants}} a_{\text{plant}} = (137 \times 10^6 \text{ plants}) (927 \text{ m}^2) = 1.27 \times 10^{11} \text{ m}^2$, or $\sim 0.085\%$ of Earth's land surface area of $1.49 \times 10^{14} \text{ m}^2$.

With a total lifetime cost per plant of $c_{\text{plant}} = \$200,000/\text{plant}$ (**Section 5.1.9**), the annual cost to install the global CO₂ capture plant network in an initial deployment period of $t_{\text{install}} = 10$ years (during 2030-2039) is $C_{\text{install}} = N_{\text{plants}} c_{\text{plant}} / t_{\text{install}} = \mathbf{\$2.74 \text{ trillion/yr for 10 years}}$. Thereafter, the plants must be replaced every $t_{\text{lifetime}} = 30$ years and so the annual cost of maintaining the network may approximate: $C_{\text{maintain}} = N_{\text{plants}} c_{\text{plant}} / t_{\text{lifetime}} = \mathbf{\$0.91 \text{ trillion per year}}$.

According to a recent analysis by Citibank,¹²¹ the economic costs associated with global climate change will amount to \$20 trillion/yr by 2060 if there is a 1.5 °C temperature increase, \$44 trillion/yr at a 2.5 °C temperature increase, and \$72 trillion/yr at a 4.5 °C temperature increase. Paying \$0.93 trillion/yr to avoid a \$20-\$72 trillion/yr worldwide cost seems like a reasonable and intelligent investment to make.

¹¹⁹ “World energy resources and consumption. Energy Consumption A1: Consumption by fuel, 1965-2008” (XLS), Statistical Review of World Energy 2009, BP, 31 July 2006; http://www.bp.com/liveassets/bp_internet/globalbp/globalbp_uk_english/reports_and_publications/statistical_energy_review_2008/STAGING/local_assets/2009_downloads/statistical_review_of_world_energy_full_report_2009.xls

¹²⁰ Neelson KH, Conrad PG. Life: past, present and future. Philos. Trans. R. Soc. Lond., B, Biol. Sci. 354(December 1999):1923-1939; <http://journals.royalsociety.org/content/7r10hq3rplg1vag/>.

¹²¹ Citi GPS, “Energy Darwinism II: Why a Low Carbon Future Doesn't have to Cost the Earth,” August 2015; <https://ir.citi.com/hsq32Jl1m4aIzicMqH8sBkPnbsqfnwy4Jgb1J2kIPYWIw5eM8yD3FY9VbGpK%2Baax>

5.2.3 Network Issues: Wind Velocity and Vertical Convection

There are many factors to be considered in the layout of a network of carbon capture devices, and a comprehensive analysis is beyond the scope of this paper. To impart the flavor of such analyses, we briefly consider one important factor: whether or not a field of CO₂ capture plants will too readily exhaust the entire local supply of atmospheric CO₂ during normal operation, causing some plants to operate at below their rated capacity.

Consider a square CO₂ capture plant field whose area is 25% occupied by capture plants, having an edge length $L_{\text{net}} = A_{\text{net}}^{1/2} = (A_{\text{plants}}/0.25)^{1/2} = 7.13 \times 10^5 \text{ m}$ across which air of density $\rho_{\text{air}} = 1.17 \text{ kg/m}^3$ at 300 K and CO₂ mass fraction $m_{\text{ratioCO}_2} = 5.881 \times 10^{-4}$ blows at a mean horizontal wind speed of v_{windH} . Let H_{extract} be the height of the air column above the capture plant field from which CO₂ can be extracted. A good proxy for H_{extract} is the thickness of the planetary boundary layer – typically¹²² ~1000 m – which is the lowest layer of the troposphere nearest the ground where wind is most turbulent and gusty, maximizing convective mixing. In this case the extraction volume $V_{\text{extract}} = H_{\text{extract}} L_{\text{net}}^2 \sim 5.08 \times 10^{14} \text{ m}^3$ and the mass of CO₂ available for extraction in that volume is $M_{\text{CO}_2} = V_{\text{extract}} m_{\text{ratioCO}_2} = 3.60 \times 10^{11} \text{ kg}(\text{CO}_2)$, where sea-level air contains $m_{\text{CO}_2} = \rho_{\text{air}} m_{\text{ratioCO}_2} = 7.09 \times 10^{-4} \text{ kg}(\text{CO}_2)/\text{m}^3$ and the CO₂ removal time from the extraction volume V_{extract} is $\tau_{\text{CO}_2} \sim M_{\text{CO}_2} / M_{\text{extract}} \sim 2.26 \times 10^5 \text{ sec}$ (~2.6 days), for $M_{\text{extract}} = 50 \times 10^{12} \text{ kg/yr} = 1.59 \times 10^6 \text{ kg}(\text{CO}_2)/\text{sec}$. To allow sufficient time for vertical mixing of fresh air from above with air nearest the surface from which CO₂ has been extracted, the vertical wind speed $v_{\text{windV}} \geq (H_{\text{extract}} / \tau_{\text{CO}_2}) \sim 0.44 \text{ cm/sec}$. The average vertical wind speed (often charted¹²³ in microbars/sec, roughly equivalent to cm/sec) is downward over most of the Earth's surface at any given time and is typically a few cm/sec,¹²⁴ so $v_{\text{windV}} \sim 1 \text{ cm/sec}$ seems reasonably conservative and appears to satisfy the vertical mixing requirement. Similarly, the horizontal surface wind velocity needed to move replacement air into the extraction volume over the CO₂ capture plant field is $v_{\text{windH}} = L_{\text{net}} / \tau_{\text{CO}_2} = M_{\text{extract}} / (H_{\text{extract}} L_{\text{net}} \rho_{\text{air}} m_{\text{ratioCO}_2}) = 3.2 \text{ m/sec}$ (~7 mph), well below the average surface wind speed of ~7 m/sec in the geographical areas of interest (see wind speed map, **Section 5.1.6**).

¹²² Jeff Haby, “The Planetary Boundary Layer,” Weather Education Website, <http://www.theweatherprediction.com/basic/pbl/>.

¹²³ Unisys, “4 Panel NAM 700 mb Plot,” http://weather.unisys.com/nam/4panel/nam_700_4panel.html.

¹²⁴ Jeff Haby, “Vertical Velocity On The 700 MB Model Progs,” Weather Education website, <http://www.theweatherprediction.com/habyhints/101/>.

6. Advanced Nanofactory-Based Atmospheric CO₂ Capture System

The system described in **Section 5** is an incremental system that does not take full advantage of nanofactory technology, hence implementation costs are high. An advanced global atmospheric management system that more fully exploits the many advantages of atomically-precise devices and low-cost nanofactory-based manufacturing gives superior results.

The previous system only has a tiny mass of components (i.e., the molecular filters) made by the nanofactory, and so cannot fully reap the cost advantages of using nanofactories. In the scenario presented in this Section, all of the system components are manufactured by nanofactories, allowing costs to fall by more than 100-fold.

In the global carbon capture system presented here, the carbon capture plants float on the surface of the ocean, forming “carbon capture islands” that remain fixed in or near a particular geographical location. Carbon dioxide is compressed into chemically inert spherical diamond tanks the size of “golfballs” that are dropped onto the ocean floor for easy disposal (image, below), where they may lie undisturbed for geological timescales. The floating carbon capture plants are manufactured in coastal nanofactories, then launched toward their destination where they congregate into compact islands and begin their carbon capture operations.



Numerous other implementations, capture systems, and disposal sites also seem workable. The scenario presented here is just one of many technical possibilities once nanofactories become available.

Section 6.1 derives the storage pressure at which the capture system will operate. **Section 6.2** describes the microscale diamond-walled pressure tanks into which the CO₂ is compressed for permanent storage, while **Section 6.3** explains how these microtanks are packed into golfball-sized diamond aggregates for convenient disposal at sea. **Section 6.4** describes the individual carbon capture plants, dubbed “golfcarts,” that float on the ocean surface and manufacture the disposable diamond “golfballs,” using solar energy and CO₂ that the “golfcarts” extract from the atmosphere. **Section 6.5** discusses where the carbon capture islands might be sited, and **Section 6.6** describes the manufacture of “golfcarts” in onshore general-purpose nanofactories, and explains the tremendous cost savings that can result from that innovation.

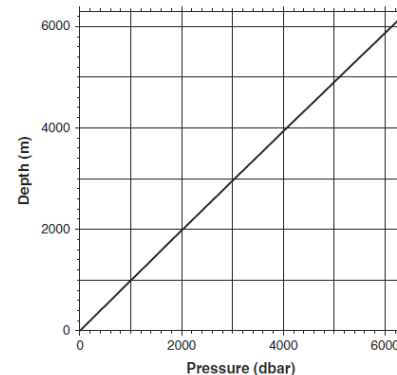
6.1 Selection of Storage Pressure

The cost of geological carbon storage (**Section 3.5.1**) is low, but there is some leakage risk. The leakage risk from carbon storage in minerals (**Section 3.5.2**) is low, but the cost appears to be relatively high. It is possible to combine the attributes of low cost and low leakage risk using a third method in which carbon dioxide is encapsulated at high pressure inside diamond-based microscopic “gas tanks”. The pressurized gas may be supplied at low cost by the use of molecular filters as described in **Section 4**.

The first task is to select a storage pressure for the CO₂ that will be entrained in the storage tanks. This is driven by two requirements: First, the CO₂ must be denser than seawater so that the tanks will sink and not float. Second, the tanks must be sufficiently more dense than seawater so that the terminal velocity will be reasonably high, allowing a fast drop from the ocean surface to the sea floor. It appears that to meet the second criterion, the density of the tanks should exceed seawater density by at least $\Delta\rho = 100 \text{ kg/m}^3$, which we adopt as our target.

We start by considering the seawater pressure/density relationship as a function of depth. The average depth of the Pacific Ocean is 4280 m, 3339 m for the Atlantic Ocean, and $d_{\text{ocean}} = 3688 \text{ m}$ for all the world’s oceans.¹²⁵ The deepest spot is the Mariana Trench, at ~11,000 m.¹²⁶ On average, oceanic pressure increases at a rate of ~0.1 atm per meter of depth, as shown in the image at right (1 dbar ~ 0.1 atm) from a station located in the northwest Pacific.¹²⁷

Temperature is a major factor only within the top 1000 m of the ocean’s surface. Below that depth, seawater temperature falls to a fairly constant 2-4 °C. At the ocean surface, temperatures outside the near-equatorial latitudes are generally 20 °C or below (**Figure 4**, below).¹²⁸ Seawater density is also a function of salinity, which varies only slightly worldwide – e.g., ranging from a low of 32 psu (parts per thousand) in the far north due to reduced evaporation, to a high of 37 psu in the southeastern area of the Pacific, but averages 35 psu worldwide. (There is also a slight variation of salinity with depth.)



¹²⁵ https://en.wikipedia.org/wiki/Pacific_Ocean; https://en.wikipedia.org/wiki/Atlantic_Ocean; <https://en.wikipedia.org/wiki/Ocean>.

¹²⁶ https://en.wikipedia.org/wiki/Mariana_Trench.

¹²⁷ Talley L, Pickard G, Emery W, Swift J. Chapter 3. Physical Properties of Seawater. Descriptive Physical Oceanography, Elsevier Ltd., 2011, pp. 29-65; http://www-pord.ucsd.edu/~ltalley/sio210/DPO/TALLEY_9780750645522_chapter3.pdf.

¹²⁸ “SST 20131220 blended Global,” NASA, 20 Dec 2013; https://en.wikipedia.org/wiki/Sea_surface_temperature#/media/File:SST_20131220_blended_Global.png.

Figure 4. Ocean surface temperature map.

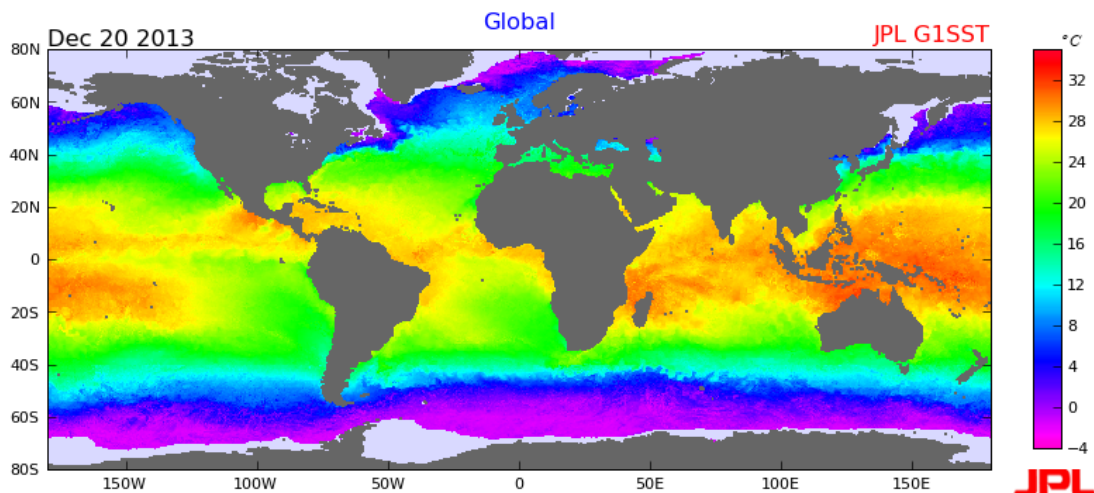


Table 2 (next page) is a summary of seawater density at all relevant ocean depths on Earth. Given a desired density differential of $\Delta\rho = 100 \text{ kg/m}^3$ between CO_2 tanks and seawater, and given that the CO_2 tanks will be loaded and initially dropped into seawater at some warm ocean surface temperature (here assumed to be $20 \text{ }^\circ\text{C}$ for illustrative purposes), the target tank density $\rho_{\text{target}} = \rho_{\text{surface}} + \Delta\rho = 1021.7 \text{ kg/m}^3$ (from **Table 2**) + $100 \text{ kg/m}^3 = 1121.7 \text{ kg/m}^3$.

Table 2. Density of seawater and CO₂ as a function of depth, pressure, and temperature.¹²⁹

Ocean Depth (m)	Seawater Pressure (bar)	Seawater or CO ₂ Pressure (atm)	Seawater Density (kg/m ³)	Seawater Temperature (°C)	CO ₂ Density (kg/m ³)
0	0	0	1021.7	20	1.7
1000	100.96	99.6 atm	1032.4	4	954.2
2000	202.37	199.7 atm	1037.2	3	1009.5
3000	304.25	300.3 atm	1041.8	2	1048.8
4000	406.59	401.3 atm	1046.3	2	1077.2
5000	509.42	502.8 atm	1050.7	2	1100.7
6000	612.73	604.7 atm	1055.0	2	1121.5
7000	716.53	707.2 atm	1059.3	2	1140.0
8000	820.83	810.1 atm	1063.4	2	1156.5
9000	925.63	913.5 atm	1067.5	2	1171.8
10,000	1030.95	1017.5 atm	1071.6	2	1185.8
		1032.0 atm		20	1150.3
		1032.0 atm		2	1187.6
11,000	1136.78	1121.9 atm	1075.5	2	1198.9

¹²⁹ Data on seawater computed using “Sea Water Equation of State Calculator,” <http://fermi.jhuapl.edu/denscalc.html>. Data on CO₂ computed using “CO₂ Calculator” (<http://www.energy.psu.edu/tools/CO2-EOS/index.php>) which encodes a mathematical model from Span R, Wagner W. A new equation of state for carbon dioxide covering the fluid region from the triple-point temperature to 1100K at pressures up to 800 MPa. J. Phys. Chem. Ref. Data. 1996;25:1509-1596; <http://library.certh.gr/libfiles/PDF/GEN-SPIN-317-A-NEW-by-WAGNER-in-JPCRD-V-25-ISS-6-PP-1509-1596-Y-1996.pdf>.

6.2 Building and Loading Diamond Microtanks

The maximum radius of a microscopic spherical diamond pressure tank of wall thickness t_{wall} and wall failure strength σ_w that can tolerate a maximum pressure of P_{max} before bursting is approximated by $R_{\text{max}} = 2 t_{\text{wall}} \sigma_w / P_{\text{max}}$. For $t_{\text{wall}} \ll R_{\text{max}}$, the empty mass of a spherical diamond tank with wall material of density ρ_{wall} is $M_{\text{tankempty}} = \rho_{\text{wall}} V_{\text{tankwall}}$ where tank wall volume $V_{\text{tankwall}} = V_{\text{tankext}} - V_{\text{tankint}}$, exterior tank volume is $V_{\text{tankext}} = (4\pi/3) R_{\text{max}}^3$, and interior tank volume $V_{\text{tankint}} = (4\pi/3) (R_{\text{max}} - t_{\text{wall}})^3$. Taking $P_{\text{max}} = 1032 \text{ atm} = 10.46 \times 10^7 \text{ N/m}^2$, $\rho_{\text{wall}} = 3510 \text{ kg/m}^3$ for diamond, $\sigma_w = 2 \times 10^{10} \text{ N/m}^2$ (~ 0.2 times the failure strength of diamond¹³⁰) and $R_{\text{max}} = 2 \text{ }\mu\text{m}$ then $t_{\text{wall}} = 5.23 \text{ nm}$ for diamond walls, $V_{\text{tankext}} = 3.35 \times 10^{-17} \text{ m}^3/\text{microtank}$, $V_{\text{tankint}} = 3.32 \times 10^{-17} \text{ m}^3/\text{microtank}$, $V_{\text{tankwall}} = 2.62 \times 10^{-19} \text{ m}^3/\text{microtank}$, and $M_{\text{tankempty}} = 9.20 \times 10^{-16} \text{ kg/microtank}$. A tank of CO_2 at 1032 atm pressure and 20 °C has $n_{\text{CO}_2} = \rho_{\text{CO}_2} N_A / \text{MW}_{\text{CO}_2} = (1150.3 \text{ kg/m}^3) (6.023 \times 10^{23} \text{ molecules/mole}) / (0.044 \text{ kg/mole}) = 1.57 \times 10^{28} \text{ CO}_2 \text{ molecules/m}^3$. CO_2 has a mass of $m_{\text{CO}_2} = 7.31 \times 10^{-26} \text{ kg/molecule CO}_2$, so the mass of gas encapsulated within a single diamond microtank is $M_{\text{gas}} = V_{\text{tankint}} n_{\text{CO}_2} m_{\text{CO}_2} = (3.32 \times 10^{-17} \text{ m}^3) (1.57 \times 10^{28} \text{ CO}_2 \text{ molecules/m}^3) (7.31 \times 10^{-26} \text{ kg/molecule CO}_2) = 3.82 \times 10^{-14} \text{ kg CO}_2/\text{microtank}$, which is $M_{\text{gas}}/M_{\text{tankempty}} = 42$ times larger than the mass of the empty tank. The computed density of one full microtank is therefore $\rho_{\text{fulltank}} = (M_{\text{tankempty}} + M_{\text{gas}}) / V_{\text{tankext}} = (9.20 \times 10^{-16} \text{ kg/microtank} + 3.82 \times 10^{-14} \text{ kg CO}_2/\text{microtank}) / (3.35 \times 10^{-17} \text{ m}^3/\text{microtank}) = 1168.8 \text{ kg/m}^3 > \rho_{\text{target}} (=1121.7 \text{ kg/m}^3)$.

How much energy is required to load one diamond microtank with compressed CO_2 gas extracted from the atmosphere? From Eqn. (3) in **Section 4.1**, the total energy required to separate atmospheric CO_2 from air and compress it into the diamond microtank at 1032 atm pressure is:

$$E_{\text{loadtank}} = N_{\text{CO}_2} (\Delta G_c + \Delta G_s) = 5.11 \times 10^{-8} \text{ J/microtank} \quad (4)$$

where the number of CO_2 molecules in the microtank is $N_{\text{CO}_2} = M_{\text{gas}} / m_{\text{CO}_2} = (3.82 \times 10^{-14} \text{ kg CO}_2/\text{microtank}) / (7.31 \times 10^{-26} \text{ kg/molecule CO}_2) = 5.23 \times 10^{11} \text{ CO}_2 \text{ molecules/microtank}$, $\Delta G_s = 36.6 \text{ zJ/molecule CO}_2$ for direct air capture of 0.0004 atm CO_2 at $T = 300 \text{ K}$, and the compression energy $\Delta G_c = k_B T \ln(c_2/c_1) = 61.2 \text{ zJ/molecule CO}_2$, where $k_B = 0.01381 \text{ zJ/K}$ (Boltzmann constant), $c_1 = 0.0004 \text{ atm}$, and $c_2 = P_{\text{max}} = 1032 \text{ atm}$.

How much energy is required to fabricate one empty diamond microtank, prior to loading with compressed CO_2 gas? The minimum thermodynamic energy cost to convert one molecule of CO_2 into one carbon atom in a diamond microtank is $E_{\text{CO}_2\text{-C}} = 657.3 \text{ zJ/atom C}$.¹³¹ For a carbon atom

¹³⁰ Freitas RA Jr. Nanomedicine, Vol. I, Landes Bioscience, 1999, Table 9.3; <http://www.nanomedicine.com/NMI/Tables/9.3.jpg>.

¹³¹ $\text{CO}_2 (\text{gas}) + 94.04 \text{ kcal/mole} (657.3 \text{ zJ}) \rightarrow \text{C} (\text{diamond}) + \text{O}_2 (\text{gas})$ using standard enthalpies of formation. To accomplish this, a specific sequence of mechanosynthetic reactions must be devised in which oxygen atoms are mechanically pulled from the CO_2 molecule one by one, after which the carbon is installed in a growing diamond structure using positionally-controlled tip-based site-specific single-atom chemistry. For mechanosynthesis theory work generally, see: Freitas RA Jr, Merkle RC. A Minimal Toolset for Positional Diamond Mechanosynthesis. *J Comput Theor Nanosci.* 2008 May;5:760-861; <http://www.molecularassembler.com/Papers/MinToolset.pdf>. For experimental work on mechanosynthesis,

mass $m_C = 1.99 \times 10^{-26}$ kg/atom C, the number of carbon atoms in a diamond microtank of mass $M_{\text{tankempty}}$ is $n_{\text{tankemptyC}} = M_{\text{tankempty}} / m_C = (9.20 \times 10^{-16} \text{ kg}) / (1.99 \times 10^{-26} \text{ kg/atom}) = 4.62 \times 10^{10}$ carbon atoms. If we reasonably assume that the energy efficiency of positionally-controlled mechanosynthesis in a second-generation nanofactory is $\epsilon_{\text{mechano}} \sim 90\%$, then the energy required to build one empty microtank is:

$$\begin{aligned} E_{\text{buildtank}} &= n_{\text{tankemptyC}} E_{\text{CO}_2\text{-C}} / \epsilon_{\text{mechano}} & (5) \\ &= (4.62 \times 10^{10} \text{ carbon atoms}) (657.3 \text{ zJ/atom C}) / (0.90) \\ &= 3.37 \times 10^{-8} \text{ J/microtank.} \end{aligned}$$

Note that obtaining the $n_{\text{tankemptyC}}$ carbon atoms used to build the microtank requires the removal of $n_{\text{tankemptyC}}$ molecules of CO_2 from the atmosphere, a gas mass of $M_{\text{diamCO}_2} = M_{\text{tankempty}} (0.044 \text{ kg/mole CO}_2 / 0.012 \text{ kg/mole C}) = 3.37 \times 10^{-15} \text{ kg CO}_2/\text{microtank}$. Thus the total amount of CO_2 removed from the atmosphere to build and to load each microtank is $M_{\text{removeCO}_2} = M_{\text{gas}} + M_{\text{diamCO}_2} = (3.82 \times 10^{-14} \text{ kg CO}_2/\text{microtank}) + (3.37 \times 10^{-15} \text{ kg CO}_2/\text{microtank}) = 4.16 \times 10^{-14} \text{ kg CO}_2/\text{microtank}$.

The total energy required to fabricate one diamond microtank of diameter 4 μm is:

$$E_{\text{tank}} = E_{\text{buildtank}} + E_{\text{loadtank}} = 8.48 \times 10^{-8} \text{ J/microtank,} \quad (6)$$

or about $E_{\text{tank}} p_{\text{elect}} / M_{\text{removeCO}_2} = (8.48 \times 10^{-8} \text{ J/microtank}) (1.94 \times 10^{-8} \text{ \$/J}) / (4.16 \times 10^{-14} \text{ kg CO}_2/\text{microtank}) = \mathbf{\$39/\text{tonne CO}_2}$ if the energy had to be supplied from the commercial electrical power grid at an energy cost of $\$0.07/\text{kWh}$ ($= p_{\text{elect}} = 1.94 \times 10^{-8} \text{ \$/J}$). Since our system will be getting its electrical power from a cheaper source, **the total cost per tonne will be significantly lower than this** (see Section 6.6).

Note that a worldwide annual atmospheric CO_2 removal rate of $M_{\text{extract}} = 50 \times 10^{12} \text{ kg/yr}$ (50 gigatonnes (Gt) per yr) requires the annual building and loading of $N_{\text{microtanks}} = M_{\text{extract}} / M_{\text{removeCO}_2} = (50 \times 10^{12} \text{ kg/yr}) / (4.16 \times 10^{-14} \text{ kg CO}_2/\text{microtank}) = 1.20 \times 10^{27} \text{ microtanks/yr}$ which will have an energy cost of:

$$\begin{aligned} E_{\text{extract}} &= N_{\text{microtanks}} E_{\text{tank}} & (7) \\ &= (1.20 \times 10^{27} \text{ microtanks/yr}) (8.48 \times 10^{-8} \text{ J/microtank}) / (3.14 \times 10^7 \text{ sec/yr}) \\ &= 3.24 \text{ terawatts.} \end{aligned}$$

It should also be pointed out that if instead of entraining compressed CO_2 inside a hollow diamond microtank, we simply built a solid diamond microsphere measuring 4 microns in diameter, the energy cost of building such a solid ‘‘tank’’ would increase to $E_{\text{buildtankD}} = V_{\text{tankext}} \rho_{\text{wall}} E_{\text{CO}_2\text{-C}} / \epsilon_{\text{mechano}} m_C = (3.35 \times 10^{-17} \text{ m}^3/\text{microtank}) (3510 \text{ kg/m}^3 \text{ for diamond}) (657.3 \text{ zJ/atom C}) / (0.90) (1.99 \times 10^{-26} \text{ kg/atom C}) = 4.31 \times 10^{-6} \text{ J/microtank}$, or ~ 51 times more than the $8.48 \times 10^{-8} \text{ J/microtank}$ total energy cost of the gas-filled microtank. Compressing gas is much less energy-intensive than ripping molecules apart into their component atoms.

see: Sugimoto Y, Pou P, Custance O, Jelinek P, Abe M, Perez R, Morita S. Complex Patterning by Vertical Interchange Atom Manipulation Using Atomic Force Microscopy. Science. 2008 Oct 17;322:413-417; <http://www.sciencemag.org/content/322/5900/413.full>.

6.3 Golfballs: Carbon Disposal at Sea

For disposal at sea, it is desirable for the discarded object to fall as quickly as possible through seawater, traveling from ocean surface to ocean floor in the minimum possible time thus minimizing possible interactions with marine life, submersible watercraft, surface ships, and the like.

The terminal velocity of microscopic particles of radius R falling through seawater may be estimated using Stokes Law for Sedimentation,¹³² which is valid in the viscous regime (i.e., Reynolds number $Re \ll 1$)¹³³:

$$v_t = 2 g R^2 (\rho_{\text{particle}} - \rho_{\text{fluid}}) / 9 \eta \quad (8)$$

$$= 0.72 \mu\text{m}/\text{sec}$$

taking the acceleration of gravity $g = 9.81 \text{ m}/\text{sec}^2$, $R = R_{\text{max}} = 2 \mu\text{m}$ for diamond microtanks, $\rho_{\text{particle}} = \rho_{\text{fulltank}} = 1168.8 \text{ kg}/\text{m}^3$, $\rho_{\text{fluid}} = 1021.7 \text{ kg}/\text{m}^3$ for seawater at the ocean surface, and the coefficient of viscosity $\eta = 1.77 \times 10^{-3} \text{ kg}/\text{m}\cdot\text{sec}$ for seawater at $2 \text{ }^\circ\text{C}$.¹³⁴ Assuming a roughly constant fall rate, the average fall time to the ocean floor would be $t_{\text{fall}} = d_{\text{ocean}} / v_t = (3688 \text{ m}) / (0.72 \times 10^{-6} \text{ m}/\text{sec}) = 5.12 \times 10^9 \text{ sec} \sim 163 \text{ yr}$. Releasing microtanks at the ocean surface would quickly produce a murky ocean filled with a dense suspension of gritty diamond particles that would take almost two centuries to settle out to the ocean floor, with major health impacts on marine life, corrosive sandblasting effects on ship propellers, and related problems. This is clearly unacceptable.



A better solution is to pack the microtanks into golfball-size aggregates of radius $R_{\text{golfball}} = 2 \text{ cm}$, forcing them out of the viscous drag regime. The diamond surfaces of loaded microtanks readily can be chemically functionalized, allowing them to be covalently bonded together into a tightly-packed

ball. The volumetric packing factor for closely-packed spheres of equal radius is $f_{\text{pack}} = (3\pi^2 / 64)^{1/2} = 68.017\%$.¹³⁵ Taking the volume of the “golfball” as $V_{\text{golfball}} = (4\pi/3) R_{\text{golfball}}^3 = 3.35 \times 10^{-5} \text{ m}^3/\text{golfball}$, and assuming the interstices between microtanks of density $\rho_{\text{microtank}} = 1168.8 \text{ kg}/\text{m}^3$ are filled with seawater of density $\rho_{\text{seawater}} = 1021.7 \text{ kg}/\text{m}^3$, then golfball mass $M_{\text{golfball}} = [f_{\text{pack}} \rho_{\text{microtank}} + (1 - f_{\text{pack}}) \rho_{\text{seawater}}] V_{\text{golfball}} = [(0.68017) (1168.8 \text{ kg}/\text{m}^3) + (0.31983) (1021.7 \text{ kg}/\text{m}^3)] (3.35 \times 10^{-5} \text{ m}^3/\text{golfball}) = 0.0376 \text{ kg}/\text{golfball}$ with a mean density of $\rho_{\text{golfball}} = M_{\text{golfball}} / V_{\text{golfball}} =$

¹³² https://en.wikipedia.org/wiki/Stokes'_law.

¹³³ For the microtanks, Reynolds number $Re = 2 R \rho_{\text{seawater}} v_{\text{fall}} / \eta = 2 (2 \mu\text{m}) (1021.7 \text{ kg}/\text{m}^3) (0.72 \mu\text{m}/\text{sec}) / (1.77 \times 10^{-3} \text{ kg}/\text{m}\cdot\text{sec}) = 1.66 \times 10^{-6}$.

¹³⁴ “Sea Water Properties – specific volume, specific heat and absolute viscosity,” The Engineering Toolbox; http://www.engineeringtoolbox.com/sea-water-properties-d_840.html.

¹³⁵ Gasson PC. Geometry of Spatial Forms, John Wiley & Sons, New York, 1983.

$(0.0376 \text{ kg}) / (3.35 \times 10^{-5} \text{ m}^3/\text{golfball}) = 1121.7 \text{ kg/m}^3 = \rho_{\text{target}}$. The design and bonding procedure must take care to avoid entrainment of air bubbles in the interstices between microtanks, as these could produce unwanted buoyancy forces.

The number of microtanks packed into each golfball is $N_{\text{tanks/golfball}} = f_{\text{pack}} V_{\text{golfball}} / V_{\text{tankext}} = (0.68017) (3.35 \times 10^{-5} \text{ m}^3/\text{golfball}) / (3.35 \times 10^{-17} \text{ m}^3/\text{microtank}) = 6.80 \times 10^{11}$ microtanks/golfball. Since the energy cost to build and load each microtank is $E_{\text{tank}} = 8.48 \times 10^{-8}$ J/microtank, the energy cost to manufacture each golfball is $E_{\text{golfball}} \sim N_{\text{tanks/golfball}} E_{\text{tank}} = (6.80 \times 10^{11} \text{ microtanks/golfball}) (8.48 \times 10^{-8} \text{ J/microtank}) = 57,700 \text{ J/golfball}$.

A worldwide annual atmospheric CO₂ removal rate of $M_{\text{extract}} = 50 \times 10^{12} \text{ kg/yr}$ requiring an annual building and loading of $N_{\text{microtanks}} = 1.20 \times 10^{27}$ microtanks/yr will produce a total of $N_{\text{golfballs}} = N_{\text{microtanks}} / N_{\text{tanks/golfball}} = (1.20 \times 10^{27} \text{ microtanks/yr}) / (6.80 \times 10^{11} \text{ microtanks/golfball}) = 1.76 \times 10^{15}$ golfballs/yr = 5.61×10^7 golfballs/sec. The total power requirement to build and load this many golfballs is $P_{\text{golfballs}} = N_{\text{golfballs}} E_{\text{golfball}} = (5.61 \times 10^7 \text{ golfballs/sec}) (57,700 \text{ J/golfball}) = 3.24 \times 10^{12}$ watts = 3.24 terawatts.

How fast will a diamond golfball fall from the ocean surface down to the ocean floor? The ratio of inertial to viscous forces is called the Reynolds number $R_e = 2 R_{\text{golfball}} \rho_{\text{seawater}} v_{\text{fall}} / \eta = 2 (2 \text{ cm}) (1021.7 \text{ kg/m}^3) (0.33 \text{ m/sec}) / (1.77 \times 10^{-3} \text{ kg/m-sec}) = 7600$, indicating non-laminar flow. In this flow regime, the terminal velocity of the diamond golfball is:¹³⁶

$$\begin{aligned} v_{\text{fall}} &= (2 g V_{\text{golfball}} (\rho_{\text{golfball}} - \rho_{\text{seawater}}) / \pi R_{\text{golfball}}^2 \rho_{\text{seawater}} C_d)^{1/2} \\ &= 0.33 \text{ m/sec} \end{aligned} \quad (9)$$

where $C_d = 0.47$ is the drag coefficient for a sphere moving in a fluid with $R_e \sim 10,000$.¹³⁷ While the values of several of the constituent variables in Eqn. (9) change slightly as the golfball falls to greater depths, the time to fall from the surface to the average ocean bottom depth is roughly on the order of $t_{\text{fall}} \sim d_{\text{ocean}} / v_{\text{fall}} = (3688 \text{ m}) / (0.33 \text{ m/sec}) = 11,200 \text{ sec} = 3.1 \text{ hr}$.

¹³⁶ https://en.wikipedia.org/wiki/Terminal_velocity.

¹³⁷ https://en.wikipedia.org/wiki/Drag_coefficient.

6.4 Golfcarts: Golfball Manufacturing at Sea

The golfcart is a machine that floats on the ocean surface, absorbing atmospheric CO₂, converting it into diamond golfballs, and then dropping the golfballs overboard, into the sea. The golfcart measures 1 m² x 20 cm in size, about the same as a sofa seat cushion. Its volume is mostly composed of ultralightweight nanomaterial that easily floats in water.

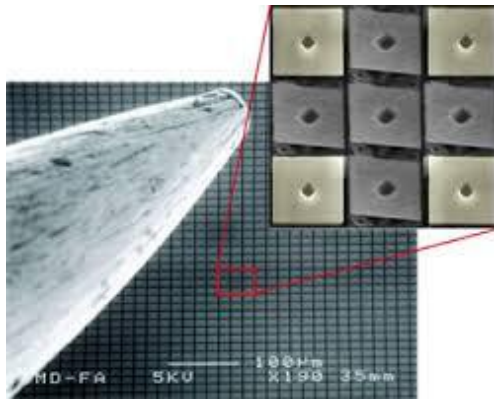


The golfcart's uppermost surface is coated with photovoltaics (**Section 6.4.1**) that absorb sunlight and produce electricity for onboard energy. Under the photovoltaic layer is a grillwork of nanofilter sheets (**Section 5.1.7**), oriented to allow sufficient airflow (**Section 6.4.3**) for efficient CO₂ extraction via molecular filters using sorting rotors (**Section 6.4.2**). Once extracted, the CO₂ is fed into a compact onboard nanofactory (**Section 6.4.4**) that breaks down some of the CO₂, releasing free oxygen and using the liberated carbon atoms to build diamond microtanks. These pure-carbon microtanks are then stuffed with CO₂ molecules at 1032 atm pressure, sealed, aggregated into diamond golfballs, and dropped into the ocean.

Each golfcart is equipped with an onboard nanocomputer, GPS navigation and communication antenna, and two motorized paddlewheels (one for motion in X, another for motion in Y) that provide each golfcart with slow mobility (**Section 6.4.5**). This controlled mobility allows large populations of golfcarts to display “herding” behavior – newcomer machines joining the fleet at the periphery will seek to remain close to their fellows and to maneuver as closely as possible to the center of the population, causing the geographical footprint of the fleet to compactify into a roughly circular shape, forming an artificial floating island of carbon-capture plants. Movements of individual machines, if properly coordinated, can also enforce stationkeeping of the whole “carbon capture island” over a particular geographical spot or circulation region within the ocean. Alternatively, large golfcart assemblies could be compliantly tethered together and then anchored to the seabed floor to prevent accidental migration into commercial shipping lanes.

6.4.1 Onboard Solar Power

The uppermost surface of the golfcart is coated with photocells that absorb sunlight and produce electricity for onboard energy. The solar collector area $A_{\text{solar}} = 1 \text{ m}^2$ will consist of an array of



millions of movable solar cells perhaps resembling the tiny motorized micromirrors in the image at left¹³⁸ that can actively track sun angle (image, below)¹³⁹ for maximum collection efficiency. Conventional research-grade photocells have already demonstrated



efficiencies up to 46% (see **Figure 2**), and nanostructured solar collectors (e.g., nanoantennas or “nantennas”; see image, below)¹⁴⁰ have a theoretical peak efficiency $>90\%$ in specific narrow bandwidths,¹⁴¹ so we’ll assume that a photovoltaic conversion efficiency of $e_{\text{solar}} \sim 50\%$ may be available¹⁴² for solar-tracking microphotocells manufactured by nanofactories. A daily average solar insolation of $I_{\text{solar}} = 200 \text{ W/m}^2$ is readily available in equatorial and mid-latitude ocean sites (see **Figure 1**), so the average continuous electrical power production onboard each golfcart will be $P_{\text{golfcart}} = e_{\text{solar}} I_{\text{solar}} A_{\text{solar}} = (0.50) (200 \text{ W/m}^2) (1 \text{ m}^2) =$

¹³⁸ “Digital micromirror device,” https://en.wikipedia.org/wiki/Digital_micromirror_device; image at https://encrypted-tbn0.gstatic.com/images?q=tbn:ANd9GcSI05Saq9As4sRUnXcnH_JhqXvlRGEmOblDwG6aVol0lZqMuJie.

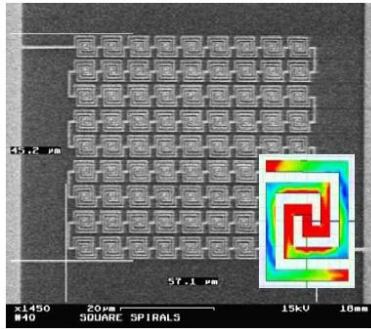
¹³⁹ “Solar tracker,” https://en.wikipedia.org/wiki/Solar_tracker; image at https://en.wikipedia.org/wiki/Solar_tracker#/media/File:8MW_horizontal_single_axis_tracker_in_Greece.JPG.

¹⁴⁰ Sadashivappa G, Sharvari NP. Nanoantenna – a review. Intl. J. Renewable Energy Technol. Res. 4(January 2015):1-9; http://www.ijretr.org/IJRETR_Vol.%204,%20No.%201,%20January%202015/nanoantenna%20.pdf.

¹⁴¹ Kotter DK, Novack SD, Slafer WD, Pinhero P. Solar nantenna electromagnetic collectors. Proc. Energy Sustainability 2008, 10-14 Aug 2008, Paper ES2008-54016; <http://www.univie.ac.at/photovoltaik/vorlesung/ss2013/unit13/nantenna.pdf>. See also: <https://en.wikipedia.org/wiki/Nantenna>.

¹⁴² Our design conclusions are not particularly sensitive to this choice.

100 watts. If the thin film¹⁴³ photovoltaic collectors and support machinery have a thickness of $t_{\text{solar}} = 30 \mu\text{m}$ and are made of diamond of density $\rho_{\text{diamond}} = 3510 \text{ kg/m}^3$, then the mass of the solar collection system on each golfcart is $M_{\text{solar}} = \rho_{\text{diamond}} t_{\text{solar}} A_{\text{solar}} = (3510 \text{ kg/m}^3) (30 \mu\text{m}) (1 \text{ m}^2) = 0.1 \text{ kg}$.



If up to $f_{\text{elect}} = 80\%$ of the golfcart's electrical power supply can be devoted to golfball manufacturing at need, then each golfcart has sufficient energy to manufacture $r_{\text{golfballs}} = f_{\text{elect}} P_{\text{golfcart}} / E_{\text{golfball}} = (0.80) (100 \text{ watts/golfcart}) / (57,700 \text{ J/golfball}) = 1.39 \times 10^{-3} \text{ golfballs/golfcart-sec} \sim 5 \text{ golfballs per golfcart per hr}$.

Each golfcart will also carry an onboard battery to allow operation during periods of darkness or inclement weather and for brief periods of burst power. Research-grade rechargeable lithium-ion batteries (image, right) have already demonstrated energy densities of 9.3 MJ/kg ;¹⁴⁴ using such batteries, 0.5 day of energy storage would require a storage capacity of $(80 \text{ W}) (86400 \text{ sec/day}) (0.5 \text{ day}) = 3.46 \text{ MJ}$ and a battery mass of $(3.46 \text{ MJ}) / (9.3 \text{ MJ/kg}) = 0.37 \text{ kg}$ with a battery volume of $\sim 0.0002 \text{ m}^3$.



If $N_{\text{golfballs}} = 5.61 \times 10^7 \text{ golfballs/sec}$ must be manufactured to meet the worldwide removal target of $M_{\text{extract}} = 50 \times 10^{12} \text{ kg CO}_2/\text{yr}$, this requires fielding and maintaining a steady-state fleet population of $N_{\text{golfcarts}} = N_{\text{golfballs}} / r_{\text{golfballs}} = (5.61 \times 10^7 \text{ golfballs/sec}) / (1.39 \times 10^{-3} \text{ golfballs/golfcart-sec}) = 4.04 \times 10^{10} \text{ golfcarts}$.

Following this deployment, the total surface area of the Earth that would be covered by oceangoing golfcarts is $A_{\text{AllGolfcarts}} = N_{\text{golfcarts}} A_{\text{solar}} = 4.04 \times 10^{10} \text{ m}^2$. That's just $(4.04 \times 10^{10} \text{ m}^2) / (3.619 \times 10^{14} \text{ m}^2) \sim 0.01\%$ of the total area¹⁴⁵ of all Earth's oceans.

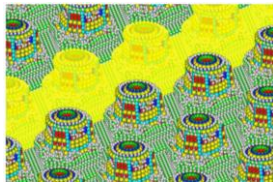
¹⁴³ https://en.wikipedia.org/wiki/Thin-film_solar_cell.

¹⁴⁴ Christopher DeMorro, "New Battery Boasts 7 Times More Energy Density," CleanTechnica, 30 July 2014; <http://cleantechnica.com/2014/07/30/new-battery-boasts-7-times-energy-density/>.

¹⁴⁵ http://www.ngdc.noaa.gov/mgg/global/etop01_ocean_volumes.html.

6.4.2 Number and Area of Sorting Rotors

The total amount of CO₂ that must be removed from the atmosphere to build and to load each microtank is $M_{\text{removeCO}_2} = 4.16 \times 10^{-14}$ kg CO₂/microtank, and there are $N_{\text{tanks/golfball}} = 6.80 \times 10^{11}$ microtanks/golfball, hence to meet their production goal each golfcart must extract $M_{\text{golfcartCO}_2} = M_{\text{removeCO}_2} N_{\text{tanks/golfball}} r_{\text{golfballs}} = (4.16 \times 10^{-14} \text{ kg CO}_2/\text{microtank}) (6.80 \times 10^{11} \text{ microtanks/golfball}) (1.39 \times 10^{-3} \text{ golfballs/golfcart-sec}) = 3.93 \times 10^{-5} \text{ kg CO}_2/\text{golfcart-sec}$, or $N_{\text{golfcartCO}_2} = M_{\text{golfcartCO}_2} / m_{\text{CO}_2} = (3.93 \times 10^{-5} \text{ kg CO}_2/\text{golfcart-sec}) / (7.31 \times 10^{-26} \text{ kg/molecule CO}_2) = 5.38 \times 10^{20}$ molecules CO₂/golfcart-sec.



We will extract the CO₂ using sheets of ~100,000-atom sorting rotors of mass $m_{\text{rotor}} = 2 \times 10^{-21}$ kg/rotor. Taking the atmospheric CO₂ diffusion-limited maximum cycle time of 1800 Hz per binding site (**Section 5.1.5**) and assuming 5 binding sites on our sorting rotors (**Section 4.1**) are exposed to atmosphere at any one time, we can run the rotors at $v_{\text{rotors}} \sim 10,000 \text{ Hz} = 10,000 \text{ molecules CO}_2/\text{rotor-sec}$ and all binding sites will stay fully occupied. This means the required number of sorting rotors is $N_{\text{golfcartRotors}} = N_{\text{golfcartCO}_2} / v_{\text{rotors}} = (5.38 \times 10^{20} \text{ molecules CO}_2/\text{golfcart-sec}) / (10,000 \text{ molecules CO}_2/\text{rotor-sec}) = 5.38 \times 10^{16}$ rotors/golfcart, having a mass $M_{\text{golfcartRotors}} = m_{\text{rotor}} N_{\text{golfcartRotors}} = (2 \times 10^{-21} \text{ kg/rotor}) (5.38 \times 10^{16} \text{ rotors/golfcart}) = 1.08 \times 10^{-4} \text{ kg/golfcart}$ and a surface area $A_{\text{golfcartRotors}} = (5.38 \times 10^{16} \text{ rotors/golfcart}) (7 \text{ nm} \times 14 \text{ nm per rotor}) = 5.27 \text{ m}^2$, and a volume of $V_{\text{golfcartRotors}} = M_{\text{golfcartRotors}} / \rho_{\text{diamond}} = (1.08 \times 10^{-4} \text{ kg/golfcart}) / (3510 \text{ kg/m}^3) = 3 \times 10^{-8} \text{ m}^3$ rotors/golfcart.

6.4.3 Air Throughput Rate

Assume the golfcart filtration volume is 0.05 m^3 ($1 \text{ m}^2 \times 5 \text{ cm}$ high) and therefore contains (2.37×10^{25} molecules CO_2/m^3 at STP) ($400 \text{ ppm CO}_2 - 200 \text{ ppm CO}_2$) ($7.31 \times 10^{-26} \text{ kg/molecule CO}_2$) (0.05 m^3) = $1.73 \times 10^{-5} \text{ kg}$ of extractable CO_2 , again taking CO_2 concentration in the airflow as 400 ppm at entry and 200 ppm at exit. To extract $3.93 \times 10^{-5} \text{ kg CO}_2/\text{golfcart-sec}$ requires about ($3.93 \times 10^{-5} \text{ kg CO}_2/\text{golfcart-sec}$) / ($1.73 \times 10^{-5} \text{ kg of CO}_2$) ~ 2.3 whole-volume air exchanges per second, a total airflow of (0.05 m^3) ($2.3 \text{ exchanges/sec}$) = $0.12 \text{ m}^3/\text{sec}$. If the 1 m^2 golfcart is square, measuring $1 \text{ m} \times 1 \text{ m} \times 0.05 \text{ m}$, with baffles installed on both sides to prevent water entry, then the frontal area facing into the wind is $1 \text{ m} \times 0.05 \text{ m} = 0.05 \text{ m}^2$ and the minimum wind speed required to clear the whole golfcart filtration volume 2.3 times/sec is ($0.12 \text{ m}^3/\text{sec}$) / (0.05 m^2) = 2.4 m/sec . The mean horizontal ocean surface wind speeds are typically 2-5 times higher than this at most places in the world having high solar irradiance (**Section 5.1.6**).

The $A_{\text{golfcartRotors}} = 5.27 \text{ m}^2$ of thin sheets containing the molecular filters are arranged side by side in the golfcart filtration volume, oriented along the direction of airflow, in sheets of size ($1 \text{ m} \times 0.05 \text{ m} = 0.05 \text{ m}^2$) each. The nanofilter sheets are (5.27 m^2) / (0.05 m^2) = 105 in number, and each sheet is spaced at most ($1 \text{ m volume length}$) / (105 sheets) = 0.95 cm apart from its neighboring sheet. Each sheet is held in a rigid frame and includes connector plumbing to allow the purified 1032 atm CO_2 gas to be transferred to the onboard nanofactory that manufactures the golfballs. A subsystem capable of automatically cleaning and keeping salt- and dust-free the nanofilter sheets, possibly including electrostatic filters, sheet wipers, sprayers, or other means, along with specific structures and methods for minimizing binding site fouling, will likely be essential but their precise design is beyond the scope of this basic scaling study.

An alternative carbon capture architecture that should be investigated is the possibility of using a low number density of smooth-surfaced root tendrils embedded with sorting rotors, dangling a short distance in the water below each golfcart to gather dissolved CO_2 from the sea. This approach might offset possible gas collection limitations due to slow vertical convection in the open ocean, ideally without entangling wildlife. The mass-weighted CO_2 concentration in seawater is $\sim 10^{-4}$, comparable to the air concentration. Extraction of this CO_2 would effectively alkalize seawater, slowly drawing more CO_2 out of the atmosphere (and into the oceans) over a timescale of many decades.

6.4.4 Onboard Nanofactory

A mature nanofactory has been described¹⁴⁶ that has a production rate for atomically-precise products of ~1 kg/hr, ~1 kg of active components ($m_{NF} = 0.00028$ kg/sec per kg nanofactory), a volume of 0.05 m^3 ($v_{NF} = 0.0056$ kg/sec per m^3 of nanofactory), and a functional lifetime of at least 10 years.

An onboard nanofactory of this type (one per golfcart) that is specialized to produce only diamond golfballs and nothing else will thus have a mass of $M_{NF} = M_{\text{golfballMfg}} r_{\text{golfballs}} / m_{NF} = (0.0266 \text{ kg/golfball}) (1.39 \times 10^{-3} \text{ golfballs/golfcart-sec}) / (0.00028 \text{ kg/sec per kg nanofactory}) = 0.132 \text{ kg}$ of nanofactory per golfcart and a volume of $V_{NF} = M_{\text{golfballMfg}} r_{\text{golfballs}} / v_{NF} = (0.0266 \text{ kg/golfball}) (1.39 \times 10^{-3} \text{ golfballs/golfcart-sec}) / (0.0056 \text{ kg/sec per } \text{m}^3 \text{ of nanofactory}) = 0.0066 \text{ m}^3$ of nanofactory per golfcart, where the manufactured mass comprising each golfball is $M_{\text{golfballMfg}} = f_{\text{pack}} \rho_{\text{microtank}} V_{\text{golfball}} = (0.68017) (1168.8 \text{ kg/m}^3) (3.35 \times 10^{-5} \text{ m}^3/\text{golfball}) = 0.0266 \text{ kg}$ per golfball, a figure that excludes the interstitial seawater mass component of a submerged golfball.

¹⁴⁶ Drexler KE, Nanosystems, Wiley, 1992, Chapter 14.

6.4.5 Paddlewheel Motive Power

Each golfcart has two paddlewheel mechanisms to provide motive power across the ocean surface. Ocean currents in the Gulf Stream and the Somali Current can reach 1.5-2 m/sec, but in most of the ocean peak surface currents on the order of 0.3-1 m/sec are more typical.¹⁴⁷

For a 1 m/sec mobility system, paddlewheel power $P_{\text{paddlewheel}} = (1/2) e_{\text{paddle}} \rho_{\text{seawater}} A_{\text{paddle}} v_{\text{paddle}}^3 = 2.6$ watts, taking paddlewheel efficiency $e_{\text{paddle}} = 50\%$,¹⁴⁸ seawater density $\rho_{\text{seawater}} = 1021.7 \text{ kg/m}^3$ (at 20 °C), paddle surface area $A_{\text{paddle}} = 5 \text{ cm} \times 10 \text{ cm} = 0.01 \text{ m}^2$, and paddle velocity $v_{\text{paddle}} = 1 \text{ m/sec}$. Note that an efficiency of 50% means that 5.2 watts must be applied to each paddlewheel to obtain 2.6 watts of motive power. Paddlewheel paddle volume $V_{\text{paddle}} = t_{\text{paddle}} A_{\text{paddle}} = 0.000005 \text{ m}^3$ and paddle mass $M_{\text{paddle}} = V_{\text{paddle}} \rho_{\text{diamond}} = 0.01755 \text{ kg}$, taking paddle thickness $t_{\text{paddle}} = 0.5 \text{ mm}$ and paddle density $\rho_{\text{diamond}} = 3510 \text{ kg/m}^3$ for diamond. With 2 paddlewheels, total power draw is 10.4 watts, paddle mass is 0.0351 kg and paddle volume is 0.00001 m^3 . Allowing additional unspecified motors, machinery, control circuits and other components having a mass of 0.0649 kg and a volume of 0.00002 m^3 gives us a total of 0.1 kg and 0.00003 m^3 for the entire paddlewheel assembly.

Propeller-driven mobility systems should also be considered but have not been reviewed here. Another alternative is to include a small retractable sail to gain extra advantage for power and steering from wind power, should that become necessary. But all such elaborations are beyond the scope of this paper.

A golfcart motoring cross-current on the sea surface at 1 m/sec could traverse a 1000 km journey from coastal shore nanofactory to mid-ocean deployment site (**Section 6.5**) in $\sim 10^6 \text{ sec} = 11.6$ days. Mobility system velocities much higher than the ~ 10 -watt system described above should be available if needed, given access at need to up to ~ 100 watts of onboard power.

¹⁴⁷ “Chapter 31. Ocean Currents: Types and Causes of Currents,” http://msi.nga.mil/MSISiteContent/StaticFiles/NAV_PUBS/APN/Chapt-32.pdf; “Speed of Ocean Currents,” The Physics Factbook, <http://hypertextbook.com/facts/2002/EugeneStatnikov.shtml>.

¹⁴⁸ Li Y, Zhang Q, Wang Z, Wu X, Cong W. Evaluation of power consumption of paddle wheel in an open raceway pond. *Bioprocess Biosyst Eng.* 2014 Jul;37(7):1325-36; <http://www.ncbi.nlm.nih.gov/pubmed/24346764>.

6.4.6 Summary of Golfcart Mass, Volume and Productivity

Table 3 summarizes the masses and volumes of the subsystems described earlier in this Section. Components which have not yet been identified are lumped together in the “unassigned” category and are given a mass of 0.27 kg and a volume of 0.14 m³ – a net density of 1.9 kg/m³ which is about twice the density of commercially-available ~1 kg/m³ silica aerogel.¹⁴⁹

In sum: The golfcart has dimensions of 1 m x 1 m x 20 cm, a mass of ~1 kg, a volume of 0.2 m³, onboard power generation of ~100 watts, and a production rate of ~5 golfballs/hr (~ 3.7 x 10⁻⁵ kg/sec of golfballs) that are made of diamond and packed with liquid CO₂ at 1032 atm pressure.

Table 3. Golfcart mass and volume estimates.		
Golfcart Component	Estimated Mass (kg)	Estimated Volume (m³)
Solar cells	0.100000	0.0000300
Battery	0.370000	0.0002000
Golfball in process	0.026600	0.0003350
Filtration volume	---	0.0500000
Sorting rotors	0.000108	---
Onboard golfball nanofactory	0.132000	0.0066000
Paddlewheel assembly	0.100000	0.0000300
<i>Subtotals</i>	<i>0.728708</i>	<i>0.0568935</i>
Unassigned	0.271292	0.1431065
Totals	1.000000	0.2000000

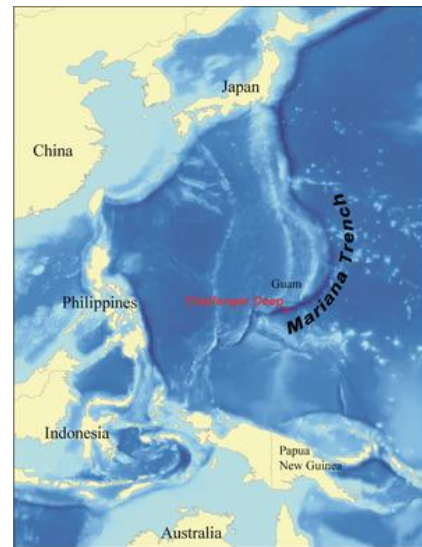
¹⁴⁹ <https://en.wikipedia.org/wiki/Aerogel>.

6.5 The Siting of Carbon Capture Islands

Meeting the worldwide removal target of $M_{\text{extract}} = 50 \times 10^{12}$ kg CO₂/yr requires fielding and maintaining a steady-state fleet population of $N_{\text{golfcarts}} = 4.04 \times 10^{10}$ golfcarts having a total ocean-covering surface area of $A_{\text{AllGolfcarts}} = 4.04 \times 10^{10} \text{ m}^2 = 40,400 \text{ km}^2$, representing $(4.04 \times 10^{10} \text{ m}^2) / (3.619 \times 10^{14} \text{ m}^2) \sim 0.01\%$ of the total area of all Earth's oceans. This global population of golfcarts may form up into one or more compact "carbon capture islands" on the sea surface. As a point of reference, a single 40,400 km² carbon capture island would be the 35th largest island in the world, slightly larger than Taiwan (35,883 km²), a bit smaller than Sri Lanka (65,268 km²), and almost twice the area of Sicily (25,662 km²).¹⁵⁰

Where should the carbon capture island(s) be sited?

Mariana Trench. One possibility would be to park a single 40,400 km² carbon capture island directly over the Mariana Trench (image, right),¹⁵¹ thus ensuring that the diamond golfballs would drop into the deepest ocean location on the planet. The Trench is 2550 km long with an average width of 69 km, for a total area of $(2550 \text{ km})(69 \text{ km}) = 175,950 \text{ km}^2$ which is more than 4 times larger than the 40,400 km² that we need for the carbon capture island. However, a circular carbon capture island of area 40,400 km² would have a diameter of $(2) [(40,400 \text{ km}^2)/\pi]^{1/2} = 227 \text{ km}$. That's much larger than the 69 km average Trench width, so the shape of the self-assembling carbon capture island would have to be engineered to form a long skinny oval or arcing rectangle (e.g., ~40 km x 1000 km), tracing the geographic curve of the Trench.



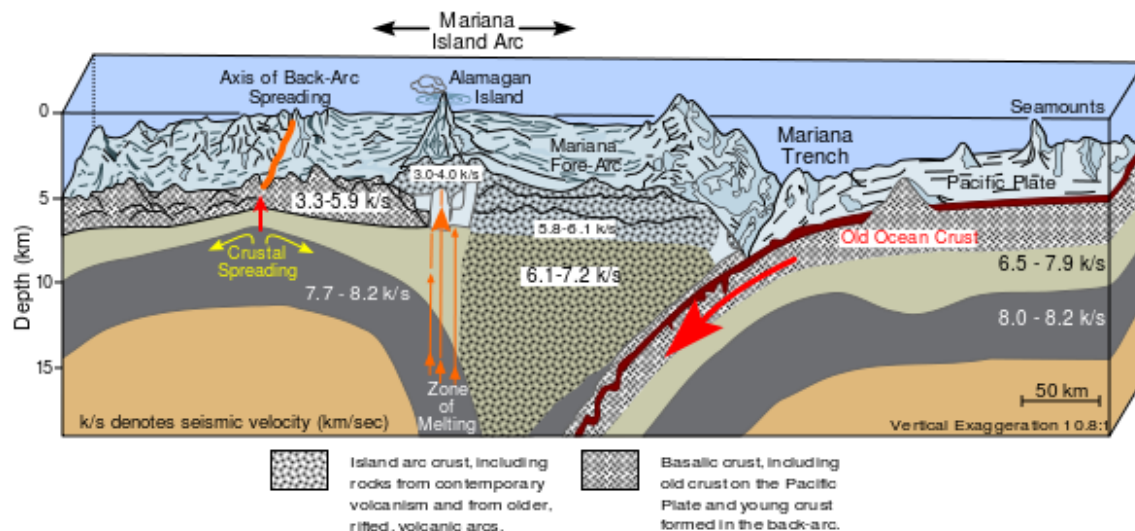
The maximum recorded depth of the Mariana Trench is 10,994 m. The pressure is 1121.9 atm at that depth, with seawater 5.3% denser than on the ocean surface. Interestingly, at that depth the compressed CO₂ is also 4.2% denser than it was at the 1032 atm microtank loading pressure (see **Table 2**), so the terminal velocity of the golfballs is not much changed near the end of its descent to the Trench floor, and the diamond walls of the microtank will have moved from resisting 1032 atm of pressure in tension to resisting 90 atm in compression, a change that should be easily handled by this material.

One additional consideration is that the Trench is located on a subduction zone. Specifically, the Pacific plate is being subducted beneath the Mariana Plate, creating the Mariana trench and the arc of the Mariana islands which are formed as water trapped in the plate is released and explodes

¹⁵⁰ https://en.wikipedia.org/wiki/List_of_islands_by_area.

¹⁵¹ https://en.wikipedia.org/wiki/Mariana_Trench.

upward to form island volcanoes (image, below).¹⁵² As with the released water, all CO₂-containing golfballs that are dropped into the Trench will be pulled into the Earth and heated at ever-higher pressures. Eventually, the microtanks might break down and release their gaseous cargo, which may find its way back into the atmosphere via volcanic activity or by other routes.¹⁵³ This is certainly a long-term consideration but probably not a near-term problem. By comparison, sea floor spreading is occurring along the mid-Atlantic Ridge,¹⁵⁴ so any carbon-capture materials deposited there might well remain undisturbed for geological times.



Cross-Section Sketch of Mariana Arc

The Mariana Islands,¹⁵⁵ located near the edge of the Trench, are inhabited and form part of Micronesia. They are U.S. territories¹⁵⁶ – the Commonwealth of the Northern Mariana Islands, and Guam. Would their inhabitants object to a 40,400 km² artificial island being permanently located on their doorstep, or would they welcome it because of all the global attention, commerce, jobs and wealth the onshore nanofactories might bring?

¹⁵² https://en.wikipedia.org/wiki/Mariana_Trench#/media/File:Cross_section_of_mariana_trench.svg.

¹⁵³ Plate subduction zones are also associated with very large megathrust earthquakes, the effects of which are unpredictable and possibly adverse to the safety of long-term disposal; https://en.wikipedia.org/wiki/Megathrust_earthquake.

¹⁵⁴ https://en.wikipedia.org/wiki/Mid-Atlantic_Ridge.

¹⁵⁵ https://en.wikipedia.org/wiki/Mariana_Islands.

¹⁵⁶ https://en.wikipedia.org/wiki/Micronesia#Mariana_Islands.

There are some minor lifeforms (e.g., giant 4-cm amoebas, shrimp, and other tiny organisms) living in the muddy “waste of firm diatomaceous ooze” on the Trench seafloor that might be disturbed by a slow rain of golfballs, and a few snailfish and large crustaceans have been observed swimming in the deep water around 8100 m depth.¹⁵⁷ If $N_{\text{golfcarts}} = 4.04 \times 10^{10}$ golfcarts drop $N_{\text{golfballs}} = 1.76 \times 10^{15}$ golfballs/yr into the Mariana Trench, randomly distributed over an $A_{\text{AllGolfcarts}} = 4.04 \times 10^{10} \text{ m}^2 = 40,400 \text{ km}^2$ footprint, then taking golfball volume $V_{\text{golfball}} = 3.35 \times 10^{-5} \text{ m}^3/\text{golfball}$ we estimate that the golfball accumulation rate on the seafloor of the Mariana Trench would approximate $d_{\text{accum}} \sim V_{\text{golfball}} N_{\text{golfballs}} / A_{\text{AllGolfcarts}} = (3.35 \times 10^{-5} \text{ m}^3/\text{golfball}) (1.76 \times 10^{15} \text{ golfballs/yr}) / (4.04 \times 10^{10} \text{ m}^2) = 1.46 \text{ m/yr}$ of golfball accumulation (~0.01% of Trench depth per year), or 0.34 m/yr if the golfballs can be distributed randomly over the entire 175,950 km^2 area of the Mariana Trench.

Oceanic Gyres. Perhaps a better solution is to split the golfcart population into several smaller tranches and to position them geographically more or less evenly around the world, perhaps ideally at the centers of the 5 major oceanic gyres where surface currents are so low that carbon capture island stationkeeping will require a minimum expenditure of motive energy by the golfcarts.

Currents in the North Pacific Gyre (**Figure 5**) have trapped exceptionally high concentrations of suspended plastic and other manmade debris in a formation known as the Pacific Trash Vortex (135°-155°W, 35°-42°N, between San Francisco and Hawaii), roughly the size of Texas.¹⁵⁸ The currents of the Sargasso Sea in the North Atlantic Gyre also accumulate a large vortex of non-biodegradable plastic waste. (The central regions of each of these gyres would be individually large enough to easily accommodate the entire golfcart population – e.g., the Sargasso Sea¹⁵⁹ has an area of 3,000,000 km^2 – but a wider geographic distribution seems advisable.)

Ideally we would locate our floating gyre-islands in areas that avoid the major shipping lanes (**Figure 6**)¹⁶⁰ where most ships may pass. A golfcart stationkeeping system employing herding behavior and self-assembly could be designed to temporarily open up internal channels to allow the occasional large ship to pass without damage to either island or ship, and for the island to reassemble itself automatically in the wake of the passing ship. But it would be better if the five carbon capture islands are marked with radio buoys so that ships can simply avoid contact with

¹⁵⁷ https://en.wikipedia.org/wiki/Mariana_Trench#Life.

¹⁵⁸ Day RH, Shaw DG, Ignell SE. Quantitative distribution and characteristics of neustonic plastic in the North Pacific Ocean. Final Report to U.S. Department of Commerce, National Marine Fisheries Service, Auke Bay Laboratory, Auke Bay, AK, 1988, pp. 247-266; http://swfsc.noaa.gov/publications/TM/SWFSC/NOAA-TM-NMFS-SWFSC-154_P247.PDF. Justin Berton, “Continent-size toxic stew of plastic trash fouling swath of Pacific Ocean,” San Francisco Chronicle, Friday, 19 October 2007, W-8; <http://www.sfgate.com/cgi-bin/article.cgi?f=/c/a/2007/10/19/SS6JS8RH0.DTL>.

¹⁵⁹ <http://www.lighthouse-foundation.org/index.php?id=131&L=1>.

¹⁶⁰ “Shipping routes red black” Halpern BS (Hengl T, Groll D); https://en.wikipedia.org/wiki/Sea_lane#/media/File:Shipping_routes_red_black.png.

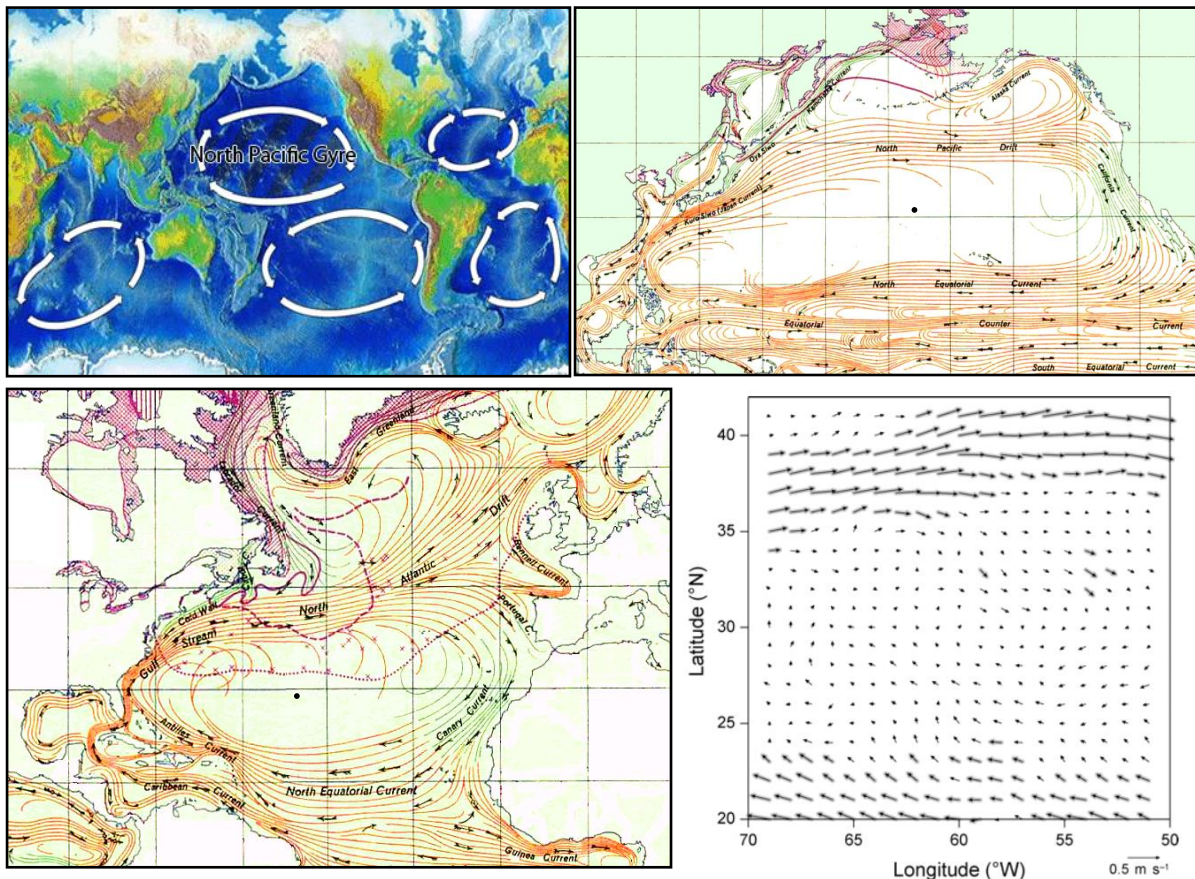
each of the roughly circular (2) $[(40,400 \text{ km}^2)/5\pi]^{1/2} \sim 100 \text{ km}$ diameter carbon capture islands that could be sited within each ocean gyre (e.g., see the two tiny black dots in **Figure 5**).

Figure 5. Top, left: The 5 major ocean gyres, including the North Pacific Gyre.¹⁶¹

Top, right: Close-up of the North Pacific Gyre.¹⁶²

Bottom, left: Close-up of Sargasso Sea in North Atlantic Gyre.¹⁶³

Bottom, right: Sargasso Sea surface current velocity map.¹⁶⁴



(The two tiny black dots, in images top right and bottom left, mark the location of carbon capture islands and are each $\sim 8080 \text{ km}^2$ in size.)

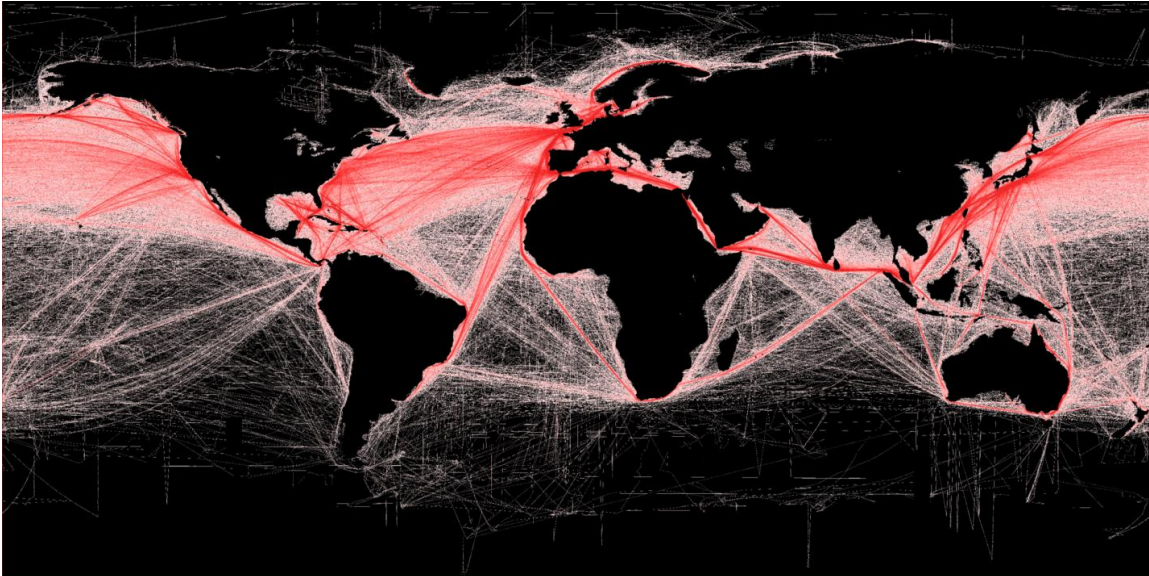
¹⁶¹ http://en.wikipedia.org/wiki/File:North_Pacific_Gyre_World_Map.png.

¹⁶² http://en.wikipedia.org/wiki/File:North_Pacific_Gyre.png.

¹⁶³ http://en.wikipedia.org/wiki/File:North_Atlantic_Gyre.png.

¹⁶⁴ Friedland KD, Miller MJ, Knights B. Oceanic changes in the Sargasso Sea and declines in recruitment of the European eel. ICES Journal of Marine Science. (2007) 64(3):519-530; <http://icesjms.oxfordjournals.org/content/64/3/519.full>.

Figure 6. Map of the world's major shipping lanes (sea lanes).



The seabed under the ocean gyres typically has a depth of ~ 4000 m, although a few places in the Sargasso are as deep as 7000 m.¹⁶⁵ If $N_{\text{golfcarts}} = 4.04 \times 10^{10}$ golfcarts drop $N_{\text{golfballs}} = 1.76 \times 10^{15}$ golfballs/yr into each of five gyres, randomly distributed over an $A_{\text{AllGolfcarts}} = 4.04 \times 10^{10} \text{ m}^2 = 40,400 \text{ km}^2$ footprint, then taking golfball volume $V_{\text{golfball}} = 3.35 \times 10^{-5} \text{ m}^3/\text{golfball}$ we estimate that the golfball accumulation rate on the seafloor under each ocean gyre would approximate $d_{\text{accum}} \sim V_{\text{golfball}} N_{\text{golfballs}} / 5 A_{\text{AllGolfcarts}} = (3.35 \times 10^{-5} \text{ m}^3/\text{golfball}) (1.76 \times 10^{15} \text{ golfballs/yr}) / (5) (4.04 \times 10^{10} \text{ m}^2) = 0.29 \text{ m/yr}$ of golfball accumulation ($\sim 0.007\%$ of gyre seafloor depth per year).

However, the each of the ocean gyres is far larger than the $\sim 8080 \text{ km}^2$ footprint of the carbon capture island to be ensconced within each gyre. For example, the North Atlantic Gyre is $3,000,000 \text{ km}^2$ in extent, and the North Pacific Subtropical Gyre is $700,000 \text{ km}^2$ to $15,000,000 \text{ km}^2$ in size. If it can be arranged for each carbon capture island to slowly circulate around an area of $A_{\text{circulate}} \sim 1,000,000 \text{ km}^2 (= 1 \times 10^{12} \text{ m}^2)$ within each gyre, then the golfball accumulation rate on the seafloor under each ocean gyre could be reduced to $d_{\text{accum}} \sim V_{\text{golfball}} N_{\text{golfballs}} / 5 A_{\text{circulate}} = (3.35 \times 10^{-5} \text{ m}^3/\text{golfball}) (1.76 \times 10^{15} \text{ golfballs/yr}) / (5) (1 \times 10^{12} \text{ m}^2) = 0.01 \text{ m/yr} (= 1 \text{ cm/yr})$ of golfball accumulation ($\sim 0.0003\%$ of gyre seafloor depth per year). In this circumstance, the seafloor deposition plain of the much larger area $A_{\text{circulate}}$ would be receiving a coating of **one golfball monolayer every ~ 4 years.**¹⁶⁶

¹⁶⁵ <http://www.lighthouse-foundation.org/index.php?id=131&L=1>.

¹⁶⁶ It might be possible to use diamond golfballs as landfill to build artificial seamounts, ultimately enabling the creation of above-sea-level artificial islands. Ignoring numerous engineering challenges, the annual worldwide golfball disposal volume of $V_{\text{golfball}} N_{\text{golfballs}} = (3.35 \times 10^{-5} \text{ m}^3/\text{golfball}) (1.76 \times 10^{15} \text{ golfballs/yr}) = 5.90 \times 10^{10} \text{ m}^3/\text{yr}$ would suffice to create above-sea-level artificial island surface at a maximum build rate of $(5.90 \times 10^{10} \text{ m}^3/\text{yr}) / (4000 \text{ m}) = 1.47 \times 10^7 \text{ m}^2/\text{yr} \sim 15 \text{ km}^2/\text{yr}$ from a seafloor at average depth 4000 m.

Once the golfballs arrive on the ocean floor, will they stay put? Deep sea currents do exist, but they are very slow, typically ~1-3 cm/sec,¹⁶⁷ which seems too weak to dislodge or roll golfballs that have settled onto the seabed floor. Later-arriving golfballs that settle onto a layer of existing golfballs coating the seafloor may nestle into a close-packed geometry and not be easily dislodged by such weak currents. The low impact velocity of $v_{\text{fall}} = 0.33$ m/sec (**Section 6.3**) seems unlikely to damage the diamond golfball structure. Golfballs descending into the ocean depths are moving slowly enough that any physical impact with living creatures seems unlikely to cause material damage to either.

Will falling golfballs bother the fish? The steady-state number density of golfballs in transit through the seawater under an extended circulation area for all 5 gyres is $n_{\text{gb}} = N_{\text{golfballs}} d_{\text{ocean}} / (5 A_{\text{circulate}} d_{\text{ocean}} v_{\text{fall}}) = 3.41 \times 10^{-5}$ golfballs/m³. The encounter rate between sea animals such as fish and golfballs is $r_{\text{gb}} \sim n_{\text{gb}} A_{\text{fish}} v_{\text{fish}} = 3.41 \times 10^{-8}$ golfballs/sec ~ 1 golfball/yr, for animals with an encounter area of $A_{\text{fish}} = 100$ cm² and a daily average swimming speed of $v_{\text{fish}} = 0.1$ m/sec. Thus the average fish swimming in a gyre might encounter a falling golfball about once a year. In the unlikely event that a chemically inert golfball is swallowed by a larger animal such as a shark or whale, the object should either pass through the digestive system unmolested or will first be chewed and broken into smaller pieces – each of which will be equally chemically inert and indigestible, all the way down in size to the individual microtanks of which the golfball is composed. The physical breakage of a few microtanks, resulting in some compressed CO₂ release, will produce a fizzy acidic taste that will likely cause the items to be harmlessly spat out of the large animal's mouth.

In general, the ocean gyres are nutrient-poor regions of the sea and don't contain a lot of fish; "benthic" life on the ocean floor is mostly microscopic. Low nutrient concentrations and thus a low density of living organisms characterize the surface waters of the gyres. The deep benthic habitats of the ocean gyres have been thought to typically consist of some of the most food-poor regions on the planet.¹⁶⁸ "At the depths of the gyre lies a sea floor of fine-grained clay sediments. This sediment is home to a community of organisms, which generally receive their nutrients as a "rain" of productivity sinking from above. At depth under the gyre lies one of the most food-poor areas on the planet, which therefore supports very low densities and biomass of benthic infauna, or animals residing in the sediment." Presumably the benthic fauna will readily adapt to the presence of the slowly-growing matrix of inert golfballs and indigenous clay, just as sea life adapts to the growing presence of carbonate deposits in coral reefs (image, right) at shallower depths.¹⁶⁹



¹⁶⁷ <http://science.howstuffworks.com/environmental/earth/oceanography/ocean-current3.htm>.

¹⁶⁸ https://en.wikipedia.org/wiki/Ecosystem_of_the_North_Pacific_Subtropical_Gyre.

¹⁶⁹ https://en.wikipedia.org/wiki/Coral_reef.

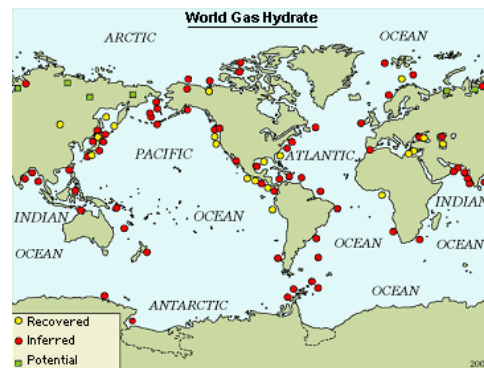
Although the carbon capture islands will be sited over biologically sparse regions of the sea, and even though the $\sim 8080 \text{ km}^2$ footprint of each carbon capture island blocks only $\sim 0.8\%$ of the extended circulation area of $\sim 1,000,000 \text{ km}^2$ within each gyre, ecologists will need to study the degree to which the local reduction of sunlight may impact biological diversity. The movement of the carbon capture islands within a larger circulation area inside each gyre should ensure access to sunlight for most of the time to most of the ocean area. If necessary, golfcarts can be programmed to jostle their neighbors, opening temporary holes in random locations to allow the periodic penetration of sunlight. Alternatively, the carbon capture island architecture could be re-designed to include persistently open holes, gaps, or strips to ensure that no deployment ever leaves the local marine flora in permanent shadow or significantly reduces biodiversity.

There is no absolute requirement for all golfcarts to be accreted into large single islands. Small numbers of smaller carbon capture islands, or even large populations of non-accreted individual golfcarts, are technically possible. The impact of such scenarios, e.g., on marine navigation by commercial shipping vessels, should be studied further but is beyond the scope of this paper. The stability of carbon capture islands, and individual golfcarts, during episodes of high winds should also be investigated, with carbon capture islands located as far away from seasonal hurricane and monsoon tracks as possible.



The arrival of golfballs on the deep ocean floor should not affect the disposition of methane clathrates (aka. methane hydrates; image, left) – methane trapped in water-ice lattice on the ocean floor. Apparently there are $5\text{-}25 \times 10^{14} \text{ kg}$ of methane locked up in marine clathrates.¹⁷⁰ However, this hydrate forms in only a narrow range of depths (continental shelves); methane clathrates in continental rocks are trapped in beds of sandstone or siltstone at ocean depths of less than 800 m.¹⁷¹ Their

typical depth profile and geological locations (map, right)¹⁷² suggest that clathrates will be present only at low concentrations on the seabed floors under the ocean gyres where golfballs would be dropped, and, when present, would likely be mixed with benthic sediments that should not be mechanically disturbed by the gentle arrival of isothermal golfballs.



¹⁷⁰ Milkov AV. Global estimates of hydrate-bound gas in marine sediments: how much is really out there? *Earth-Sci Rev.* 2004; 66 (3–4):183-197; <http://www.sciencedirect.com/science/article/pii/S0012825203001296>.

¹⁷¹ https://en.wikipedia.org/wiki/Methane_clathrate.

¹⁷² <http://www.azimuthproject.org/azimuth/show/Methane+clathrate>.

6.6 Manufacturing Golfcarts Using Onshore Nanofactories

Diamondoid golfcarts would be manufactured using general-purpose nanofactories located onshore in coastal regions nearest the deployment site(s). If $N_{\text{golfballs}} = 5.61 \times 10^7$ golfballs/sec must be manufactured to meet the worldwide removal target of $M_{\text{extract}} = 50 \times 10^{12}$ kg CO₂/yr, this requires fielding and maintaining a steady-state fleet population of $N_{\text{golfcarts}} = 4.04 \times 10^{10}$ golfcarts.

If golfcarts have a lifetime of $\tau_{\text{golfcart}} = 10$ years (after which time they are returned to shore for recycling or in a few cases gracefully scuttled at sea if inoperable), then to maintain a population of 4.04×10^{10} golfcarts we must manufacture $N_{\text{golfcarts}} / \tau_{\text{golfcart}} = 4.04 \times 10^9$ golfcarts/yr at 1 kg per golfcart, or $r_{\text{golfcarts}} = 4.04 \times 10^9$ kg/yr of diamondoid golfcarts.

Using second-generation nanofactories producing ~ 1 kg/day of product, manufacturing this many golfcarts would require $(4.04 \times 10^9 \text{ kg/yr}) / (365 \text{ kg/nanofactory-yr}) = 11$ million onshore nanofactories, each of mass ~ 100 kg and volume $\sim 1 \text{ m}^3$, for a total mass of ~ 1.1 million tonnes of onshore nanofactories having a total volume of 11 million m^3 (an $\sim 11 \text{ km}^2$ factory floor footprint).

Using mature nanofactories producing ~ 1 kg/hr of product, manufacturing this many golfcarts would require $(4.04 \times 10^9 \text{ kg/yr}) / (8760 \text{ kg/nanofactory-yr}) = 461,000$ onshore nanofactories, each of mass ~ 1 kg and volume $\sim 0.05 \text{ m}^3$ (**Section 6.4.4**), for a total mass of ~ 461 tonnes of onshore nanofactories having a volume of 23,000 m^3 . Given these superior numbers, it may make sense to delay the full global deployment program until mature nanofactories are widely available for molecular manufacturing.

If the energy cost of synthesizing diamondoid materials from hydrocarbon feedstocks in onshore nanofactories is $\sim 10^8 \text{ J/kg}$,¹⁷³ then the power requirement for all the onshore nanofactories needed to make all the floating golfcarts is $(\sim 10^8 \text{ J/kg}) (4.04 \times 10^9 \text{ kg/yr}) / (3.14 \times 10^7 \text{ sec/yr}) = 12.9 \text{ GW}$. This modest power requirement could be entirely supplied from “green” sources, e.g., by any one of the three largest hydroelectric power plants in the world,¹⁷⁴ or by a handful of custom-built 2-5 GW nuclear power plants (of which there already exist at least 74 such plants in the world).¹⁷⁵ Of course, nanofactory-manufactured atomically-precise photovoltaic systems are likely to be vastly cheaper to build and operate per delivered watt of solar power than present-day conventional hydroelectric, wind, geothermal, or nuclear-electric systems.

At a $p_{\text{mfg}} = \$1/\text{kg}$ manufacturing cost in onshore-based mature nanofactories, the manufacturing cost to set up the initial global system over a $\tau_{\text{rollout}} = 10$ yr rollout period is $C_{\text{install}} = 10 p_{\text{mfg}} r_{\text{golfcarts}} = (10) (\$1/\text{kg}) (4.04 \times 10^9 \text{ kg/yr}) = \40.4 billion, or $C_{\text{install}} / \tau_{\text{rollout}} = \4.04 billion/yr on an annual

¹⁷³ Drexler KE, Nanosystems, Wiley, 1992, Section 13.3.7(b).

¹⁷⁴ https://en.wikipedia.org/wiki/List_of_conventional_hydroelectric_power_stations.

¹⁷⁵ https://en.wikipedia.org/wiki/List_of_nuclear_power_stations.

basis during the 10-yr initial deployment. Thereafter, the annual manufacturing cost to indefinitely maintain the system is $C_{\text{annual}} = p_{\text{mfg}} r_{\text{golfcarts}} = \4.04 billion/yr.

Thus the net (manufacturing) cost for a **worldwide annual atmospheric CO₂ removal** rate of $M_{\text{extract}} = 50 \times 10^{12}$ kg CO₂/yr (=50 x 10⁹ tonne CO₂/yr) is $C_{\text{annual}} =$ **\$4.04 billion/yr.**

The net (manufacturing) **cost of atmospheric carbon capture**, using the mature nanofactory-based CO₂ capture system described in this Section, is a truly astonishing $C_{\text{annual}} / M_{\text{extract}} =$ (\$4.04 billion/yr) / (50 x 10⁹ tonne CO₂/yr) = **\$0.08/tonne CO₂.**

How is such a low cost possible? The answer is simple: the energy that is required to drive the carbon capture and mechanosynthetic chemical processes is provided – thanks to inexpensive nanofactory-based manufacturing – almost for “free”.

Specifically, the photovoltaic panel on the roof of each golfcart generates $P_{\text{golfcart}} = 100$ watts of power but has a mass of only $M_{\text{solar}} = 0.1$ kg. With a $p_{\text{mfg}} = \$1/\text{kg}$ manufacturing cost using mature onshore-based nanofactories,¹⁷⁶ the manufacturing cost to make the photovoltaic roof panel is only $p_{\text{solar}} = M_{\text{solar}} p_{\text{mfg}} = (0.1 \text{ kg}) (\$1/\text{kg}) = \$0.10$, which is a manufacturing cost of $p_{\text{solar}} / P_{\text{golfcart}} =$ **\$0.001/watt.** That’s 300 times cheaper than the estimated **\$0.30/watt** manufacturing cost of today’s least expensive crystalline silicon solar cells.¹⁷⁷

Assuming a lifetime of $\tau_{\text{golfcart}} = 10$ years in service, the lifetime cost per joule of energy delivered to the golfcarts for carbon capture is $p_{\text{lifetime}} = p_{\text{solar}} / [P_{\text{golfcart}} \tau_{\text{golfcart}}] = (\$0.1) / [(100 \text{ watts}) (3.14 \times 10^7 \text{ sec/yr}) (10 \text{ yr})] =$ **3.18 x 10⁻¹² \$/J** (because sunlight is provided for “free”), which is 6000 times cheaper than $p_{\text{elect}} =$ **1.94 x 10⁻⁸ \$/J**, the present-day cost of industrial electricity.

¹⁷⁶ The estimated manufacturing cost for atomically precise diamondoid products using the first nanofactory is ~**\$1000/kg** of finished product, falling to ~**\$10/kg** for second-generation nanofactories that are constructed from components fabricated by the first nanofactory. Manufacturing cost for a mature later-generation nanofactory should approximate ~**\$1/kg** – see Drexler KE, Nanosystems: Molecular Machinery, Manufacturing, and Computation, John Wiley & Sons, New York, 1992; Section 14.5.6(h). Freitas RA Jr. Economic impact of the personal nanofactory. Nanotechnology Perceptions: A Review of Ultraprecision Engineering and Nanotechnology 2(May 2006):111-126, <http://www.rfreitas.com/Nano/NoninflationaryPN.pdf>. Freitas RA Jr., Merkle RC. Kinematic Self-Replicating Machines, Landes Bioscience, Georgetown, TX, 2004, pp. 202-204; <http://www.molecularassembler.com/KSRM/6.2.2.htm>).

¹⁷⁷ <http://pv.energytrend.com/pricequotes.html>. Also see chart: https://en.wikipedia.org/wiki/Cost_of_electricity_by_source#/media/File:Price_history_of_silicon_PV_cells_since_1977.svg.

7. Conclusions

Cost estimates on conventional technologies for atmospheric carbon capture optimistically estimate **\$70-\$200/tonne CO₂ and higher** (Section 3.3). This range pushes the outer limits of what seems to be economically feasible.

The new carbon capture technology proposed here, built by molecular manufacturing using first-generation nanofactories at a manufacturing cost of ~\$1000/kg, would enable the atmospheric capture of CO₂ at a total lifetime cost of about **\$21/tonne CO₂**. The molecular filter approach is far less costly than other proposed technologies and will approach the thermodynamic minimum for energy consumption in the gas separation application. The same filtration technology is readily extended to include the extraction of other greenhouse gases and atmospheric pollution gases, at no appreciable increase in system cost or performance.

Even using a first-generation nanofactory, an initial installation cost of \$2.74 trillion/yr for 10 years followed by a maintenance cost of **\$0.91 trillion per year** would allow the establishment of a network of direct atmospheric CO₂ capture plants that are powerful enough to reduce global CO₂ levels by ~50 ppm per decade, easily overwhelming current anthropogenic emission rates. This is sufficient to return Earth's atmosphere to pre-industrial carbon dioxide levels near 300 ppm within 40 years from launch of program, and thereafter to maintain the atmosphere in this ideal condition indefinitely, eliminating one of the primary drivers of global climate change on our planet. Advantages include a low environmental footprint and a fail-safe mode of operation.

Lower cost later-generation nanofactories will allow, within the same timeframe, the deployment of a global system of floating carbon capture islands, possibly sited in the stable ocean gyres, having comparable CO₂ extraction and sequestration capabilities as the simpler system described above. The annual cost to deploy (assuming a 10-year rollout period) and later to indefinitely maintain a global atmospheric carbon capture system is about **\$4.04 billion per year**. This system achieves capture and permanent sequestration of atmospheric CO₂ at a total lifetime cost of about **\$0.08/tonne CO₂**. The cost can be driven so extraordinarily low because the mature nanofactory, manufacturing atomically precise product for ~\$1/kg, can also manufacture a cheap source of solar energy to power the CO₂ capture and sequestration process.

Extracted and sequestered carbon may become a valuable resource in future decades, providing a compact cheap source of carbon to be used as a key building material in the fabrication of diamond-based consumer, commercial, and industrial products that can be manufactured in a worldwide nanofactory-based economy.